Swansea University
Prifysgol Abertawe

Cronfa
Setting Research Free

Swansea University E-Theses

Lattice reduction and list based low complexity MIMO detection and its applications.

Bai, Lin

How to cite:

Bai, Lin (2010) *Lattice reduction and list based low complexity MIMO detection and its applications..* thesis, Swansea University.
http://cronfa.swan.ac.uk/Record/cronfa42763

Use policy:

This item is brought to you by Swansea University. Any person downloading material is agreeing to abide by the terms of the repository licence: copies of full text items may be used or reproduced in any format or medium, without prior permission for personal research or study, educational or non-commercial purposes only. The copyright for any work remains with the original author unless otherwise specified. The full-text must not be sold in any format or medium without the formal permission of the copyright holder. Permission for multiple reproductions should be obtained from the original author.

Authors are personally responsible for adhering to copyright and publisher restrictions when uploading content to the repository.

Please link to the metadata record in the Swansea University repository, Cronfa (link given in the citation reference above.)

http://www.swansea.ac.uk/library/researchsupport/ris-support/

Lattice Reduction and List based Low Complexity MIMO Detection and its Applications

Swansea University
Prifysgol Abertawe

Lin Bai

School of Engineering

Swansea University

Submitted to Swansea University in fulfillment of the requirements
for the degree of

Doctor of Philosophy (Ph.D.)

Oct. 15, 2010

ProQuest Number: 10807532

All rights reserved

INFORMATION TO ALL USERS
The quality of this reproduction is dependent upon the quality of the copy submitted.

In the unlikely event that the author did not send a complete manuscript
and there are missing pages, these will be noted. Also, if material had to be removed,
a note will indicate the deletion.

ProQuest 10807532

Published by ProQuest LLC (2018). Copyright of the Dissertation is held by the Author.

All rights reserved.
This work is protected against unauthorized copying under Title 17, United States Code
Microform Edition © ProQuest LLC.

ProQuest LLC.
789 East Eisenhower Parkway
P.O. Box 1346
Ann Arbor, MI 48106 – 1346

UNIVERSITY OF WALES SWANSEA
LIBRARY

Abstract

Multiple input multiple output (MIMO) is an important technique of improving the spectral efficiency in wireless communications. In MIMO systems, it is usually required to jointly detect signals at the receiver. While the maximum likelihood (ML) MIMO detection provides an optimal performance with full receive diversity, its complexity grows exponentially with the number of transmit antennas. Thus, lattice reduction (LR) and list based detectors are developed to reduce the complexity.

In this thesis, we first apply the partial maximum a posteriori probability (PMAP) principle to the list-based method for MIMO detection. It shows that the PMAP-based list detection outperforms the conventional list detection with a reasonably low complexity. To further improve the performance for slow fading MIMO channels, we develop the column reordering criteria (CRC) for the LR-based list detection. It shows that with our proposed CRC, the LR-based list detection can provide a near ML performance with a sufficiently low complexity. Then, we develop a complexity efficient pre-voting cancellation based detection with pre-voting vector selection criteria for underdetermined MIMO systems and show that this scheme can exploit a near ML performance with full receive diversity.

An extension of MIMO systems is multiuser MIMO systems, where the user selection becomes an effective way to increase diversity (multiuser diversity). If multiple users are selected to access the channel at a time, the selection problem becomes a combinatorial problem, where an exhaustive search may leads to highly computational complexity. Therefore, we propose a low complexity greedy user selection scheme with an iterative LR updating algorithm when a LR-based MIMO detector is used. It shows that the proposed selection scheme can provide a comparable performance to the combinatorial ones with much lower complexity.

To my wife, Xin.

Declarations and Statements

DECLARATION

This work has not previously been accepted in substance for any degree and is not being concurrently submitted in candidature for any degree.

Signed.. ...(candidate)

Date.....Oct..15..2010.....

STATEMENT 1

This thesis is the result of my own investigations, except where otherwise stated. Where correction services have been used, the extent and nature of the correction is clearly marked in a footnote(s).

Other sources are acknowledged by footnotes giving explicit references. A bibliography is appended.

Signed.... .(candidate)

Date.....Oct..15..2010...

STATEMENT 2

I hereby give consent for my thesis, if accepted, to be available for photocopying and for inter-library loan, and for the title and summary to be made available to outside organizations.

Signed .....(candidate)

Date.....Oct..15..2010.....

Contents

Acknowledgements

This dissertation can not be completed without the help and guidance from the people who are acknowledged here.

First of all, I should appreciate the guidance and supervision from Prof. Jinho Choi, who is my Ph.D. supervisor as well as my MS.c. dissertation supervisor. From his instruction, I know the importance of independent investigation. From his encouragement, I understand nothing is impossible as long as you can concentrate. I have also received some priceless ideas and suggestion from him which help me succeed.

Then, I want to express my appreciation to my parents and my wife, Xin. Without their support, I can barely make the academic achievement during my postgraduate studies.

Finally, I offer my regards and blessings to all of my friends who supported me in any respect during the completion of my Ph.D.

List of Figures

List of Tables

List of Abbreviations

MIMO	Multiple Input Multiple Output
DMT	Diversity-Multiplexing Trade-Off
SNR	Signal to Noise Ratio
ML	Maximum Likelihood
ZF	Zero Forcing
MMSE	Minimum Mean Square Error
V-BLAST	Vertical Bell Laboratories Layered Space Time
SIC	Successive Interference Cancellation
LR	Lattice Reduction
LLL	Lenstra-Lenstra-Lovász
APP	A Posteriori Probability
MAP	Maximum a Posteriori Probability
ISI	Intersymbol Interference
GSD	Generalized Sphere Decoding
PMAP	Partial MAP
PVC	Pre-voting Cancellation
PVS	Post-voting Vector Selection
CSCG	Circular Symmetric Complex Gaussian
CSI	Channel State Information
APRP	A Priori Probability
MSE	Mean Square Error
DFE	Decision Feedback Equalizer
SINR	Signal to Noise plus Interference
QAM	Quadratic Amplitude Modulation
BER	Bit Error Rate
CRIS	Column Reordering Index Set
SSE	Sum of Squared Error
CLLL	Complex Valued LLL
BS	Base Station

MMI	Maximum Mutual Information
MDist	Max-Min Distance
ME	Max-Min Eigenvalue
ODR	Optimal Decision Region
MMMSE	Min-Max Mean Square Error
MD	Max-Min Diagonal
PEP	Pairwise Error Probability
DRC	Dimension Reduction Condition
PDR	Probability of Dimension Reduction
cdf	Cumulative Density Function
flops	floating point operation
CRC	Column Reordering Criteria
OD	Orthogonal Deficiency
EP	Error Probability
TSD-CR	Tree Search Decoder - Column Reordering
PVC-MIMO	PVC-based MIMO
SD	Sphere Decoding
UILS	Underdetermined Integer Least Squares
pdf	Probability Density Function
SDMA	Space Division Multiple Access
LBR	Lattice Basis Reduced
LRG	LR-based Greedy
UBLR	Updated Basis LR
UBLRG	UBLR-based Greedy

List of Notations

$\mathbf{A}/\mathbf{a}$	(Boldface upper/lower letters) complex-valued matrix/vector
$\mathbf{A}_r/\mathbf{a}_r$	(Boldface upper/lower letters) real-valued matrix/vector
$\mathbf{A}^{\mathrm{T}}, \mathbf{A}^{\mathrm{H}}, \mathbf{A}^{\dagger}$	Transpose, Hermitian transpose, Pseudo inverse, respectively
$[\mathbf{A}]_{p,q}$	The (p,q)th element of $\mathbf{A}$
$\mathbf{A}(a:b, c:d)$	The submatrix of $\mathbf{A}$ with the elements obtained from rows $a, \ldots, b$ and columns $c, \ldots, d$
$\mathbf{A}(:, n)$	The n-th column vector of $\mathbf{A}$
$\mathbf{A}(n, :)$	The n-th row vector of $\mathbf{A}$
$\det(\mathbf{A})$	Determinant of matrix $\mathbf{A}$
$\mathcal{D}(\mathbf{A})$	Length of the shortest non-zero vector of the lattice generated by $\mathbf{A}$
$\lambda_{\min}(\mathbf{A})$	Minimum eigenvalue of $\mathbf{A}$
$\mathcal{L}(\mathbf{A})$	Lattice generated by $\mathbf{A}$
$E[\cdot]$	Statistical expectation
$\Re(\cdot), \Im(\cdot)$	Real and imaginary parts
$\mathcal{CN}(\mathbf{m}, \mathbf{C})$	Complex Gaussian vector distribution with mean $\mathbf{m}$ and covariance $\mathbf{C}$
$\log(\cdot)$	Natural logarithm
$\mathbf{0}$	Matrix with all entries of 0
$\|\cdot\|$	2-norm
$\lceil \beta \rfloor$	The nearest integer to β
$\lfloor \beta \rfloor$	The closest integer which is smaller than β
$\lvert\beta\rvert$	Absolute value of scalar β
$\setminus$	Set minus
$\mathbf{I}_n$	An $n \times n$ identity matrix
$\{k_{(1)}, k_{(2)}, \ldots\}$	The collection set of $k_{(1)}, k_{(2)}, \ldots$
$\mathrm{erfc}(x)$	Complementary error function of x, i.e., $\mathrm{erfc}(x) = \frac{2}{\sqrt{\pi}} \int_x^{+\infty} e^{-z^2} dz$
$\{\exists x : f(x)\}$	There is at least one x such that a function of x, $f(x)$, is true.
$\mathbb{Z}$	Set of integer numbers.

1

Introduction

1.1 An Overview

In company with the growing requirement of the information technology in the modern society, wireless communications play an crucial role. However, the scarce wireless spectrum has posed a big challenge on wireless communication systems with the increasing data rate demands. To improve the spectral efficiency [1] in wireless communications, multiple antennas are employed at both transmitter and receiver, where the resulting system is called the multiple-input multiple-output (MIMO) system [2]. In MIMO systems, it is usually required to detect signals jointly as multiple signals are transmitted through multiple independent signal paths between the transmitter and the receiver. For coded MIMO systems, the diversity-multiplexing trade-off (DMT) [3] is widely used to measure the performance. A system is defined with spatial multiplexing gain r and spatial diversity gain d as the data rate $R(\mathrm{SNR})$ achieves [3]

$$\lim_{\mathrm{SNR}\to\infty} \frac{R(\mathrm{SNR})}{\log \mathrm{SNR}} = r, \tag{1.1}$$

and the average error probability $P_e(\mathrm{SNR})$ achieves

$$-\lim_{\mathrm{SNR}\to\infty} \frac{P_e(\mathrm{SNR})}{\log \mathrm{SNR}} = d, \tag{1.2}$$

where SNR denotes the signal to noise ratio. If we consider uncoded systems, we can also use spatial diversity [1] as a performance metric, especially when

different MIMO detection methods are adopted. Note that a full receive diversity gain is considered with its diversity order equals the number of receive antennas in MIMO systems.

By using exhaustive search, maximum likelihood (ML) detector can be used to detect the joint signals to achieve an optimal performance with a full receive diversity order. Since the complexity of the ML detection grows exponentially with the number of transmit antennas, it is normally not used in practical systems. Instead, for MIMO detection, various computationally efficient approaches have been proposed. Learned as linear detectors, the zero-forcing (ZF) and the minimum mean square error (MMSE) detectors are considered which take the signals from the other antennas as the interference. In general, they have low complexity, but the performance is not good enough for some cases, specially at a high SNR. Since linear detectors can not provide a reasonably good performance and a full receive diversity order from multiple receive antennas, other approaches are considered. For example, the vertical Bell laboratories layered space-time (V-BLAST), known as the successive interference cancellation (SIC), is proposed in [4]. It is shown that an MMSE detector with SIC can improve the performance, but suffers from the error propagation. By ordering the signal detection and cancellation, the error propagation can be mitigated.

Clearly, linear detectors and the ML detector have two desirable features we want to achieve, low computational complexity and optimal performance. This thesis aims to design good MIMO detectors with features of a comparable complexity to that of linear detectors and a near ML performance. To achieve the design goals, we rethink of several existing approaches and methods, including list and lattice reduction (LR) based detection.

With the ML detector, exhaustive search is performed for all the possible decision vectors. While the list-based detectors [5, 6, 7, 8, 9, 10, 11] construct a list of candidate decision vectors and then choose the best candidate as the final decision, the computational complexity can be considerably reduced. By regarding some bits/symbols as unreliable, the list is constructed in [6]. In [7], the list of the parallel detector is generated by employing a separate low-complexity detector for each possible value of the first symbol to be detected. In [10], a list sphere detection is proposed by considering the candidate list in a sphere.

Furthermore, a family of list-based Chase detectors is proposed in [12, 13, 14, 15, 16, 17]. The principle of the Chase detection is to separate the detection procedure into two layers. In the first layer, one symbol is chosen to be detected separately and a list of candidates for this symbol will be constructed. On the second layer, the contribution from the detected symbol is treated as the interference and will be canceled from the received signal. The residual signal will be detected by the sub-detectors to decompose the remaining symbols. The final hard decision symbol vector is determined by MMSE over the concerned vectors. Note that different algorithms can be employed as the sub-detectors in the detection.

Taking the channel matrix as a basis for a lattice, various approaches based on the properties of lattice are considered. Since a lattice can be generated by different bases or channel matrices, in order to mitigate the interference between multiple signals, we can find a matrix whose column vectors are nearly orthogonal to generate the same lattice. Based on the Lenstra-Lenstra-Lovász (LLL) algorithm [18], a lattice reduced matrix with a nearly orthogonal basis is generated. By employing various low complexity detectors (e.g., MMSE and MMSE-SIC detectors) with the lattice reduced matrix, the LR-based detection [19, 20, 21, 22, 23, 24, 25, 26] is carried out, which can provide a full receive diversity gain with a good performance. Furthermore, its complexity is significantly lower than that of the ML detector using an exhaustive search. Although the LR can be performed with a complex-valued channel matrix as in [23, 24, 25] or a real-valued one converted from the complex-valued one as in [19, 22], they can provide the same performance as shown in [23, 25]. Since the LR with a complex-valued matrix has a lower complexity [23], in general, we consider the LR with a complex-valued matrix.

Some other approaches are also proposed to reduce the complexity for MIMO detection. By regarding the ML detection problem with a partial information of a posteriori probability (APP), the partial maximum a posteriori probability (MAP) principle is applied in [27] to reduce a higher-dimensional ML detection problem to two lower-dimensional subdetection problems to mitigate the inter-symbol interference (ISI) and reduce the complexity. In [28], a complexity efficient LR-based list detection is studied to reduce a large MIMO detection problem into multiple small sub-detection problems.

A channel matrix is called square or tall if the number of transmit antennas M is equal to, or smaller than the number of receive antennas N. For most detectors, it is usually assumed that channel matrix is square or tall. However, there could be the cases where the channel matrices are fat ($M > N$), which results in underdetermined or rank-deficient MIMO systems. Note that the LR-based detection is only considered for the cases of tall or square channel matrices. Although the list detection can be employed to such underdetermined MIMO systems, it can not provide a good performance with a full receive diversity. Therefore, some generalized sphere decoding (GSD) approaches [29, 30, 31, 32, 33] are developed for such MIMO systems. In [34], two sub-optimal group detectors are introduced. A geometrical approach based detection for underdertermined MIMO systems is studied in [35]. To further reduce the complexity, a computationally efficient GSD-based detector with column reordering is proposed in [36].

In MIMO systems, a rich spatial diversity gain can be obtained by employing various MIMO detectors (e.g., ML and LR-based detectors) to MIMO systems. Consider that multiple users are able to access the MIMO channel with different locations and channel conditions. Due to users' different locations and channel conditions, it is possible to exploit another diversity gain, where the performance can be maximized by choosing the user of the best channel at a time. The resulting system and its corresponding diversity gain are named as the multiuser MIMO system [37] with the multiuser diversity gain [38]. Conventionally, the SNR is used as a user selection criterion to investigate the multiuser diversity [39] [40], which highly depends on the channel capacity. Hence, the user which has the highest channel capacity is chosen, when multiuser MIMO systems are carried out. Although SNR-based or throughput-based optimal user selection schemes are adopted in user selection, the actual performance can be different from the expected one if non-ideal or suboptimal MIMO detectors are employed for joint detection. In [41], the error probability is considered as the user selection criteria, which choose the user who has the smallest error probability for given MIMO detectors. The user selection criteria with ML detector as well as other low complexity suboptimal detectors are derived. It is shown that a near optimal performance with a full diversity gain (i.e., multiuser diversity and multiple

antenna diversity) can be achieved using those user selection criteria proposed in [41] with LR-based detectors.

1.2 Contributions

Although various complexity efficient MIMO detection schemes are proposed, in many cases, they can not provide a near ML performance. Furthermore, their complexity is still considerably high. In order to improve the performance and reduce the complexity, in this thesis, we first propose a complexity efficient partial MAP (PMAP) based list detection for MIMO systems. Then, an error probability based column reordering strategy is studied with the LR-based list MIMO detection to further improve the performance when slow fading MIMO channels are considered. For underdetermined MIMO systems, a pre-voting cancellation (PVC) based detection is developed which provides a near optimal performance with a low complexity. Furthermore, we consider user selection problems in multiuser MIMO systems, where an actual low complexity MIMO detection is employed. Using a LR updating method, we investigate a group of low complexity greedy user selection criteria for multiuser MIMO systems. The detailed contributions are organized as follows:

- The PMAP principle can be applied to reduce the complexity of the MIMO detection through the SIC. In Chapter 3, we apply the PMAP principle to the list detection method for MIMO detection, where the SIC is performed with a list of candidates. The PMAP principle helps to choose candidate symbol vectors in the list detection. It is shown that the proposed method outperforms the conventional list detection method with a reasonable complexity.

- A computationally efficient LR-based list detection is studied to reduce a large MIMO detection problem into multiple small sub-detection problems. In Chapter 4, based on the error probability analysis, we study column reordering schemes for channel matrices to improve performance. It is shown

that by employing our proposed column reordering, a significant performance improvement can be obtained with a low complexity for slow fading MIMO channels.

- Various detection methods including the ML detection have been studied for MIMO systems. While it is usually assumed that the channel matrix is square or tall in most cases, there could be the cases where the channel matrices are fat, which results in underdetermined/rank-deficient MIMO systems. In Chapter 5, we employ the PVC-based detection for underdetermined MIMO systems and show that the proposed detectors can exploit a full receive diversity. Furthermore, the post-voting vector selection (PVS) criteria for the proposed detectors are taken into account to further improve the performance. We also show that our proposed scheme has a lower computational complexity compared to existed approaches, in particular when slow fading MIMO channels are considered.

- User selection plays a crucial role in multiple access channels (e.g., uplink channels of cellular systems). It is known that the multiuser diversity can be exploited in user selection to maximize a total throughput or achievable rate. While the achievable rate is adopted as a performance indicator to see an overall performance, it may not be proper if a suboptimal detector or decoder is employed. In particular, for MIMO systems, a low complexity suboptimal MIMO detector can be used as optimal MIMO detectors require prohibitively high computing power. Under this practical circumstance, it may be desirable to derive user selection criteria based on the error probability for given MIMO detectors. In Chapter 6, we propose a low complexity greedy user selection scheme with an iterative LR updating algorithm when a LR-based MIMO detector is used. We also analyze the diversity gain for combinatorial user selection approaches with various MIMO detectors. From simulation results, we can confirm that the proposed greedy user selection approach can provide a comparable performance to the combinatorial ones with much lower complexity.

1.2.1 Publications

1.2.1.1 Journal Papers

Published/Accepted

(J1) L. Bai, and J. Choi, "Partial MAP-based list detection for MIMO systems," *IEEE Trans. Vehicular Tech.*, pp. 2544-2548, June 2009.

(J2) L. Bai, C. Chen, J. Choi, and C. Ling, "Greedy user selection using a lattice reduction updating method for multiuser MIMO systems," *IEEE Trans. Vehicular Tech.* (accepted)

(J3) L. Bai, C. Chen, and J. Choi, "Error probability based column reordering criterion for lattice reduction based list MIMO detection," *IET Electronics Letters*, vol. 46, issue 12, June, 2010.

(J4) L. Bai, C. Chen, and J. Choi, "Pre-voting cancellation based detection for underdetermined MIMO systems," *EURASIP Journal on Wireless Communications and Networking (JWCN).* (accepted)

(J5) C. Chen, L. Bai, B. Wu, and J. Choi, "Downlink throughput maximization for OFDMA systems with feedback channel capacity constraints," *IEEE Trans. Signal Processing.* (accepted)[1]

(J6) C. Chen, L. Bai, K. Cai, J. He, and H. Xiang, "A network coding based interference cancelation scheme for wireless ad hoc networks," *Wiley Journal on Wireless Communications and Mobile Computing (WCMC), vol. 10, August 2010.*[2]

[1]Lin Bai has improved the joint sub-carrier and power allocation algorithm in the paper with an iteratively search approach.

[2]Lin Bai has derived the geometrical relations between nodes in adjacent regions for the case of hexagonal region and presented numerical results to validate the derivations.

Under Revision

(JR1) C. Chen, L. Bai, J. He, H. Xiang, and J. Choi, "On the capacity improvement for multicast traffics with physical-layer network coding," submitted to *Journal of Communications and Networks (JCN).* (minor revision)[1]

Submitted

(JS1) C. Chen, L. Bai, B. Wu, and J. Choi, "Resource allocation for maximizing outage throughput in OFDMA systems with finite-rate feedback," submitted to *EURASIP Journal on Wireless Communications and Networking (JWCN).*[2]

(JS2) C. Chen, L. Bai, B. Wu, and J. Choi, "Signal beamforming and relay selection criteria for cooperative Bi-directional transmissions with physical layer network coding," submitted to *IET Communications.*[3]

1.2.1.2 Conference Papers

(C1) L. Bai, C. Chen, and J. Choi, "Lattice reduction aided detection for underdetermined MIMO systems: a pre-voting cancellation approach," *IEEE. Vehicular Tech. Conf.*, spring 2010.

(C2) L. Bai, C. Chen, J. Choi, and C. Ling, "Updated basis lattice reduction based sequential user selection for multiuser MIMO systems," submitted to *IEEE Globecom*, 2010. (accepted)

(C3) C. Chen, L. Bai, B. Wu, D. To, and J. Choi, "Outage throughput maximization for OFDMA systems with feedback channel capacity constraints," submitted to *IEEE Globecom*, 2010. (accepted)

[1]Lin Bai has made the proof of Lemma 4.8 with more scientific precision, where Lemma 4.8 is a key point to generate the main results of this paper.

[2]Lin Bai has improved the power allocation algorithm and provided the numerical results to validate the effectiveness of the algorithm.

[3]Lin Bai has derived the error probability of the second scenario and provided the numerical results to validate the derivations.

(C4) C. Chen, L. Bai, J. He, H. Xiang, and J. Choi, "On the capacity improvement of multicast throughput in wireless Ad Hoc networks with physical-layer network coding," *International Wireless Communication and Mobile Computing Conference (IWCMC)*, 2010.

(C5) B. Wu, C. Chen, L. Bai, W. Guan, and H. Xiang, "Resource allocation for OFDMA systems with guaranteed outage probabilities," *International Wireless Communication and Mobile Computing Conference (IWCMC)*, 2010.

1.2.2 Externally Funded Research Projects

(P1) Member, Project on "Wireless broadband access for high speed trains", 2009-2010. Funded by Huawei Technologies Co., Ltd. China[1].

(P2) Member, Project on "Design of low complexity MIMO detectors", 2007-2008. Funded by Huawei Technologies Co., Ltd. China[2].

[1]In this project, we propose a new detection algorithm called LR based list detector which uses list detection and lattice aided detection techniques as the key ingredients to develop low complexity and high performance MIMO detector. The study of implementation possibility on hardware is also carried out. The study provides reference for implementing true silicon architecture. Finally, the proposed detector will be applied to the 3G systems for long-term evolution services. Lin Bai has improved the LR-based list detection algorithm and analyzed the performance and complexity trade-off, where simulation results are provided to validate the effectiveness of the algorithm.

[2]In this project, we study a wireless access system for high speed trains. A distributed antenna system is considered for wireless communications between trains and access points on ground. It is assumed that trains are equipped with two antenna arrays for efficient communications with road side access points. We focus on two key approaches, namely joint power allocation and cyclic beamforming. A joint two-point power allocation problem is formulated to allocate powers for wireless links between antenna arrays on trains and RSAPs. For cyclic beamforming, beamformer has been designed to provide a certain signal to interference plus noise ratio. Lin Bai has derived the cyclic beamforming in conjunction with the joint power allocation to minimize the intra and inter fluctuation, where the cyclic beamforming design is the key point to generate the main results of this work.

1.3 Outline

The rest of this thesis is organized as follows. Background of conventional MIMO detectors and multiuser MIMO user selection is presented in Chapter 2. A computationally efficient PMAP-based list detection for MIMO systems is shown in Chapter 3. Then, an error probability based column reordering strategy is studied for the LR-based list MIMO detection in Chapter 4. In Chapter 5, a pre-voting cancellation based detection is developed for underdetermined MIMO systems. The greedy user selection using an iterative LR updating method for multiuser MIMO systems is proposed in Chapter 6. Some concluding remarks and future works are represented in Chapter 7. Finally, the appendices show the details of some derivations.

2

Background of MIMO Detection and User Selection

In this chapter, we provide a brief summary of the existing well-known MIMO detection approaches. Then, list detection and LR-based detection are presented. After that, we introduce the multi-user MIMO user selection.

2.1 Conventional Approaches

2.1.1 System Model

Consider a MIMO system with M transmit and N receive antennas. Let $\mathbf{H}_l$ denote an $N \times M$ channel matrix at symbol time l, where $l = 0, 1, \ldots, L-1$ and L is the length of a data packet. Define $s_{m,l}$ and $y_{n,l}$ as the the data symbol transmitted by the mth transmit antenna and the received signal at the nth receive antenna during the lth symbol interval, respectively. Assume that a common signal alphabet, denoted by $\mathcal{S}$, is used for all s_m. That is, $s_m \in \mathcal{S}$, $m = 1, 2, \ldots, M$. Then, the received signal vector over a flat-fading MIMO channel is given by

$$\begin{aligned} \mathbf{y}_l &= [y_{1,l}\ y_{2,l}\ \cdots\ y_{N,l}]^{\mathrm{T}} \\ &= \mathbf{H}_l \mathbf{s}_l + \mathbf{n}_l, l = 0, 1, \ldots, L-1, \end{aligned} \tag{2.1}$$

where the manuscript T denotes the transpose, $\mathbf{s}_l = [s_{1,l},\ s_{2,l},\ \ldots,\ s_{M,l}]^{\mathrm{T}}$ and $\mathbf{n}_l = [n_{1,l},\ n_{2,l},\ \ldots,\ n_{N,l}]^{\mathrm{T}}$ denote the transmit signal vector and the noise vec-

tor which is assumed to be a zero-mean circular symmetric complex Gaussian (CSCG) random vector with $E[\mathbf{n}\mathbf{n}^{\mathrm{H}}] = N_0\mathbf{I}$. Note that H represents the Hermitain transpose, respectively. Furthermore, it is assumed that the channel state information (CSI) is perfectly known at the receiver.

According to [1], the MIMO channel capacity grows linearly with $\min(M, N)$. Note that there is a fundamental trade-off between receive diversity gain and multiplexing diversity gain [3]. Thus, we may prefer that $M = N$ which results in that $\mathbf{H}_l$ is square.

2.1.2 ML Detection

For the sake of simplification, we omit the symbol-duration index l in (2.1) and rewirte the received signal as

$$\mathbf{y} = \mathbf{H}\mathbf{s} + \mathbf{n}. \tag{2.2}$$

Here, $\mathbf{H}$ is the channel matrix which can also be written as

$$\mathbf{H} = [\mathbf{h}_1, \mathbf{h}_2, \ldots, \mathbf{h}_M], \tag{2.3}$$

where $\mathbf{h}_m$ denotes the mth column vector of $\mathbf{H}$. Define the number of the elements of $\mathcal{S}$ by $K = |\mathcal{S}|$, and $\mathcal{S}^M$ denotes the M-dimensional Cartesian product of $\mathcal{S}$, the maximum likehood function of the ML detection is given by

$$\begin{aligned} \mathbf{s}_{\mathrm{ml}} &= \arg\max_{\mathbf{s}\in\mathcal{S}^M} f(\mathbf{y}|\mathbf{s}) \\ &= \arg\min_{\mathbf{s}\in\mathcal{S}^M} ||\mathbf{y} - \mathbf{H}\mathbf{s}||^2. \end{aligned} \tag{2.4}$$

Since an exhaustive search is carried out to identify the ML vector and the number of candidate vectors for $\mathbf{s}$ is K^M, the complexity grows exponentially with the number of transmit antenna M.

Let $\mathbf{b}$ denote the bit-level symbol vector of $\mathbf{s}$, where the elements of $\mathbf{b}$ are binary and $\mathbf{b} = [b_1\ b_2\ \ldots\ b_{\bar{M}}]^{\mathrm{T}}$, $\bar{M} = M\log_2 K$. Denote *a priori* probability (APRP) of $\mathbf{b}$ by $\Pr(\mathbf{b})$, the MAP detection is given by

$$\begin{aligned} \mathbf{b}_{\mathrm{map}} &= \arg\max_{\mathbf{b}} \Pr(\mathbf{b}|\mathbf{y}) \\ &= \arg\max_{\mathbf{b}} f(\mathbf{y}|\mathbf{b})\Pr(\mathbf{b}). \end{aligned} \tag{2.5}$$

Furthermore, the APP of each bit is given by

$$\begin{aligned}\Pr(b_i = +1|\mathbf{y}) &= \sum_{\mathbf{b}\in\mathcal{B}_i^+} \Pr(b|y) \\ \Pr(b_i = -1|\mathbf{y}) &= \sum_{\mathbf{b}\in\mathcal{B}_i^-} \Pr(b|y),\end{aligned} \tag{2.6}$$

where $\mathcal{B}_i^{\pm} = \left\{[b_1\ b_2\ \ldots\ b_{\bar{M}}]^{\mathrm{T}} \mid b_i = \pm 1, b_m \in \{+1,-1\}, \forall m \neq i\right\}$.

For the ML detection, although its performance is optimal, the extremely highly computational complexity makes it unrealistic to be employed in practical systems when M is large.

2.1.3 ZF and MMSE Detection

For complexity reduction, linear detectors are considered. With linear detectors, the received signal $\mathbf{y}$ is multiplied by an estimator $\mathbf{W}$.

The ZF estimator and the estimated transmit symbol vector are given by

$$\mathbf{W}_{\mathrm{zf}} = \mathbf{H}(\mathbf{H}\mathbf{H}^{\mathrm{H}})^{-1} \tag{2.7}$$

and

$$\begin{aligned}\hat{\mathbf{s}}_{\mathrm{zf}} &= \mathbf{W}_{\mathrm{zf}}^{\mathrm{H}}\mathbf{y} \\ &= (\mathbf{H}\mathbf{H}^{\mathrm{H}})^{-1}\mathbf{H}^{\mathrm{H}}\mathbf{y} \\ &= \mathbf{s} + (\mathbf{H}\mathbf{H}^{\mathrm{H}})^{-1}\mathbf{H}^{\mathrm{H}}\mathbf{n}.\end{aligned} \tag{2.8}$$

It is shown that when $\mathbf{H}$ tends to zero, $(\mathbf{H}\mathbf{H}^{\mathrm{H}})^{-1}\mathbf{H}^{\mathrm{H}}\mathbf{n}$ tends to infinity.

To reduce the impact from noise, the MMSE detector generates an estimator with taking account of the noise component. The MMSE estimator is found by minimizing the mean-square error as

$$\begin{aligned}\mathbf{W}_{\mathrm{mmse}} &= \arg\min_{\mathbf{W}} E\left[||\mathbf{s} - \mathbf{W}^{\mathrm{H}}\mathbf{y}||^2\right] \\ &= \left(E\left[\mathbf{y}\mathbf{y}^{\mathrm{H}}\right]\right)^{-1} E\left[\mathbf{y}\mathbf{s}^{\mathrm{H}}\right] \\ &= \left(\mathbf{H}\mathbf{H}^{\mathrm{H}} + N_0\mathbf{I}\right)^{-1}\mathbf{H}.\end{aligned} \tag{2.9}$$

The result estimated symbol vector is given by

$$\begin{aligned}\hat{\mathbf{s}}_{\text{mmse}} &= \mathbf{W}_{\text{mmse}}^{\text{H}}\mathbf{y} \\ &= \mathbf{H}^{\text{H}}\left(\mathbf{H}\mathbf{H}^{\text{H}} + N_0\mathbf{I}\right)^{-1}\mathbf{y} \end{aligned} \tag{2.10}$$

and the mean-square error (MSE) follows that

$$\begin{aligned}\text{MSE} &= E\left[\left(\mathbf{s} - \mathbf{W}_{\text{mmse}}^{\text{H}}\mathbf{y}\right)\left(\mathbf{s} - \mathbf{W}_{\text{mmse}}^{\text{H}}\mathbf{y}\right)^{\text{H}}\right] \\ &= \mathbf{I} - \mathbf{H}^{\text{H}}\left(\mathbf{H}\mathbf{H}^{\text{H}} + N_0\mathbf{I}\right)^{-1}\mathbf{H} \\ &= \left(\mathbf{I} + \frac{1}{N_0}\mathbf{H}^{\text{H}}\mathbf{H}\right)^{-1}. \end{aligned} \tag{2.11}$$

2.1.4 SIC Detection

Based on the QR factorization of the channel matrix $\mathbf{H}$, a SIC method is proposed and analyzed in [42, 43]. For convenience, assume that $\mathbf{H}$ is square or tall and $M \leq N$, $\mathbf{H}$ is factorized as

$$\mathbf{H} = \mathbf{Q}\mathbf{R}, \tag{2.12}$$

where an $N \times N$ sized $\mathbf{Q}$ is unitary, an $N \times M$ sized $\mathbf{R} = \left[\bar{\mathbf{R}}^{\text{T}}\ \mathbf{0}\right]^{\text{T}}$, and a $M \times M$ sized $\bar{\mathbf{R}}$ is upper triangular. By multiplying $\mathbf{Q}^{\text{H}}$, (2.2) is rewritten as

$$\begin{aligned}\mathbf{x} &= \mathbf{Q}^{\text{H}}\mathbf{y} \\ &= \mathbf{R}\mathbf{s} + \mathbf{Q}^{\text{H}}\mathbf{n}, \end{aligned} \tag{2.13}$$

where $\mathbf{Q}^{\text{H}}\mathbf{n}$ is a zero-mean complex Gaussian random vector. Since $\mathbf{Q}^{\text{H}}\mathbf{n}$ and $\mathbf{n}$ have the same statistical properties, $\mathbf{Q}^{\text{H}}\mathbf{n}$ can be used to denote $\mathbf{n}$. We have (2.13) as

$$\mathbf{x} = \mathbf{R}\mathbf{s} + \mathbf{n}. \tag{2.14}$$

Denoted by $r_{p,q}$, x_k, and n_k the (p,q)-th entry of $\mathbf{R}$, kth element of $\mathbf{x}$, and kth element of $\mathbf{n}$, respectively. Since $\bar{\mathbf{R}}$ is upper triangular, we have

$$\begin{aligned} x_N &= n_N \\ &\vdots \\ x_M &= r_{M,M}s_M + n_M \\ x_{M-1} &= r_{M-1,M}s_M + r_{M-1,M-1}s_{M-1} + n_{M-1} \\ &\vdots \end{aligned} \tag{2.15}$$

This results in a sequential detection procedure. Firstly, s_M can be detected from x_M, since there is no interference. Then, the contribution of s_M is to be canceled in detecting s_{M-1} from x_{M-1}. This sequential detection procedure is terminated till all the elements in $\mathbf{s}$ are detected. The mth element of $\mathbf{s}$, s_m, can be detected after canceling $M-m$ data symbols as

$$u_m = x_m - \sum_{m=k+1}^{M} r_{k,m}\hat{s}_m, \ k \in \{1, 2, \ldots, M-1\}, \tag{2.16}$$

where $\hat{s}_m$ denotes the hard-decision estimate of s_m from u_m. Note that when $\mathbf{H}$ is fat and $M > N$, the $N \times M$ sized matrix $\mathbf{R}$ after QR factorization of $\mathbf{H}$ is not upper triangular, thus, the sequential detection based SIC method can not be employed.

Since $\mathbf{Q}^{\mathrm{H}}$ is used to perform nulling processing in (2.13), a ZF decision feedback equalizer (DFE) over ISI channels is considered. In order to improve the performance, by taking account of the background noise, the MMSE-DFE based SIC is carried out. From (2.2), with the MMSE-DFE based SIC, the MMSE estimator for symbol s_1 is given by

$$\begin{aligned} \mathbf{w}_{\mathrm{mmse},1} &= \arg\min_{\mathbf{w}} E\left[|s_1 - \mathbf{w}^{\mathrm{H}}\mathbf{y}|^2\right] \\ &= \left(\mathbf{H}\mathbf{H}^{\mathrm{H}} + N_0\mathbf{I}\right)^{-1}\mathbf{h}_1, \end{aligned} \tag{2.17}$$

where $\mathbf{h}_k$ denotes the kth column of $\mathbf{H}$ and $k \in \{1, \ldots, M\}$. Then, a hard-decision is carried out to detect s_1 which is based on

$$\hat{s}_{1,\mathrm{mmse}} = \mathbf{w}_{\mathrm{mmse},1}\mathbf{y}. \tag{2.18}$$

Assume that s_1 is successfully detected and its contribution is canceled from $\mathbf{y}$, we have

$$\mathbf{y}_1 = \sum_{m=2}^{M} \mathbf{h}_m s_m + \mathbf{n}, \tag{2.19}$$

on which the MMSE method can be employed to detect s_2. With the MMSE-based cancellation method repeated, the detection of the s_m's can be performed.

Note that the performance of the MMSE-DFE based SIC highly depends on the reliability of detected symbols in the early stages. To improve the performance, a pre-ordering method for SIC detection is proposed and discussed in

[43, 44]. Furthermore, a simple strategy is considered by selecting the first symbol to be detected has the smallest MSE (i.e., equivalently, highest signal to interference plus noise ratio (SINR)) as

$$\left\{k_{(1)}, \mathbf{w}_{k_{(1)}}\right\} = \arg \min_{k} \min_{\mathbf{w}} E\left[|s_k - \mathbf{w}^{\mathrm{H}}\mathbf{y}|^2\right], \tag{2.20}$$

where $k_{(1)}$ and $\mathbf{w}_{k_{(1)}}$ denote the index of the first detected symbol and its corresponding MMSE filtering vector, respectively. Then, the cancellation is carried out as

$$\bar{\mathbf{y}} = \mathbf{y} - \mathbf{h}_{k_{(1)}}\hat{\mathbf{s}}_{k_{(1)}}, \tag{2.21}$$

where $\hat{\mathbf{s}}_{k_{(1)}}$ denotes a hard-decision of $\mathbf{s}_{k_{(1)}}$ from $\mathbf{w}_{k_{(1)}}^{\mathrm{H}}\mathbf{y}$. With $\bar{\mathbf{y}}$, the next symbol to be detected is found as

$$\left\{k_{(2)}, \mathbf{w}_{k_{(2)}}\right\} = \arg \min_{k \in I} \min_{\mathbf{w}} E\left[|s_k - \mathbf{w}^{\mathrm{H}}\hat{\mathbf{y}}|^2\right], \tag{2.22}$$

where $I = \{1, 2, \ldots, M\} \setminus k_{(1)}$ and $\setminus$ denotes the set minus. The cancellation and MMSE filtering is repeated until all symbols are detected.

2.1.5 Simulation Results

We consider uncoded 16-quadratic amplitude modulation (QAM) 2×2 and 16-QAM 4×4 MIMO systems for the simulations. The elements of the MIMO channels are generated as independent complex Gaussian random variables with mean zero and unit variance. The SNR is defined by the energy per bit to the noise power spectral density ratio E_b/N_0. In Figs. 2.1 and 2.2, we show the bit error rate (BER) performance of the ML detector, the ZF detector, and the ZF-SIC detector. Since an exhaustive search is considered with the ML detector, the optimal performance with full receive diversity gain is obtained at the cost of high complexity. While the ZF has the lowest complexity, it provides the worst performance. We also note that the ZF-SIC detector has a trade-off between the performance and complexity.

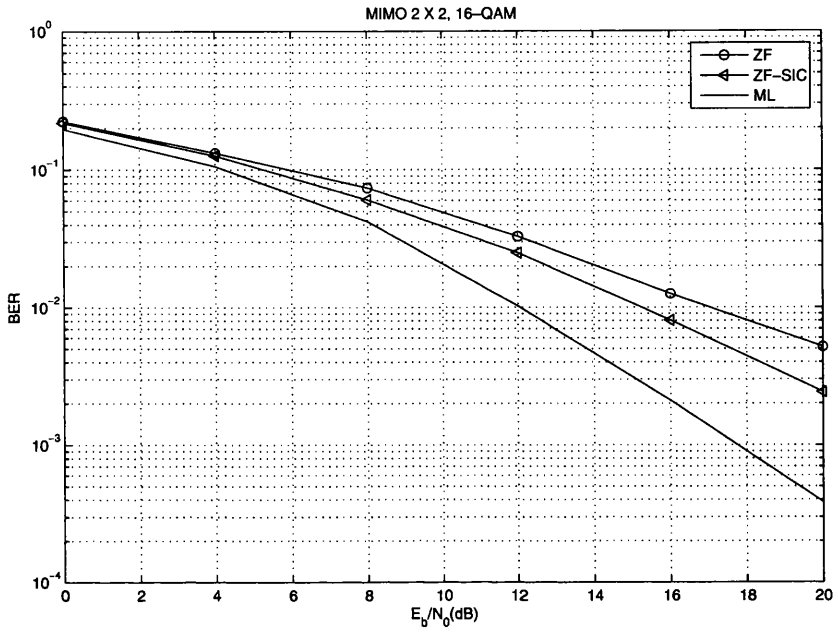

Figure 2.1: BER performance of conventional detectors in a 16-QAM 2×2 MIMO system.

2.1.6 Conclusion and Remarks

In this section, we introduced 3 conventional approaches for MIMO detection. While an optimal performance is obtained by the ML detection, a prohibitively high complexity makes it unrealistic to be employed. There are some suboptimal approaches which can provide a relatively low complexity (e.g., ZF and ZF-SIC detectors). However, their performance is not comparable with that of the ML, especially at a high SNR. Therefore, some techniques are carried out to improve the performance of these conventional suboptimal approaches. In the following sections, we explain the list and LR-based detection.

2.2 List Detection

By dividing the symbol to be detected in two layers, a complexity efficient SIC-based list detection [5, 6, 7, 8, 9, 10, 11] is studied. In this section, we introduce a

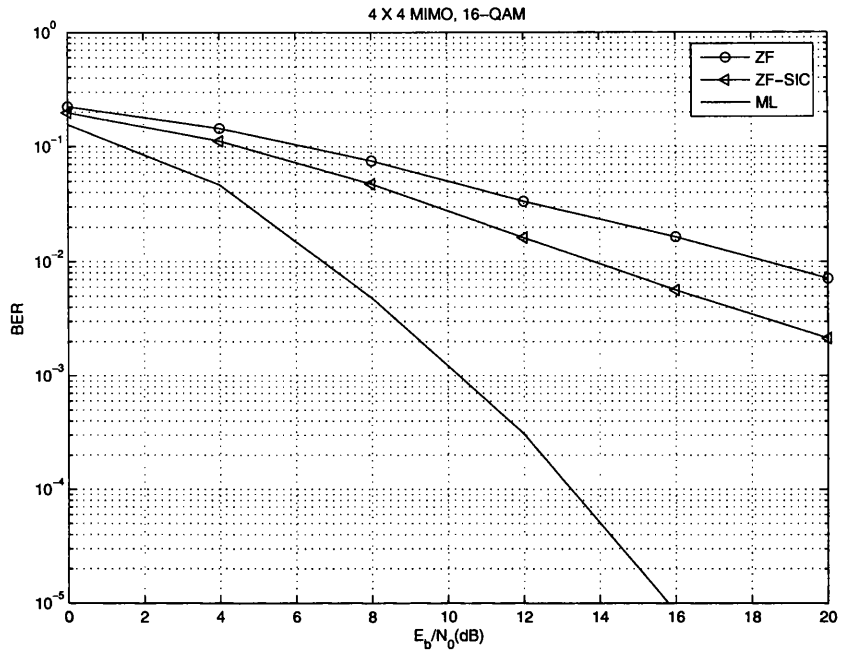

Figure 2.2: BER performance of conventional detectors in a 16-QAM 4×4 MIMO system.

class of list-based detectors for MIMO channels, namely, list-based Chase detector [12, 13, 14, 15, 16, 17].

2.2.1 Chase Algorithms

In this subsection, we first review the list-based Chase algorithm using the linear filter to perform a two-step detection. Note that this class of Chase detection can be implemented with any M and N. Furthermore, for the case of $M \leq N$, the QR factorization-based Chase detection is studied to improve the performance.

Consider the column swapping of channel matrix $\mathbf{H}$, from (2.2), we have

$$\mathbf{y} = \mathbf{H}_{\mathcal{K}}\mathbf{s}_{\mathcal{K}} + \mathbf{n}, \tag{2.23}$$

where the $N \times M$ channel matrix $\mathbf{H}_{\mathcal{K}} = \left[\mathbf{h}_{k_{(1)}}, \ldots, \mathbf{h}_{k_{(M)}}\right]$, the transmit signal vector $\mathbf{s}_{\mathcal{K}} = \left[s_{k_{(1)}}, \ldots, s_{k_{(M)}}\right]^{\mathrm{T}}$. Note that $\mathbf{h}_{k_{(m)}}$ denotes the $k_{(m)}$th col-

umn vector of $\mathbf{H}_{\mathcal{K}}$ and the column reordering index set (CRIS) is denoted by $\mathcal{K} = \{k_{(1)}, \ldots, k_{(M)}\}$, which is a permutation of $\{1, 2, \ldots, M\}$.

By defining the sub-CRIS as $\mathcal{U} = \{k_{(1)}, \ldots k_{(M-1)}\}$, we have $\mathbf{H}_{\mathcal{K}} = \left[\mathbf{H}_{\mathcal{U}}\ \mathbf{h}_{k_{(M)}}\right]$ and $\mathbf{s}_{\mathcal{K}} = \left[\mathbf{s}_{\mathcal{U}}^{\mathrm{T}}\ s_{k_{(M)}}\right]^{\mathrm{T}}$. Then, (2.23) is rewritten as

$$\mathbf{y} = \mathbf{H}_{\mathcal{U}}\mathbf{s}_{\mathcal{U}} + \mathbf{h}_{k_{(M)}} s_{k_{(M)}} + \mathbf{n}, \tag{2.24}$$

where the size of sub-vector $\mathbf{s}_{\mathcal{U}}$ is $(M-1) \times 1$.

Based on the system models in (2.23) and (2.24), the linear filter-based Chase detection is summarized as follows [13]:

a) Select the sub-vectors $\mathbf{s}_{\mathcal{U}}$ and $s_{k_{(M)}}$ from $\mathbf{s}$ which fit the one in (2.24). Note that the channel matrix $\mathbf{H}_{\mathcal{K}} = \left[\mathbf{H}_{\mathcal{U}}\ \mathbf{h}_{k_{(M)}}\right]$ is generated accordingly.

b) Generate a list of Q candidate values for $s_{k_{(M)}}$, say $\{\hat{s}^1_{k_{(M)}}, \hat{s}^2_{k_{(M)}}, \ldots, \hat{s}^Q_{k_{(M)}}\}$, where $Q \leq |\mathcal{S}|$ and $\hat{s}^q_{k_{(M)}}$ denotes the qth closest symbol to $\hat{y}$, $q = 1, 2, \ldots, Q$. Here, $\hat{y} = \mathbf{w}^{\mathrm{H}}_{k_{(M)}}\mathbf{y}$ and $\mathbf{W}_{\mathcal{K}} = \left[\mathbf{w}_{k_{(1)}}, \ldots, \mathbf{w}_{k_{(M)}}\right]$ represents the linear (ZF or MMSE) filter of $\mathbf{H}_{\mathcal{K}}$.

c) By canceling the contribution of the symbol vector $s_{k_{(M)}}$ to $\mathbf{y}$ using each candidate of $s_{k_{(M)}}$ in the list, a set of Q residual vectors $\{\mathbf{y}_1, \mathbf{y}_2, \ldots, \mathbf{y}_Q\}$ is generated as

$$\mathbf{y}_q = \mathbf{y} - \mathbf{h}_{k_{(M)}} \hat{s}^q_{k_{(M)}}. \tag{2.25}$$

d) Apply an independent sub-detector to each $\mathbf{y}_q$ and obtain decision of the remaining $M-K$ symbols $\{\hat{\mathbf{s}}^1_{\mathcal{U}}, \hat{\mathbf{s}}^2_{\mathcal{U}}, \ldots, \hat{\mathbf{s}}^Q_{\mathcal{U}}\}$ (MIMO detectors that work for square or tall MIMO channels can be used when $K \geq M - N$). Let $\hat{\mathbf{s}}^q_{\mathcal{K}} = \begin{bmatrix} \hat{\mathbf{s}}^q_{\mathcal{U}} \\ \hat{s}^q_{k_{(M)}} \end{bmatrix}$. As a result, the Q candidate hard decision vectors $\{\hat{\mathbf{s}}^1_{\mathcal{K}}, \hat{\mathbf{s}}^2_{\mathcal{K}}, \ldots, \hat{\mathbf{s}}^Q_{\mathcal{K}}\}$ can be obtained.

e) From the candidates $\{\hat{\mathbf{s}}^1_{\mathcal{K}}, \hat{\mathbf{s}}^1_{\mathcal{K}}, \ldots, \hat{\mathbf{s}}^Q_{\mathcal{K}}\}$, obtain the final hard decision vector $\mathbf{s}_{\mathcal{K}}$ that best represents the observation vector $\mathbf{y}$ in the sense of the sum of squared error (SSE) as

$$\hat{\mathbf{s}}_{\mathcal{K}} = \arg \min_{\hat{\mathbf{s}}^q_{\mathcal{K}} \in \{\hat{\mathbf{s}}^1_{\mathcal{K}}, \ldots, \hat{\mathbf{s}}^Q_{\mathcal{K}}\}} \| \mathbf{y} - \mathbf{H}_{\mathcal{K}} \hat{\mathbf{s}}^q_{\mathcal{K}} \|^2 . \tag{2.26}$$

Since a linear detector to obtain a list of candidate vectors for $s_{k_{(M)}}$ suffers from the interference, a good performance cannot be achieved with the Chase detector. In order to improve the performance by mitigating the impact from the interference, a class of QR factorization-based Chase detection is considered. However, it can not be used for underdetermined MIMO systems when $M > N$.

Assume that the channel matrix $\mathbf{H}_{\mathcal{K}}$ is square and sized $M \times M$. Using the QR factorization $\mathbf{H}_{\mathcal{K}} = \mathbf{QR}$ (i.e., $M \times M$ matrices $\mathbf{Q}$ and $\mathbf{R}$ are unitary and upper triangular, respectively), from (2.23), we have $\mathbf{x} = \mathbf{Q}^{\mathrm{H}}\mathbf{y} = \mathbf{R}\mathbf{s}_{\mathcal{K}} + \mathbf{n}$. Let $\mathbf{x} = \left[\mathbf{x}_1^{\mathrm{T}}\ x_2^{\mathrm{T}}\right]^{\mathrm{T}}$ and $\mathbf{n} = \left[\mathbf{n}_1^{\mathrm{T}}\ n_2^{\mathrm{T}}\right]^{\mathrm{T}}$ (i.e., $\mathbf{x}_1$ and $\mathbf{n}_1$ are $(M-1) \times 1$ sub-vectors of $\mathbf{x}$ and $\mathbf{n}$, respectively), $\mathbf{x}$ is rewritten as

$$\begin{bmatrix} \mathbf{x}_1 \\ x_2 \end{bmatrix} = \begin{bmatrix} \mathbf{A} & \mathbf{C} \\ 0 \cdots 0 & r_{M,M} \end{bmatrix} \begin{bmatrix} \mathbf{s}_{\mathcal{U}} \\ s_{k_{(M)}} \end{bmatrix} + \begin{bmatrix} \mathbf{n}_1 \\ n_2 \end{bmatrix}, \tag{2.27}$$

where sub-matrix $\mathbf{A}$ of sized $(M-1) \times (M-1)$ is triangular from $\mathbf{R}$ and $r_{M,M}$ represents the (M,M)-th entry of $\mathbf{R}$.

Based on the system model in (2.27), the QR factorization-based Chase detection is summarized as follows [14]:

a) Generate a list of Q candidate values for $s_{k_{(M)}}$, say $\{\hat{s}^1_{k_{(M)}}, \hat{s}^2_{k_{(M)}}, \ldots, \hat{s}^Q_{k_{(M)}}\}$, where $Q \leq |\mathcal{S}|$ and $\hat{s}^q_{k_{(M)}}$ denotes the qth closest symbol to $\hat{x}_2$, $q = 1, 2, \ldots, Q$. Here, $\hat{x}_2 = r^{-1}_{M,M} x_2$.

b) By canceling the contribution of the symbol vector $\hat{s}_{k_{(M)}}$ to $\mathbf{x}_1$ using each candidate of $\hat{s}_{k_{(M)}}$ in the list, a set of Q residual vectors $\{\hat{\mathbf{x}}^1_1, \hat{\mathbf{x}}^2_1, \ldots, \hat{\mathbf{x}}^Q_1\}$ is generated as

$$\hat{\mathbf{x}}^q_1 = \mathbf{x}_1 - \mathbf{C}\hat{s}^q_{k_{(M)}}. \tag{2.28}$$

c) Apply an independent subdetector for each $\hat{\mathbf{x}}^q_1$ and obtain decision of the remaining $M-1$ symbols $\{\hat{\mathbf{s}}^1_{\mathcal{U}}, \hat{\mathbf{s}}^2_{\mathcal{U}}, \ldots, \hat{\mathbf{s}}^Q_{\mathcal{U}}\}$. Let $\hat{\mathbf{s}}^q_{\mathcal{K}} = \begin{bmatrix} \hat{\mathbf{s}}^q_{\mathcal{U}} \\ \hat{s}^q_{k_{(M)}} \end{bmatrix}$. As a result, the Q candidate hard decision vectors $\{\hat{\mathbf{s}}^1_{\mathcal{K}}, \hat{\mathbf{s}}^2_{\mathcal{K}}, \ldots, \hat{\mathbf{s}}^Q_{\mathcal{K}}\}$ can be obtained.

d) From the candidates $\{\hat{\mathbf{s}}^1_{\mathcal{K}}, \hat{\mathbf{s}}^1_{\mathcal{K}}, \ldots, \hat{\mathbf{s}}^Q_{\mathcal{K}}\}$, obtain the final hard decision vector $\mathbf{s}_{\mathcal{K}}$ that best represents the observation vector $\mathbf{x}$ in the sense of the SSE as

$$\hat{\mathbf{s}}_{\mathcal{K}} = \arg \min_{\hat{\mathbf{s}}^q_{\mathcal{K}} \in \{\hat{\mathbf{s}}^1_{\mathcal{K}}, \ldots, \hat{\mathbf{s}}^Q_{\mathcal{K}}\}} \| \mathbf{x} - \mathbf{R}\hat{\mathbf{s}}^q_{\mathcal{K}} \|^2 . \tag{2.29}$$

With the Chase detector, a low-complexity can be obtained with a small list length Q. The performance of above detection highly depends on the reliability of detected $s_{k_{(M)}}$.

2.2.2 Ordering

In order to avoid an error propagation, the first symbol $s_{k_{(M)}}$ should be properly selected.

For the linear filter-based Chase detector, a simply strategy to choose $s_{k_{(M)}}$ is based on the maximum SINR or MSE, which is shown as

$$k_{(M)} = \arg \min_{\hat{k}_{(M)} \in \{1, \ldots, M\}} E\left[s_{\hat{k}_{(M)}} - \mathbf{w}^{\mathrm{H}}_{\hat{k}_{(M)}} \mathbf{y} \right], \tag{2.30}$$

where $k_{(M)}$ denotes the index of the first detected symbol that has the smallest MSE and $\mathbf{w}_{\hat{k}_{(M)}}$ denotes its corresponding linear filter represented in step *b*) of the linear filter-based Chase detection.

Note that although a correct detection for the first symbol (first layer detection) is highly guaranteed with maximizing SINR, the performance of the sub-detection on reduced size sub-matrix (second layer detection) is not considered. In this case, a trade-off between the performance of the first and second layer detection is discussed in [13]. In [14], the S-Chase detector is proposed to improve the performance with reordering columns of matrix $\mathbf{H}_{\mathcal{K}}$ as

1) $\mathcal{M} = \{1, 2, \ldots, M\}$

2) if $Q > \frac{3|\mathcal{S}|}{4}$

3) $\quad p = -1$

4) else

5) $\quad p = 1$

6) end

7) for $i = 1$ to M

8) $k_{(i)} = \arg\max_{k=1,\ldots,\text{size}(\mathcal{M})} \| \mathbf{h}_k \|^p$

9) $\mathcal{M} = \mathcal{M} \setminus k_{(i)}$

10) end

For the QR factorization-based Chase detection, we can rewrite that $\mathbf{H}_{\mathcal{K}} = \mathbf{Q}_{\mathcal{K}}\mathbf{R}_{\mathcal{K}}$. Define the effective SNR gain, G_Q (which is illustrated in the next subsection), with respects to list length Q, the SNR of the first detected symbol, $s_{k_{(M)}}$, and the remaining $M-1$ symbols become

$$\text{SNR}_M^{\mathcal{K}} = \frac{G_Q |r_{M,M}^{\mathcal{K}}|^2}{N_0} \tag{2.31}$$

and

$$\text{SNR}_m^{\mathcal{K}} = \frac{|r_{m,m}^{\mathcal{K}}|^2}{N_0}, \quad m \in \{1, 2, \ldots, M-1\}, \tag{2.32}$$

respectively. Here, $r_{M,M}^{\mathcal{K}}$ and $r_{m,m}^{\mathcal{K}}$ represent the Mth and mth diagonal elements of $\mathbf{R}_{\mathcal{K}}$, respectively. According to the SNR, two strategies of ordering are carried out, namely B-Chase ordering [13] and BLAST ordering [45, 46].

With the B-Chase algorithm, the CRIS is found by maximizing the minimum SNR, which is shown as follows:

$$\mathcal{K} = \arg\max_{\hat{\mathcal{K}}} \min \left\{ \text{SNR}_1^{\hat{\mathcal{K}}}, \text{SNR}_2^{\hat{\mathcal{K}}}, \ldots, \text{SNR}_M^{\hat{\mathcal{K}}} \right\}, \tag{2.33}$$

where $\hat{\mathcal{K}}$ represents a permutation of $\{1, 2, \ldots, M\}$. Since there are $M!$ possible permutation CRIS, the computational complexity cost by B-Chase ordering could be high. Furthermore, when $Q = 1$ is considered with the B-Chase ordering, it becomes the conventional BLAST ordering since there is no SNR gain enjoyed for the detection of the first symbol and $G_1 = 1$.

2.2.3 Performance Analysis

For the list detection, the performance can be improved with a larger list length Q due to a higher possibility of successive cancellation is considered for the first symbol. Note that a larger Q leads to a higher computational complexity for detection.

Let d_Q denote the distance from the transmitted symbol to the nearest decision boundary when a length Q list detection is considered. In order to estimate the performance with the impact of the list length, in [13, 47], the effective SNR gain of the length Q list detection is considered and given by

$$G_Q = \left(\frac{d_Q}{d_1}\right)^2. \tag{2.34}$$

Denote by $s = |a|e^{j\omega}$ the transmitted symbol with 4-QAM as its modulation method, where $\omega \in \{\pm\frac{\pi}{4}, \pm\frac{3\pi}{4}\}$. Suppose that $s = e^{j\frac{\pi}{4}}$ is transmitted. With the list length $Q = 1$, the decision region of list detection becomes the conventional decision region, where $|\omega - \frac{\pi}{4}| < \frac{\pi}{4}$. Then, we can have $d_1 = \frac{1}{\sqrt{2}}$. With $Q = 2$, the successive list detection in above happens when $|\omega - \frac{\pi}{4}| < \frac{\pi}{2}$, where $d_2 = 1$. Therefore, compare to the conventional detection ($Q = 1$), the length $Q = 2$ list detection can provide an effective SNR gain of $G_2 = \left(\frac{d_2}{d_1}\right)^2 = 2$. Similarly, since the same minimum distance from transmitted symbol to decision boundary is considered for $Q = 2$ and $Q = 3$, we can show that $G_3 = 2$.

Using the same strategy, [13, 47] shows that for 16-QAM, we have $G_2 = 2$, $G_3 = 2$, $G_8 = 8$, and $G_{10} = 10$; for 64-QAM, we have $G_4 = 4$, $G_8 = 8$, $G_{18} = 20$, $G_{33} = 40$, and $G_{48} = 58$. It is noteworthy that for the cases of $Q = 1$ (conventional detection) and $Q = |\mathcal{S}|$ (full length), the SNR gain leads to $G_1 = 1$ and $G_{|\mathcal{S}|} = \infty$, respectively, since there would be no decision boundary for the case of full length. Although the decision regions based SNR gain is considered as an approximate performance metric, as shown in [47], it provides an accurate result to a certain extend (for an error probability of 0.01, it is accurate within 1 dB for a 16-QAM list detector with $Q \in \{1, \ldots, 9\}$ and for a 64-QAM list detector with $Q \in \{1, \ldots, 41\}$).

The correlation between list length and SNR gain is further analyzed by Liu, Ling, and Stehlé in [48]. By viewing the channel matrix as a basis for a lattice,

a list of candidate lattice points is built up, where the closest lattice point is found to perform the list-based detection. Taking the real-valued channel matrix transformation (as shown in (2.46)), the channel matrix in (2.23) is generated as a $n \times m$ real-valued matrix and [48] shows that

$$Q = \left(\frac{8em}{G_Q}\right)^{G_Q/4}, \quad G_Q < 8m. \tag{2.35}$$

It represents the relation between G_Q and Q. Furthermore, in order to achieve a near-ML performance, one can be found in [48] that the list length follows

$$Q = (e\rho_0)^{2m/\rho_0} \tag{2.36}$$

under the condition that

$$\text{PF} \approx G_Q = \frac{8m}{\rho_0}, \quad \rho_0 > 1, \tag{2.37}$$

where PF denotes the proximity factor in [49].

The computational complexity of Chase detection depends on the ordering, the list length, and the sub-detection methods. Without taking account of the ordering, the computational complexity of Chase detection is linearly proportional to the list length Q under the condition that an actual sub-detector is employed. Nevertheless, the complexity is mainly affected by the type of the sub-detector.

Denote by C_{sub} and C_{sel} the complexity of the sub-detector (e.g., ML, MMSE, and MMSE-SIC) employed for the list detection and the complexity of the ordering, respectively. The overall complexity of Chase detection is given by

$$C_{\text{chase}} = QC_{\text{sub}} + C_{\text{sel}}. \tag{2.38}$$

Depending on different applications, we can choose different sub-detectors for list detection (ML is used for good performance and MMSE is used for low complexity), where the complexity and performance trade-off need to be considered. We should also note that the list-based detection can not provide a full receive diversity, which is illustrated through the simulation results.

2.2.4 Simulation Results

In Figs. 2.3 and 2.4, we show the BER performance of the various detectors in 2×2 and 4×4 uncoded MIMO systems, respectively. We use 16-QAM for signaling. Note that the ZF-SIC detector is used as the subdetector for the linear filter-based Chase detection, where the S-Chase is carried out to perform a symbol ordering. In general, it shows that the Chase detection has a significant performance improvement compared to conventional suboptimal detectors (e.g., ZF detector or ZF-SIC detector). In Fig. 2.3, we can show that the Chase detection with $Q = 4$ provides a sufficiently good performance compared to the ML detection. Fig. 2.4 shows that the Chase detection is not suitable to be employed in a large MIMO system, since there is a big gap compared to the ML performance. It is also noteworthy that the Chase detection can not exploit a full receive diversity.

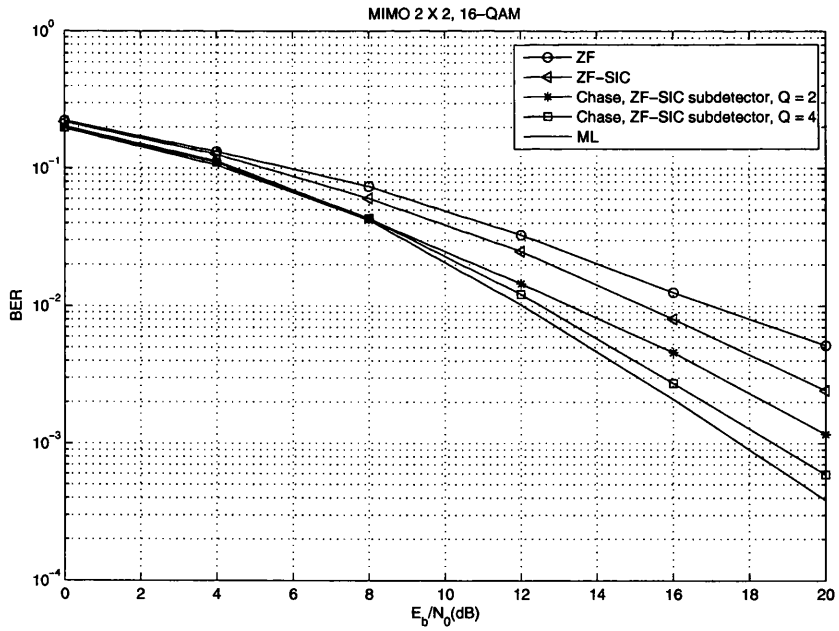

Figure 2.3: BER performance of different detectors in a 16-QAM 2×2 MIMO system.

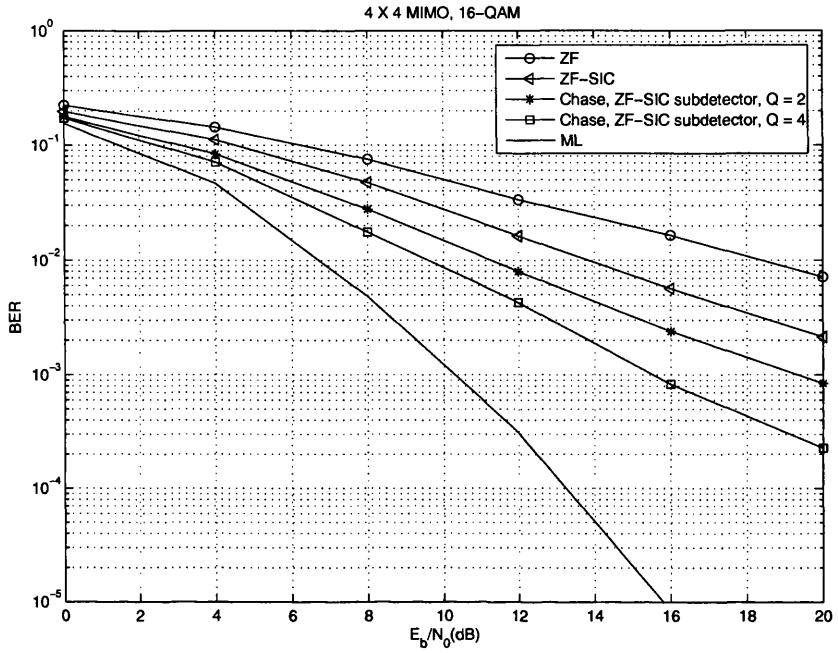

Figure 2.4: BER performance of different detectors in a 16-QAM 4×4 MIMO system.

2.2.5 Conclusion and Remarks

In this section, we introduced the list-based Chase detection for MIMO systems. It has been shown that the performance of conventional suboptimal detectors (e.g., ZF and ZF-SIC detectors) can be improved by using the list-based techniques. However, the Chase detector can not exploit a full receive diversity, especially when a large MIMO system is considered (i.e., more layers of interference).

2.3 Lattice Reduction based Detection

In this section, we introduce the LR-based detection [19, 20, 21, 22, 23, 24, 25, 26] for MIMO systems. Conventionally, the LLL algorithm [18] is developed to transform a basis to a near-orthogonal one. Taking the channel matrix as a basis for a lattice, using the LLL algorithm, LR-based detectors have been proposed

for MIMO systems.

2.3.1 MIMO Systems with Lattice

Consider a basis $\mathbf{B}$ consists of M real valued linearly independent basis vectors which is given by

$$\mathbf{B} = \{\mathbf{b}_1, \mathbf{b}_2, \ldots, \mathbf{b}_M\}. \tag{2.39}$$

Since a lattice can be generated from an integer linear combination of a basis, with $\mathbf{B}$, we can have a lattice defined by

$$\mathbf{\Lambda} = \left\{ \mathbf{u} | \mathbf{u} = \sum_{m=1}^{M} \mathbf{b}_m z_m, \ z_m \in \mathbb{Z} \right\}, \tag{2.40}$$

where $\mathbb{Z}$ denotes the set of integer numbers. Note that a lattice can be generated by different bases or matrices.

Denote by $\mathbf{H}$ and $\mathbf{G}$ two bases that generate the same lattice, where each column vector of a basis is an integer linear combination of the column vectors of the other basis. For example, consider that

$$\mathbf{H} = \begin{bmatrix} 2 & 1 \\ 1 & 1 \end{bmatrix} \tag{2.41}$$

and

$$\mathbf{G} = \begin{bmatrix} 1 & 0 \\ 0 & 1 \end{bmatrix}. \tag{2.42}$$

We can easily show that

$$\begin{bmatrix} 2 \\ 1 \end{bmatrix} = 2 \times \begin{bmatrix} 1 \\ 0 \end{bmatrix} + \begin{bmatrix} 0 \\ 1 \end{bmatrix} \tag{2.43}$$

and

$$\begin{bmatrix} 1 \\ 1 \end{bmatrix} = \begin{bmatrix} 1 \\ 0 \end{bmatrix} + \begin{bmatrix} 0 \\ 1 \end{bmatrix}. \tag{2.44}$$

Thus, bases $\mathbf{H}$ and $\mathbf{G}$ have the same lattice. It is also shown that

$$\mathbf{G} = \mathbf{HU}, \tag{2.45}$$

where $\mathbf{U}$ is an unimodular matrix.

By viewing the received signal as the lattice points spanned by the basis (i.e., a channel matrix), MIMO systems with lattice are developed.

Consider the system model of MIMO channels represented in (2.2). For convenience, in this section, we assume that the channel matrix $\mathbf{H}$ is square of sized $M \times M$. Although the LR can be performed with a complex-valued $\mathbf{H}$ as in [23, 24, 25] or a real-valued which is converted from $\mathbf{H}$ as in [19, 22], there is no performance difference shown in [23, 25]. In general, the LR with a complex-valued $\mathbf{H}$ is suitable for performance analysis, while that with a real-valued $\mathbf{H}$ is convenient to introduce the system. In this and next subsection, we use the real-valued channel matrix to introduce the MIMO system with lattice. Taking the real-valued channel matrix transformation, (2.2) can be written as

$$\begin{bmatrix} \Re(\mathbf{y}) \\ \Im(\mathbf{y}) \end{bmatrix} = \begin{bmatrix} \Re(\mathbf{H}) & -\Im(\mathbf{H}) \\ \Im(\mathbf{H}) & \Re(\mathbf{H}) \end{bmatrix} \begin{bmatrix} \Re(\mathbf{s}) \\ \Im(\mathbf{s}) \end{bmatrix} + \begin{bmatrix} \Re(\mathbf{n}) \\ \Im(\mathbf{n}) \end{bmatrix}, \tag{2.46}$$

where $\Re(.)$ and $\Im(.)$ denote the real and imaginary parts operation, respectively. Furthermore, we define that the real-valued vectors and matrix as $\mathbf{y}_r = \left[\Re(\mathbf{y})^{\mathrm{T}}\ \Im(\mathbf{y})^{\mathrm{T}}\right]^{\mathrm{T}}$, $\mathbf{s}_r = \left[\Re(\mathbf{s})^{\mathrm{T}}\ \Im(\mathbf{s})^{\mathrm{T}}\right]^{\mathrm{T}}$, $\mathbf{n}_r = \left[\Re(\mathbf{n})^{\mathrm{T}}\ \Im(\mathbf{n})^{\mathrm{T}}\right]^{\mathrm{T}}$, and $\mathbf{H}_r = \begin{bmatrix} \Re(\mathbf{H}) & -\Im(\mathbf{H}) \\ \Im(\mathbf{H}) & \Re(\mathbf{H}) \end{bmatrix}$. Then, (2.46) is written as

$$\mathbf{y}_r = \mathbf{H}_r \mathbf{s}_r + \mathbf{n}_r. \tag{2.47}$$

Suppose that A-QAM is used as the modulation method for $\mathbf{s}$, we can show that

$$\mathcal{S} = \left\{ a + jb | a, b \in \{-\sqrt{A}+1, -\sqrt{A}+3, \ldots, -1, 1, \ldots, \sqrt{A}-3, \sqrt{A}-1\} \right\} \tag{2.48}$$

and $\mathbf{s} \in \mathcal{S}^M$. Here, the symbol energy is represented by $E_s = \frac{2(A-1)}{3}$. Thus, with a proper scaling and transformation, we can have the real-valued transmit symbol vector $\mathbf{s}_r \in \mathbb{Z}^{2M}$.

By taking the real-valued channel matrix $\mathbf{H}_r$ as a basis of lattice, according to the definition in (2.40), the lattice and its applications can be applied to MIMO systems.

2.3.2 Lattice Reduction based MIMO Detection

Since a lattice can be generated by different bases or channel matrices, in order to mitigate the interference between multiple signals, we can find a matrix whose column vectors are nearly orthogonal to generate the same lattice. This technique is regarded as the LR. LR can be applied to MIMO systems, where the resulting detection methods are regarded as the LR-based MIMO detection [19, 20, 21, 22, 23, 24, 25, 26]. In this subsection, we study the LR-based detection for MIMO systems.

Consider that real-valued matrix $\mathbf{H}_r$ and $\mathbf{G}_r$ span the same lattice, according to (2.45), we have

$$\mathbf{H}_r = \mathbf{G}_r \mathbf{U}_r, \tag{2.49}$$

where $\mathbf{U}_r$ is unimodular. From (2.47), we can show that

$$\mathbf{y}_r = \mathbf{G}_r \mathbf{U}_r \mathbf{s}_r + \mathbf{n}_r = \mathbf{G}_r \mathbf{c}_r + \mathbf{n}_r, \tag{2.50}$$

where $\mathbf{c}_r = \mathbf{U}_r \mathbf{s}_r$. With the unimodular matrix $\mathbf{U}_r$ which consists of integers, we have $\mathbf{c}_r \in \mathbb{Z}^{2M}$.

Here, the LLL algorithm can be employed to generate $\mathbf{G}_r$ from $\mathbf{H}_r$, which will be introduced in the next subsection. The matrix generated by the LLL algorithm is regarded as the lattice reduced matrix.

Based on (2.50), conventional low complexity detectors (e.g., linear detector and MMSE-SIC detector) are able to be carried out to detect $\mathbf{c}_r$. Note that although the ML detection can be applied to the lattice reduced matrices, there is no performance gain due to an exhaustive search is carried out.

The LR-based linear detectors [22] are carried out to detect $\mathbf{c}_r$ as

$$\hat{\mathbf{c}}_r = \lfloor \mathbf{W}_r^{\mathrm{H}} \mathbf{y}_r \rceil, \tag{2.51}$$

where the linear filter $\mathbf{W}_r = \mathbf{G}_r \left(\mathbf{G}_r \mathbf{G}_r^{\mathrm{H}}\right)^{-1}$ for the LR-based ZF detector and $\mathbf{W}_r = \left(\mathbf{G}_r \mathbf{G}_r^{\mathrm{H}} + \frac{N_0}{E_s}\mathbf{I}\right)^{-1} \mathbf{G}_r$ for the LR-based MMSE detection. Here, $\lfloor . \rceil$ denotes the rounding operation. From $\hat{\mathbf{c}}_r$, the estimation of $\mathbf{s}_r$ is given by

$$\hat{\mathbf{s}}_r = \mathbf{U}_r^{-1} \hat{\mathbf{c}}_r. \tag{2.52}$$

For the LR-based MMSE-SIC detector [23], the system represented in (2.47) is rewritten as

$$\begin{bmatrix} \mathbf{y}_r \\ \mathbf{0} \end{bmatrix} = \begin{bmatrix} \mathbf{H}_r \\ \sqrt{\frac{N_0}{E_s}}\mathbf{I}_{2N} \end{bmatrix} \mathbf{s}_r + \begin{bmatrix} \mathbf{n}_r \\ -\sqrt{\frac{N_0}{E_s}}\mathbf{s}_r \end{bmatrix}, \tag{2.53}$$

where $\tilde{\mathbf{y}}_r = \left[\mathbf{y}_r^{\mathrm{T}}\ \mathbf{0}\right]^{\mathrm{T}}$, $\tilde{\mathbf{H}}_r = \left[\mathbf{H}_r^{\mathrm{T}}\ \sqrt{\frac{N_0}{E_s}}\mathbf{I}_{2N}\right]^{\mathrm{T}}$, and $\tilde{\mathbf{n}}_r = \left[\mathbf{n}_r^{\mathrm{T}}\ -\sqrt{\frac{N_0}{E_s}}\mathbf{s}_r^{\mathrm{T}}\right]^{\mathrm{T}}$. Using the LLL algorithm with $\tilde{\mathbf{H}}_r$, the lattice reduced matrix $\tilde{\mathbf{G}}_r$ can be found as $\tilde{\mathbf{H}}_r = \tilde{\mathbf{G}}_r\tilde{\mathbf{U}}_r$, where $\tilde{\mathbf{U}}_r$ is unimodular. Then, (2.53) is rewritten as

$$\tilde{\mathbf{y}}_r = \tilde{\mathbf{G}}_r\tilde{\mathbf{c}}_r + \tilde{\mathbf{n}}_r, \tag{2.54}$$

where $\tilde{\mathbf{c}}_r = \tilde{\mathbf{U}}_r\mathbf{s}_r$.

Using the QR factorization of $\tilde{\mathbf{G}}_r = \tilde{\mathbf{Q}}_r\tilde{\mathbf{R}}_r$, the LR-based MMSE-SIC detection is carried out, where $\tilde{\mathbf{Q}}_r$ and $\tilde{\mathbf{R}}_r$ are unitary and upper triangular matrices, respectively. Multiplying $\tilde{\mathbf{Q}}_r^{\mathrm{H}}$ to $\tilde{\mathbf{y}}_r$ in (2.54), we can have

$$\tilde{\mathbf{Q}}_r^{\mathrm{H}}\tilde{\mathbf{y}}_r = \tilde{\mathbf{R}}_r\tilde{\mathbf{c}}_r + \tilde{\mathbf{n}}_r. \tag{2.55}$$

Since $\tilde{\mathbf{Q}}_r^{\mathrm{H}}\tilde{\mathbf{n}}_r$ has the same statistical property as $\tilde{\mathbf{n}}_r$, we use $\tilde{\mathbf{n}}_r$ to denote $\tilde{\mathbf{Q}}_r^{\mathrm{H}}\tilde{\mathbf{n}}_r$. Then, the MMSE-SIC detection represented in previous section is employed in (2.55) to estimate $\tilde{\mathbf{c}}_r$.

2.3.3 LLL and CLLL Algorithms

In order to find a matrix whose column vectors are nearly orthogonal to generate the same lattice, the LLL algorithm is proposed in [18]. Note that the conventional LLL algorithm is performed with a real-valued matrix which is transformed from a complex-valued matrix using the method in (2.46).

Suppose that a real-valued matrix $\mathbf{G}_r$ is generated from the $2M \times 2M$ matrix $\mathbf{H}_r$ in (2.49) using the LLL algorithm, where $\mathbf{H}_r$ is transformed from an $M \times M$ complex-valued matrix $\mathbf{H}$ using the method in (2.46). Then, $\mathbf{G}_r$ of sized $2M \times 2M$ is named LLL-reduced matrix [18] if $\mathbf{G}_r$ is QR factorized as

$$\mathbf{G}_r = \mathbf{Q}_r\mathbf{R}_r, \tag{2.56}$$

where $\mathbf{Q}_r$ of sized $2M \times 2M$ is an unitary matrix ($\mathbf{Q}_r^{\mathrm{T}}\mathbf{Q}_r = \mathbf{I}_N$) and $\mathbf{R}_r$ of sized $2M \times 2M$ is an upper triangular matrix. The elements of $\mathbf{R}_r$ satisfies the following inequalities:

$$| [\mathbf{R}_r]_{\ell,\rho} | \leq \frac{1}{2} | [\mathbf{R}_r]_{\ell,\ell} | \quad \text{with} \quad 1 \leq \ell < \rho \leq 2M \tag{2.57}$$

and

$$\delta[\mathbf{R}_r]^2_{\rho-1,\rho-1} \leq [\mathbf{R}_r]^2_{\rho,\rho} + [\mathbf{R}_r]^2_{\rho-1,\rho} \quad \text{with} \quad \rho = 2, \ldots, 2M, \tag{2.58}$$

where $[\mathbf{R}_r]_{p,q}$ denotes the (p,q)-th entry of $\mathbf{R}_r$. The parameter δ is closely related to a quality-complexity trade-off [18]. Note that for the real-valued LLL and complex-valued LLL algorithms, δ can be chosen from $(\frac{1}{4}, 1)$ and $(\frac{1}{2}, 1)$, respectively [25]. Normally, we define that $\delta = \frac{3}{4}$ to meet a good quality-complexity trade-off.

In order to generate the real-valued channel matrix $\mathbf{H}_r$ to a lattice reduced matrix $\mathbf{G}_r$, the LLL algorithm [18, 22] is summarized as follows, where the input and output are given by $\{\mathbf{H}_r\}$ and $\{\mathbf{Q}_r, \mathbf{R}_r, \mathbf{U}_r\}$, respectively.

INPUT: $\{\mathbf{H}_r\}$

OUTPUT $\{\mathbf{Q}_r, \mathbf{R}_r, \mathbf{U}_r\}$

1) $[\mathbf{Q}_r\ \mathbf{R}_r] \leftarrow \mathrm{qr}(\mathbf{H}_r)$

2) $\zeta \leftarrow \mathrm{size}(\mathbf{H}_r, 2)$

3) $\mathbf{U}_r \leftarrow \mathbf{I}_\zeta$

4) while $\rho \leq \zeta$

5) for $\ell = 1 : \rho - 1$

6) $\mu \leftarrow \lceil \mathbf{R}_r(\rho - \ell, \rho) / \mathbf{R}_r(\rho - \ell, \rho - \ell) \rfloor$

7) if $\mu \neq 0$

8) $\mathbf{R}_r(1 : \rho - \ell, \rho) \leftarrow \mathbf{R}_r(1 : \rho - \ell, \rho) - \mu \mathbf{R}_r(1 : \rho - \ell, \rho - \ell)$

9) $\mathbf{U}_r(:, \rho) \leftarrow \mathbf{U}_r(:, \rho) - \mu \mathbf{U}_r(:, \rho - \ell)$

10) end if

11) end for

12) if $\delta(\mathbf{R}_r(\rho-1,\rho-1))^2 > \mathbf{R}_r(\rho,\rho)^2 + \mathbf{R}_r(\rho-1,\rho)^2$

13) Swap the $(\rho-1)$-th and ρth columns in $\mathbf{R}_r$ and $\mathbf{U}_r$

14) $\boldsymbol{\Theta} = \begin{bmatrix} \alpha & \beta \\ -\beta & \alpha \end{bmatrix}$ with $\begin{matrix} \alpha = \frac{\mathbf{R}_r(\rho-1,\rho-1)}{\|\mathbf{R}_r(\rho-1:\rho,\rho-1)\|} \\ \beta = \frac{\mathbf{R}_r(\rho,\rho-1)}{\|\mathbf{R}_r(\rho-1:\rho,\rho-1)\|} \end{matrix}$

15) $\mathbf{R}_r(\rho-1:\rho,\rho-1:\zeta) \leftarrow \boldsymbol{\Theta}\mathbf{R}_r(\rho-1:\rho,\rho-1:\zeta)$

16) $\mathbf{Q}_r(:,\rho-1:\rho) \leftarrow \mathbf{Q}_r(:,\rho-1:\rho)\boldsymbol{\Theta}^{\mathrm{T}}$

17) $\rho \leftarrow \max\{\rho-1, 2\}$

18) else

19) $\rho \leftarrow \rho+1$

20) end if

21) end while

With the unimodular matrix $\mathbf{U}_r$, linear detectors or SIC detector can be employed with the LLL-reduced matrix $\mathbf{G}_r = \mathbf{H}_r\mathbf{U}_r$ to perform the LR-based detection. In [23, 25], the complex-valued LLL (CLLL) is proposed which can straightforwardly perform the LR on the complex-valued matrix with no extra transformation required. It shows that compared to the LLL, the CLLL can provide the same performance with a half complexity, approximately. Therefore, it is desired to consider the CLLL for LR-based detection with a reduced complexity.

Consider a complex-valued matrix $\mathbf{G}$ generated from an $M \times M$ matrix $\mathbf{H}$ using the CLLL algorithm. With the QR factorization of $\mathbf{G} = \mathbf{QR}$, where $\mathbf{Q}$ is unitary and $\mathbf{R}$ is upper triangular, $\mathbf{G}$ is CLLL-reduced if the elements of $\mathbf{R}_{(m)}$ satisfy the following inequalities [25]:

$$| \Re([\mathbf{R}]_{\ell,\rho}) | \leq \frac{1}{2} | [\mathbf{R}]_{\ell,\ell} | \quad \text{and} \quad | \Im([\mathbf{R}]_{\ell,\rho}) | \leq \frac{1}{2} | [\mathbf{R}]_{\ell,\ell} | \quad \text{for} \quad 1 \leq \ell < \rho \leq M \tag{2.59}$$

and

$$\delta|[\mathbf{R}]_{\rho-1,\rho-1}|^2 \leq |[\mathbf{R}]_{\rho,\rho}|^2 + |[\mathbf{R}]_{\rho-1,\rho}|^2 \quad \text{for} \quad \rho = 2, \ldots, M. \tag{2.60}$$

Here, $[\mathbf{R}]_{p,q}$ denotes the (p,q)-th entry of $\mathbf{R}$. Let $\delta \in (\frac{1}{2}, 1)$, the CLLL algorithm [23, 25] is summarized as follows, where the input and output are given by $\{\mathbf{H}\}$ and $\{\mathbf{Q}, \mathbf{R}, \mathbf{U}\}$, respectively.

INPUT: $\{\mathbf{H}\}$

OUTPUT $\{\mathbf{Q}, \mathbf{R}, \mathbf{U}\}$

1) $[\mathbf{Q}\ \mathbf{R}] \leftarrow \mathrm{qr}(\mathbf{H})$

2) $\zeta \leftarrow \mathrm{size}(\mathbf{H}, 2)$

3) $\mathbf{U} \leftarrow \mathbf{I}_\zeta$

4) while $\rho \leq \zeta$

5) for $\ell = 1 : \rho - 1$

6) $\mu \leftarrow \lceil \mathbf{R}(\rho - \ell, \rho) / \mathbf{R}(\rho - \ell, \rho - \ell) \rfloor$

7) if $\mu \neq 0$

8) $\mathbf{R}(1 : \rho - \ell, \rho) \leftarrow \mathbf{R}(1 : \rho - \ell, \rho) - \mu \mathbf{R}(1 : \rho - \ell, \rho - \ell)$

9) $\mathbf{U}(:, \rho) \leftarrow \mathbf{U}_r(:, \rho) - \mu \mathbf{U}(:, \rho - \ell)$

10) end if

11) end for

12) if $\delta|(\mathbf{R}(\rho - 1, \rho - 1))|^2 > |\mathbf{R}(\rho, \rho)|^2 + |\mathbf{R}(\rho - 1, \rho)|^2$

13) Swap the $(\rho - 1)$-th and ρth columns in $\mathbf{R}$ and $\mathbf{U}$

14) $\boldsymbol{\Theta} = \begin{bmatrix} \alpha^* & \beta \\ -\beta & \alpha \end{bmatrix}$ with $\begin{matrix} \alpha = \frac{\mathbf{R}(\rho-1,\rho-1)}{\|\mathbf{R}(\rho-1:\rho,\rho-1)\|} \\ \beta = \frac{\mathbf{R}(\rho,\rho-1)}{\|\mathbf{R}(\rho-1:\rho,\rho-1)\|} \end{matrix}$

15) $\mathbf{R}(\rho - 1 : \rho, \rho - 1 : \zeta) \leftarrow \boldsymbol{\Theta} \mathbf{R}(\rho - 1 : \rho, \rho - 1 : \zeta)$

16) $\quad \mathbf{Q}(:, \rho-1:\rho) \leftarrow \mathbf{Q}(:, \rho-1:\rho)\boldsymbol{\Theta}^{\mathrm{T}}$

17) $\quad \rho \leftarrow \max\{\rho-1, 2\}$

18) else

19) $\quad \rho \leftarrow \rho+1$

20) end if

21) end while

Compared to the LLL algorithm, the differences of the CLLL algorithm are shown as: *a*) the rounding operation at step 6) is carried out with complex numbers; *b*) an absolute operation is carried out at step 12); *c*) the unitary matrix $\boldsymbol{\Theta}$ is computed with complex numbers.

With the complex-valued unimodular matrix $\mathbf{U}$, low-complexity detectors (e.g., linear and MMSE-SIC detectors) are carried out with the CLLL-reduced matrix $\mathbf{G} = \mathbf{HU}$ to estimate $\mathbf{c}$. Note that in order to convert $\mathbf{c}$ to $\mathbf{s}$, a proper scaling and transformation is performed on both real and imaginary parts.

2.3.4 Performance Evaluation

In this subsection, we consider the error probability of the LR-based MIMO detection, where the elements of the complex-valued channel matrix $\mathbf{H}$ are independent and $\sim \mathcal{CN}(0,1)$, i.e., Rayleigh MIMO channels.

We can quantify the orthogonality of an $M \times M$ matrix $\mathbf{H}$ using the following metric [25].

The *orthogonality deficiency* $\eth_M$ of an $M \times M$ matrix $\mathbf{H} = [\mathbf{h}_1, \ldots, \mathbf{h}_M]$ is defined as

$$\eth_M(\mathbf{H}) = 1 - \frac{\det\left(\mathbf{H}^{\mathrm{H}}\mathbf{H}\right)}{\prod_{i=1}^{M} \|\mathbf{h}_i\|}. \tag{2.61}$$

The LR can find a new basis of the channel matrix that is more orthogonal (or less orthogonality deficiency) than the original channel matrix. Then, the system from (2.2) can be written as

$$\mathbf{y} = \mathbf{GUs} + \mathbf{n}, \tag{2.62}$$

where $\mathbf{U}$ is unimodular. From the work by Ma and Zhang [25], we can find that

$$\sqrt{1-\eth_M(\mathbf{G})} \geq 2^{\frac{M}{2}} \left(\frac{2}{2\delta-1}\right)^{-\frac{M(M+1)}{4}} \tag{2.63}$$

for both real and complex LLL-LR. Define $c_\delta := 2^{\frac{M}{2}} \left(\frac{2}{2\delta-1}\right)^{-\frac{M(M+1)}{4}}$. Then, after the LLL-LR, $\eth_M(\mathbf{G})$ is bounded by $1-c_\delta^2$.

Now we derive the error probability, $P_{e,\mathrm{LR}}$, for the LR-based linear detection. From [25], the error probability of the LR-based MMSE detector is equivalent to that of the LR-based ZF detector. Hence, for further analysis, we assume that the LR-based ZF detector is used for the MIMO detection. From (2.62), let $\mathbf{x} = \mathbf{G}^\dagger \mathbf{y}$ denote the output of the LR-based ZF detector, where $\mathbf{G}^\dagger$ denotes the pseudoinverse of $\mathbf{G}$. Then, it follows that

$$\mathbf{x} = \mathbf{U}\mathbf{s} + \mathbf{G}^\dagger \mathbf{n}. \tag{2.64}$$

The estimation of $\mathbf{s}$ can be expressed as

$$\hat{\mathbf{s}} = \mathbf{U}^{-1}\lfloor \mathbf{x} \rceil = \mathbf{s} + \mathbf{U}^{-1}\lfloor \mathbf{G}^\dagger \mathbf{n} \rceil. \tag{2.65}$$

Thus, the error probability in detecting $\mathbf{s}$ for given $\mathbf{H}$ is upper bounded by

$$P_{e,\mathrm{LR}|\mathbf{H}} \leq 1 - \Pr\left(\lfloor \mathbf{G}^\dagger \mathbf{n} \rceil = \mathbf{0} \middle| \mathbf{H}\right). \tag{2.66}$$

Let $\mathbf{G}^\dagger = [\hat{g}_1, \ldots, \hat{g}_M]^{\mathrm{T}}$, where $\hat{g}_i^{\mathrm{T}}$, $i = 1, 2, \ldots, M$, denotes the ith row of $\mathbf{G}^\dagger$ and let $\mathbf{G} = [g_1, \ldots, g_M]$, where g_i denotes the ith column of $\mathbf{G}$, and let $\mathbf{h}_{\min}$ represent the vector of the minimum non-zero norm of all the vectors in the lattice generated by $\mathbf{H}_{\mathbb{Q}}$. From (2.63) and the derivation in [25], we have

$$\begin{aligned} P_{e,\mathrm{LR}|\mathbf{H}} &\leq \Pr\left(\max_{1\leq i\leq M} |\hat{g}_i^{\mathrm{T}}\mathbf{n}| \geq \frac{1}{2} \middle| \mathbf{H}\right) \\ &\leq \Pr\left(\frac{\|\mathbf{n}\|}{\sqrt{1-\eth_N(\mathbf{G})}\cdot \min_{1\leq i\leq M}\|g_i\|} \geq \frac{1}{2} \middle| \mathbf{H}\right) \\ &\leq \Pr\left(\|\mathbf{n}\| \geq \frac{1}{2} c_\delta \|\mathbf{h}_{\min}\| \middle| \mathbf{H}\right). \end{aligned} \tag{2.67}$$

We have

$$\begin{aligned} E_{\mathbf{H}}[P_{e,\mathrm{LR}|\mathbf{H}}] &\leq E_{\mathbf{H}}\left[\Pr\left(\|\mathbf{n}\|^2 \geq \frac{1}{2}c_\delta^2\|\mathbf{h}_{\min}\|^2\middle|\mathbf{H}\right)\right] \\ &= E_{\mathbf{n}}\left[\Pr\left(\|\mathbf{h}_{\min}\|^2 \leq \frac{\|\mathbf{n}\|^2}{c_\delta^2/2}\middle|\mathbf{n}\right)\right] \\ &= c_{MM}\left(\frac{2}{c_\delta^2}\right)^M \frac{(2M-1)!}{(M-1)!}\left(\frac{1}{N_0}\right)^{-M}, \end{aligned} \tag{2.68}$$

where c_{MM} and c_δ^2 are constants and $c_\delta < 1$. Thus, the upper bound on $P_{e,\mathrm{LR}|\mathbf{H}}$ in (2.68) results from the M-th moment of Chi-square random variable, $||\mathbf{n}||^2$.

Note that M is also the maximum receive diversity order for the $M \times M$ MIMO system. Thus, a full receive diversity gain can be achieved by the proposed detectors with LR-aided linear detectors. For LR-based SIC detection, it can be deduced from [41] that the bound of its error probability results from the same moment of $||\mathbf{n}||^2$ as the LR-based linear detection.

Another more precise diversity analysis is studied by Gan, Ling, and Mow in [23], where the proximity factor [50] is used to derive the bound of error probability. Define the proximity factors for CLLL-based ZF detection by

$$\rho_{i,\mathrm{ZF}} = \sup \frac{\lambda^2(\mathbf{\Lambda})}{\| \mathbf{g}_i \|^2 \sin^2\theta_i}, \tag{2.69}$$

where sup stands for the supremum that is taken over the CLLL-reduced bases $\mathbf{G}$ and θ_i denotes the angle between $\mathbf{g}_i$ and the linear sub-space spanned by the rest $M-1$ basis vectors. Let $\rho_{\mathrm{ZF}} = \max_{1\leq i\leq M}\rho_{i,\mathrm{ZF}}$, from [50], the error probability of CLLL-based ZF detection with a given SNR is upper bounded as

$$P_e(\mathrm{SNR}) \leq \sum_{i=1}^{M} P_{e,\mathrm{LD}}\left(\frac{\mathrm{SNR}}{\rho_{i,\mathrm{ZF}}}\right) \leq M P_{e,\mathrm{LD}}\left(\frac{\mathrm{SNR}}{\rho_{\mathrm{ZF}}}\right), \tag{2.70}$$

where LD denotes the lattice decoding. Furthermore, *Lemma* 1 in [23] shows that

$$\sin\theta_i \geq \left(\frac{2}{2+\sqrt{2}}\right)^{M-i}\left(\sqrt{\alpha}\right)^{1-n}, \tag{2.71}$$

where $\alpha = \left(\delta - \frac{1}{2}\right)^{-1} \geq 2$. If $M = 2$ and $\delta = 1$, we can have $\rho_{\mathrm{ZF}} \leq 2$, which matches the result derived in [19] (the maximum loss of 3 dB). Using the similar approach, the performance of LR-based SIC detection is also analyzed in

Table 2.1: The average value of column swaps per iteration when the CLLL-based MMSE detector is used for MIMO systems with $N = 8$ and $M = 2, 3, \ldots, 8$.

Average value of column swaps per iteration							
M	2	3	4	5	6	7	8
CLLL	0.2909	0.9029	1.8022	3.0633	4.7711	7.2925	12.1228

[23]. From this, we can point out that the LR-based detection can exploit a full diversity with a countable SNR loss.

In [23, 51, 52], the complexity of CLLL is studied. It is shown that the average complexity of CLLL follows $O\left(M^3 N \log M\right)$. Moreover, the complexity of LR highly depends on the number of column swaps in step 13) of the LLL and CLLL algorithms. In Table 2.1, the average value of column swaps per iteration is shown when the CLLL-based MMSE detector is used for MIMO systems with $N = 8$ and $M = 2, 3, \ldots, 8$.

2.3.5 Simulation Results

In Figs. 2.5 and 2.6, we compare the performance of the CLLL-based detection to conventional detectors for uncoded 2×2 and 4×4 MIMO systems, respectively, where 16-QAM is used for signaling. It shows that the performance of the MMSE detection can be significantly improved by introducing the LR method. For large MIMO systems, the CLLL-based MMSE-SIC detection outperforms the LR-based MMSE detection, since the interference can be mitigated by using the SIC approach, which is illustrated in Fig. 2.6. Furthermore, simulation results show that the CLLL-based detection can exploit a full receive diversity order.

2.3.6 Conclusion and Remarks

In this section, we explained the LR and its application in MIMO detection. It has been shown that the LR can improve the performance of suboptimal detectors (e.g., MMSE and MMSE-SIC detectors) with a reasonably low complexity. More

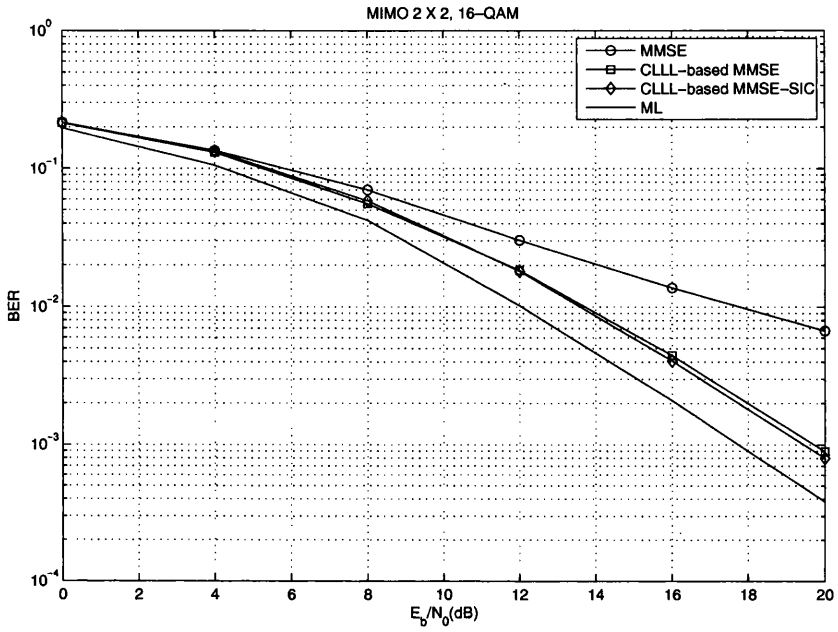

Figure 2.5: BER performance of various detectors in a 16-QAM 2×2 MIMO system.

importantly, from theoretical and numerical results, we showed that a full receive diversity is exploited with the LR-based detectors.

2.4 Multiuser MIMO User Selection

A rich spatial diversity gain can be obtained by employing various MIMO detectors (e.g., ML and LR-based detectors) to MIMO systems. Consider that multiple users are able to access the MIMO channel with different locations and channel conditions, it is possible to exploit another diversity gain, where the performance can be maximized by choosing the user of the best channel at a time. The resulting diversity gain is called the multiuser diversity gain [38] with multiuser MIMO systems [37], where the multiuser MIMO user selection [39, 40] becomes an effective way to increase the diversity. In this section, we introduce the user selection criteria for multiuser MIMO systems.

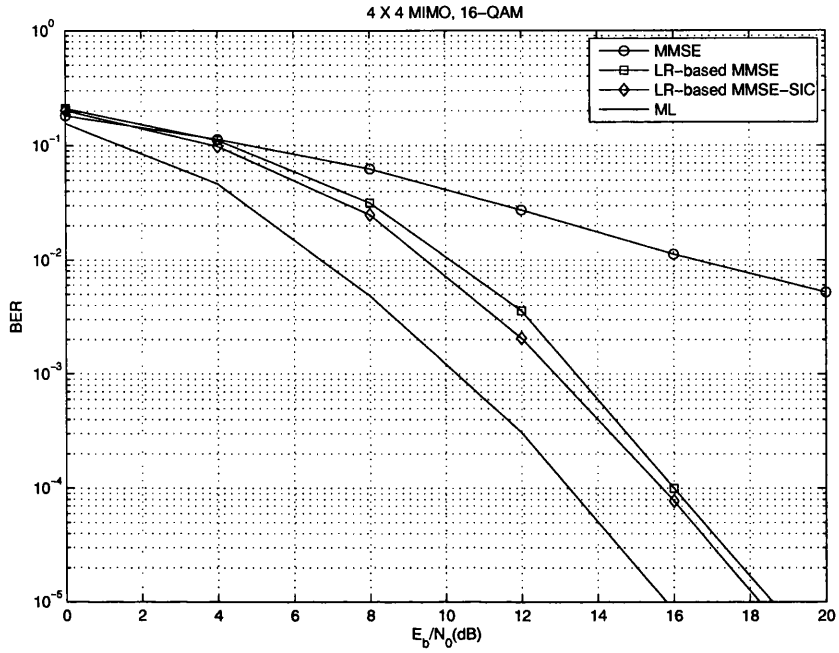

Figure 2.6: BER performance of various detectors in a 16-QAM 4×4 MIMO system.

2.4.1 System Model

We consider the multiuser MIMO system shown in Fig. 2.7 with K users in uplink channels, where each user is equipped with M transmit antennas. The based station (BS) is equipped with N receive antennas, where $N \geq M$. Each user has an $N \times M$ channel matrix and $M \times L$ signal vector to be transmitted, which are denoted by $\mathbf{H}_k$ and $\mathbf{S}_k$, respectively, where $k \in \{1, 2, \ldots, K\}$. The channel is assumed to be a quasi-static block flat-fading channel with its channel matrix is not varying over a time slot duration of L symbols. Note that one user is selected to access the channel during one time slot. For uncoded signals, in this section, we can assume $L = 1$ (Note that this assumption is used to simplify the derivation of user selection criteria, while the length of slot can be any number). Consider that the kth user is selected to transmit signal to the BS. Then, over a slot duration, the received signal at the BS is given by

$$\mathbf{y}_k = \mathbf{H}_k \mathbf{s}_k + \mathbf{n}_k, \tag{2.72}$$

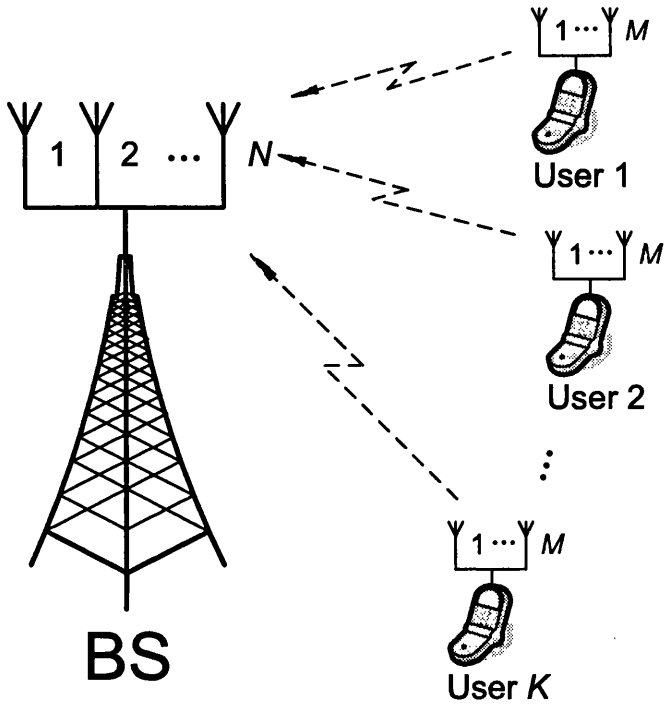

Figure 2.7: Block diagram for multiuser MIMO uplink channels of K users equipped per user with M transmit antennas and the BS equipped with N receive antennas.

where the background noise vector $\mathbf{n}_k$ is an independent zero-mean CSCG random vector with $E\left[\mathbf{n}_k\mathbf{n}_k^{\mathrm{H}}\right] = N_0\mathbf{I}$. Furthermore, we assume that the CSI is perfectly known at the receiver.

2.4.2 User Selection Criteria

In this subsection, we briefly introduce some existing user selection criteria for multiuser MIMO systems.

2.4.2.1 Maximum Mutual Information Criterion

In [53], the maximum mutual information (MMI) criterion is proposed to select the user who has the maximum mutual information between the transmitter and

receiver. The mutual information of the kth user is given by

$$I_k = \log\det\left(\mathbf{I}_M + \frac{\mathrm{SNR}}{M}\mathbf{H}_k^{\mathrm{H}}\mathbf{H}_k\right). \tag{2.73}$$

The MMI criterion is carried out to find the user index as

$$k_{\mathrm{MMI}} = \arg\max_{k=1,2,\ldots,K}(I_k). \tag{2.74}$$

Although conventional user selection schemes [39, 40] are adopted to select user of the strongest channel gain at a time, the actual performance can be different from the expected one if non-ideal or suboptimal MIMO detectors are employed for joint detection. Therefore, it is desirable to derive a user selection criterion which can maximize throughput over fading channels by exploiting multiuser diversity as well as multiple antenna diversity depending on the actual MIMO detector employed. In [54], a geometrical-based criterion is developed for the LR-based linear detection to minimum the error probability. In [41], for the user selection in uplink channels, where a single user is selected to transmit signals to a BS at a time, the error probability is used for the user selection criteria to choose the user who has the smallest error probability for given MIMO detectors (i.e., ML, MMSE, LR-based detectors).

2.4.2.2 Selection Criteria for ML and MMSE Detectors

In [41], the max-min distance (MDist) and the max-min eigenvalue (ME) criteria are derived for the ML and MMSE detectors, respectively. With the MDist and ME user selection, the user who can access the channel can be found as

$$k_{\mathrm{MDist}} = \arg\max_{k=1,2,\ldots,K}\mathcal{D}\left(\mathbf{H}_k\right) \tag{2.75}$$

and

$$k_{\mathrm{ME}} = \arg\max_{k=1,2,\ldots,K}\lambda_{\min}\left(\mathbf{H}_k^{\mathrm{H}}\mathbf{H}_k\right), \tag{2.76}$$

respectively. Here, $\mathcal{D}(\mathbf{A})$ and $\lambda_{\min}(\mathbf{A})$ denote the length of the shortest non-zero vector of the lattice generated by $\mathbf{A}$ and the minimum eigenvalue of $\mathbf{A}$, respectively. Note that although these two criteria can be used for any MIMO detector, the MDist criterion has been derived to maximize the performance with the ML detector and the ME criterion suits for the MMSE detector.

2.4.2.3 Selection Criteria for LR-based Detectors

For the LR-based detection, from (2.72), the received signal vector is rewritten as

$$\mathbf{y}_k = \mathbf{G}_k \mathbf{c}_k + \mathbf{n}_k, \tag{2.77}$$

where $\mathbf{G}_k = \mathbf{H}_k \mathbf{U}_k^{-1}$ and $\mathbf{c}_k = \mathbf{U}_k \mathbf{s}_k$. Here, $\mathbf{U}_k$ is an integer unimodular matrix and $\mathbf{G}_k$ is a CLLL-reduced matrix.

In [54], the optimal decision region (ODR) criterion for the LR-based linear detection can be simplified to the min-max mean square error (MMMSE) criterion with the lattice reduced basis $\mathbf{G}_k$ which is given by

$$k_{\text{ODR/MMMSE}} = \arg \min_{k=1,2,\ldots,K} \left\{ \max_{i=1,2,\ldots,M} \| \mathbf{w}_{k,(i)} \|^2 \right\}. \tag{2.78}$$

Here, $\mathbf{w}_{k,(i)}$ denotes the ith row of the linear filter $\mathbf{W}_k^{\text{H}}$ from $\mathbf{G}_k$ and $\mathbf{W}_k = \mathbf{G}_k \left(\mathbf{G}_k \mathbf{G}_k^{\text{H}}\right)^{-1}$.

In [41], two selection criteria are proposed for the LR-based MMSE and LR-based MMSE-SIC detectors, respectively. With the LR-based MMSE detector, the ME criterion is used as the user selection criterion by replacing $\mathbf{H}_k$ with $\mathbf{G}_k$ in (2.77). Then, the user index is selected as

$$k_{\text{ME}} = \arg \max_{k=1,2,\ldots,K} \lambda_{\min} \left(\mathbf{G}_k^{\text{H}} \mathbf{G}_k\right). \tag{2.79}$$

For the LR-based MMSE-SIC detection, $\mathbf{H}_k$ is replaced by an extended channel matrix defined as $\tilde{\mathbf{H}}_k = \left[\mathbf{H}^{\text{T}} \sqrt{\frac{N_0}{E_s}} \mathbf{I}_N\right]^{\text{T}}$, while $\mathbf{y}_k$ and $\mathbf{n}_k$ are replaced by $\tilde{\mathbf{y}}_k = \left[\mathbf{y}_k^{\text{T}} \; \mathbf{0}^{\text{T}}\right]^{\text{T}}$ and $\tilde{\mathbf{n}}_k = \left[\mathbf{n}_k^{\text{T}} \; -\sqrt{\frac{N_0}{E_s}} \mathbf{s}_k^{\text{T}}\right]^{\text{T}}$, respectively. Using the LR with $\tilde{\mathbf{H}}_k$, the lattice reduced matrix $\tilde{\mathbf{G}}_k$ can be found as $\tilde{\mathbf{H}}_k = \tilde{\mathbf{G}}_k \tilde{\mathbf{U}}_k$, where $\tilde{\mathbf{U}}_k$ is an integer unimodular matrix. The LR-based MMSE-SIC detection is carried out with the QR factorization of $\tilde{\mathbf{G}}_k = \tilde{\mathbf{Q}}_k \tilde{\mathbf{R}}_k$, where $\tilde{\mathbf{Q}}_k$ is unitary and $\tilde{\mathbf{R}}_k$ is upper triangular. Multiplying $\tilde{\mathbf{Q}}_k^{\text{H}}$ to $\tilde{\mathbf{y}}_k$ results in

$$\tilde{\mathbf{Q}}_k^{\text{H}} \tilde{\mathbf{y}}_k = \tilde{\mathbf{R}}_k \tilde{\mathbf{c}}_k + \tilde{\mathbf{Q}}_k^{\text{H}} \tilde{\mathbf{n}}_k, \tag{2.80}$$

where $\tilde{\mathbf{c}}_k = \tilde{\mathbf{U}}_k \mathbf{s}_k$. The SIC-based detection is performed with upper triangular matrix $\tilde{\mathbf{R}}_k$ in (2.80). The max-min diagonal (MD) criterion derived in [41] for

the LR-based MMSE-SIC detector is given by

$$k_{\mathrm{MD}} = \arg \max_{k=1,2,\ldots,K} \left\{ \min_{q} \mid r_{q,q}^{(k)} \mid \right\} \tag{2.81}$$

where $r_{q,q}^{(k)}$ denotes the (q,q)-th element of $\tilde{\mathbf{R}}_k$.

2.4.3 Performance Evaluation

In [41], the performance of user selection criteria with various MIMO detectors is analyzed in terms of the diversity gain.

2.4.3.1 Diversity Gain of MDist Criterion with ML Detector

The average pairwise error probability (PEP) of the ML detector with the user selected from K users under the MDist user selection criterion, denoted by P_e^{ml}, is upper-bounded as [41]

$$P_e^{\mathrm{ml}} \leq c_1 \left(\frac{\|\sigma_h^2 \mathbf{d}\|^2}{N_0} \right)^{-NK} + o\left(\left(\frac{\|\sigma_h^2 \mathbf{d}\|^2}{N_0} \right)^{-NK+1} \right), \tag{2.82}$$

where $c_1 > 0$ is constant, and $\mathbf{d} = \mathbf{s}_{(1)} - \mathbf{s}_{(2)}$ (here, $\mathbf{s}_{(i)} \in \mathcal{S}^M$ and $\mathbf{s}_{(1)} \neq \mathbf{s}_{(2)}$).

This theorem shows that a full receive diversity gain of N together with a full multiuser diversity gain of K can be achieved by the ML detectors under the MDist user selection criterion.

2.4.3.2 Diversity Gain of ME Criterion with MMSE Detector

The average PEP of the MMSE detector with the user selected from K users under the ME user selection criterion, denoted by P_e^{mmse}, is upper-bounded as [41]

$$P_e^{\mathrm{mmse}} \leq c_2 \left(\frac{\sigma_h^2 \|\mathbf{d}\|^2}{N_0} \right)^{-K} + o\left(\left(\frac{\sigma_h^2 \|\mathbf{d}\|^2}{N_0} \right)^{1-K} \right), \tag{2.83}$$

where $c_2 > 0$ is constant.

This theorem shows that for the MMSE detector, the ME user selection criterion cannot exploit a full receive diversity, however, a full multiuser diversity can be achieved.

2.4.3.3 Diversity Gain of MD Criterion with LR-based MMSE-SIC Detector

The average PEP of the LR-based MMSE-SIC detector with the user selected from K users under the MD user selection criterion, denoted by P_e^{lr}, is upper-bounded as [41]

$$P_e^{\text{lr}} \leq c_3 \left(\frac{\|\sigma_k^2 \mathbf{d}\|^2}{N_0}\right)^{-NK} + o\left(\left(\frac{\|\sigma_k^2 \mathbf{d}\|^2}{N_0}\right)^{-NK+1}\right), \tag{2.84}$$

where $c_3 > 0$ is constant.

This theorem shows that a full receive diversity gain of N together with a full multiuser diversity gain of K, as with the ML detector, can be achieved by the LR-based detector under the MD user selection criterion. From these results, we can see that the LR-based detector is as good as the ML detector with respect to the diversity gains.

2.4.4 Simulation Results

In order to illustrate the impact of the multiuser diversity gain to multiuser MIMO systems, we present the BER simulation results of various multiuser MIMO systems in Fig. 2.8. Three multiuser MIMO systems are considered with $M = 2$ and $K = \{1, 2\}$, namely *i*): MMSE detection under ME criterion, *ii*): CLLL-based MMSE-SIC detection under MD criterion, *iii*): ML detection under MDist criterion. Note that 16-QAM is used for signaling for all the systems. It shows that Systems *ii*) and *iii*) with $K = 2$ can provide a full diversity gain (i.e., multiuser diversity $\times$ multiple antenna diversity $= 4$), which outperforms that with $K = 1$. Furthermore, we can see that Systems *i*) can not exploit a full multiple antenna diversity, however, a full multiuser diversity can be achieved which is K.

2.4.5 Conclusion and Remarks

In this section, we introduced multiuser MIMO systems and the multiuser MIMO user selection criteria. Using the error probability based selection criteria, we showed that the LR-based detection can exploit the same diversity as that of the ML detection in multiuser MIMO systems.

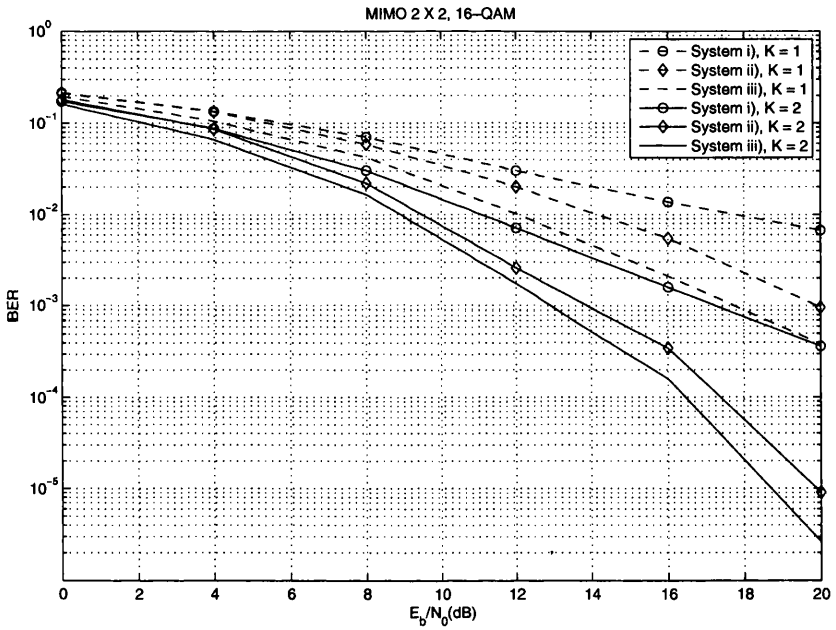

Figure 2.8: BER performance of various multiuser MIMO systems with 16-QAM, $M = 2$, and $K = \{1, 2\}$.

3

Partial MAP based List Detection for MIMO Systems

3.1 Introduction

In [55, 56], it has been shown that the capacity of wireless channels can be significantly improved by using MIMO systems. In MIMO systems, it is often desirable to use the ML detection to achieve the best performance. However, since the complexity of the ML detection grows exponentially with the number of transmit antennas, the ML detection approach is not practical for higher dimensional detection problems of large MIMO systems.

To reduce the computational complexity of the MIMO detection, the V-BLAST approach [44] has been proposed by employing the nulling and cancellation operations with the SIC in MIMO systems. In [27], the PMAP principle is considered to reduce the complexity of the MIMO detection. With the SIC, the PMAP detection can reduce a higher dimensional detection problem to multiple lower dimensional sub-detection problems.

Note that [27] discusses the PMAP solution with the chosen candidate that has the maximum APP among the candidate set in the first sub-detection, after separating the detection problem into two sub-detection problems, dimensionally. In this chapter, we use a list decoding approach [5, 6, 7, 8, 9, 10, 11] to extend the PMAP solution with any list of the candidates involved in the first sub-detection, thus, the best candidate can be chosen among the list in the second

sub-detection as the final decision. In particular, we focus on a family of list detection algorithms named the Chase detectors [12, 13, 14, 15, 16, 17] to work with the PMAP principle.

With the PMAP principle, the SIC can be implemented to reduce the complexity of MIMO detection under certain condition and probability. In [27], the condition and probability is given out with a specific list length. In this chapter, we extended the condition and probability of the SIC with any list length. Note that the PMAP principle is used to choose candidate symbol vectors in the list detection. Using this, we propose a computationally efficient algorithm for the detection problem in MIMO systems. It can be shown that compared to the conventional list detection which was proposed as the S-Chase detector in [14], the method we proposed has improved performance with a reasonable complexity.

This chapter is organized as follows. The MIMO system is presented in Section 3.2. The condition and probability of the SIC contributed by the PMAP based list detection are derived in Section 3.3. In addition, the proposed list detection algorithm based on the PMAP principle is explained. Simulation results are presented in Section 3.4. Finally, we conclude this chapter in Section 3.5.

3.2 System Model

Consider a MIMO system with N transmit antennas and N receive antennas. The received signal vector over a flat fading MIMO channel is written as

$$\mathbf{y} = \mathbf{H}\mathbf{s} + \mathbf{n}, \tag{3.1}$$

where the $N \times N$ matrix $\mathbf{H}$ is the channel matrix, the $N \times 1$ vector $\mathbf{s}$ is the transmit signal vector, and the $N \times 1$ vector $\mathbf{n}$ is a zero-mean white Gaussian noise vector with $E[\mathbf{n}\mathbf{n}^{\mathrm{H}}] = N_0\mathbf{I}$. Using the unitary matrix $\mathbf{Q}$ from the QR factorization [57] of the channel matrix $\mathbf{H}$, we have

$$\mathbf{Q}^{\mathrm{H}}\mathbf{y} = \mathbf{R}\mathbf{s} + \mathbf{Q}^{\mathrm{H}}\mathbf{n}, \tag{3.2}$$

where $\mathbf{H} = \mathbf{Q}\mathbf{R}$. With the upper triangular matrix $\mathbf{R}$, the received signal vector from (3.2) becomes

$$\begin{bmatrix} \mathbf{r} \\ \mathbf{z} \end{bmatrix} = \begin{bmatrix} \mathbf{A}_1 & \mathbf{A}_2 \\ \mathbf{0} & \mathbf{B} \end{bmatrix} \begin{bmatrix} \mathbf{s}_1 \\ \mathbf{s}_2 \end{bmatrix} + \begin{bmatrix} \mathbf{n}_1 \\ \mathbf{n}_2 \end{bmatrix}, \tag{3.3}$$

where the $N_1 \times 1$ vector $\mathbf{r}$ and $N_2 \times 1$ vector $\mathbf{z}$ are the first and second sub-vectors of $\mathbf{Q^H y}$, respectively, and $N = N_1 + N_2$. In addition, $\mathbf{s}_i$ and $\mathbf{n}_i$ are the i-th sub-vectors of $\mathbf{s}$ and $\mathbf{Q^H n}$, respectively, and $\mathbf{A}_1$, $\mathbf{A}_2$, and $\mathbf{B}$ are the sub-matrices of $\mathbf{H}$. Furthermore, we can show that $\mathbf{n}_1$ and $\mathbf{n}_2$ are the zero-mean Gaussian noise vectors and that

$$E\left[\begin{bmatrix} \mathbf{n}_1 \\ \mathbf{n}_2 \end{bmatrix} \begin{bmatrix} \mathbf{n}_1^H & \mathbf{n}_2^H \end{bmatrix} \right] = N_0 \mathbf{I}. \tag{3.4}$$

In addition, we assume that $\mathbf{s}_1 \in \beta^{N_1}$ and $\mathbf{s}_2 \in \beta^{N_2}$, where β denotes the signal alphabet and β^N denotes the N dimensional Cartesian product of β.

From (3.3), the detection of $\mathbf{s}$ can be decomposed into the two sub-detection of $\mathbf{s}_1$ and $\mathbf{s}_2$, which have N_1 and N_2 elements, respectively. Due to no interference from $\mathbf{s}_1$, the sub-detection of $\mathbf{s}_2$ can be done independently, while the sub-detection of $\mathbf{s}_1$ is not straightforward as $\mathbf{s}_2$ becomes an interfering signal through $\mathbf{A}_2$. In the next section, we study the sub-detection of $\mathbf{s}_1$ with list decoding [5, 6, 7, 8] and PMAP principle [27] to deal with the interference effectively. Note that we have assumed that the number of receive antennas is identical to that of transmit antennas for convenience. The decomposition in (3.3) would also be possible when the numbers are different.

3.3 Partial MAP based List Detection

As shown in [27], the PMAP principle can be applied to the sub-detection of $\mathbf{s}_1$ by using the APRP of $\mathbf{s}_2$, which can be obtained from the result of the sub-detection of $\mathbf{s}_2$. Here, we focus on the sub-detection of $\mathbf{s}_1$ under the assumption that the APRP of $\mathbf{s}_2$ is available.

While the SIC is used to mitigate the interference of $\mathbf{s}_2$ in [27], we use the list decoding approach [5, 6, 7, 8] to effectively deal with the interference of $\mathbf{s}_2$. Basically, instead of exhaustive searching for all the possible decision vectors in the detection problem, the list decoding creates a list of candidate vectors and then chooses the best candidate within the list for the final decision. In this section, we drive the PMAP solution with the SIC, by generating a list of candidate decision vectors of $\mathbf{s}_2$ for the final decision.

Let us define the finite set of all the possible candidate vectors for $\mathbf{s}_2$ as $\{\mathbf{s}_2^1, \mathbf{s}_2^2, \cdots, \mathbf{s}_2^M\}$, where M is the number of all the possible candidate vectors (for example, $M = 16^2$ if the size $\mathbf{s}_2$ is 2×1 and 16-QAM is used), and the APRPs of the candidate vectors are denoted by $\Pr(\mathbf{s}_2 = \mathbf{s}_2^1)$, $\Pr(\mathbf{s}_2 = \mathbf{s}_2^2)$, $\cdots$, $\Pr(\mathbf{s}_2 = \mathbf{s}_2^M)$. Furthermore, we assume that $\Pr(\mathbf{s}_2 = \mathbf{s}_2^1) \geq \Pr(\mathbf{s}_2 = \mathbf{s}_2^2) \geq \cdots \geq \Pr(\mathbf{s}_2 = \mathbf{s}_2^M)$. Moreover, suppose that the partial APPs for each candidate are available and denoted by $\Pr(\mathbf{s}_2 = \mathbf{s}_2^n \mid \mathbf{r})$, where $n \in \{1, 2, \cdots, M\}$.

3.3.1 The Case of List Length $Q = 1$

When $Q = 1$, the list detection is the same as the SIC in [27]. With the APRP of $\mathbf{s}_2$, the PMAP detection of $\mathbf{s}_1$ and $\mathbf{s}_2$ with $\mathbf{r}$ in (3.3) is defined as

$$\begin{aligned}\{\hat{\mathbf{s}}_1, \hat{\mathbf{s}}_2\} = &\arg\min_{\mathbf{s}_1, \mathbf{s}_2} \frac{1}{N_0} \parallel \mathbf{r} - (\mathbf{A}_1\mathbf{s}_1 + \mathbf{A}_2\mathbf{s}_2) \parallel^2 \\ &+ \log \frac{1}{\Pr(\mathbf{s}_2)},\end{aligned} \tag{3.5}$$

where $\Pr(\mathbf{s}_2)$ stands for the APRP of $\mathbf{s}_2$. Furthermore, the log - APP ratio [58] is defined as

$$L(\mathbf{s}_2 \mid \mathbf{r}) = \log \frac{\Pr(\mathbf{s}_2 = \mathbf{s}_2^1 \mid \mathbf{r})}{\max_{\mathbf{s}_2^n \neq \mathbf{s}_2^1} \Pr(\mathbf{s}_2 = \mathbf{s}_2^n \mid \mathbf{r})}. \tag{3.6}$$

If $L(\mathbf{s}_2 \mid \mathbf{r}) \geq 0$, then we can have $\Pr(\mathbf{s}_2 = \mathbf{s}_2^1 \mid \mathbf{r}) \geq \max_{\mathbf{s}_2^n \neq \mathbf{s}_2^1} \Pr(\mathbf{s}_2 = \mathbf{s}_2^n \mid \mathbf{r})$. Therefore, $\Pr(\mathbf{s}_2 = \mathbf{s}_2^1 \mid \mathbf{r})$ becomes the maximum among all the partial APPs, and the PMAP solution of $\mathbf{s}_2$ becomes $\mathbf{s}_2^1$. According to [27], a sufficient condition to make sure that $L(\mathbf{s}_2 \mid \mathbf{r}) \geq 0$ is as follows:

$$\min_{\mathbf{s}_1} \frac{1}{N_0} \parallel \mathbf{r} - (\mathbf{A}_1\mathbf{s}_1 + \mathbf{A}_2\mathbf{s}_2^1) \parallel^2 \leq \log \frac{\Pr(\mathbf{s}_2 = \mathbf{s}_2^1)}{\Pr(\mathbf{s}_2 = \mathbf{s}_2^2)}. \tag{3.7}$$

If (3.7) is satisfied, the PMAP detection problem in (3.5) can be simplified as

$$\mathbf{s}_1^1 = \arg\min_{\mathbf{s}_1} \frac{1}{N_0} \parallel \mathbf{r}_2^1 - \mathbf{A}_1\mathbf{s}_1 \parallel^2, \tag{3.8}$$

where $\mathbf{r}_2^1 = \mathbf{r} - \mathbf{A}_2\mathbf{s}_2^1$. The condition in (3.7) is called the dimension reduction condition (DRC). It is to say, if we can have the DRC satisfied, then the N dimensional detection problem can be decomposed into an N_1 dimensional and

N_2 dimensional detection problems which can reduce the complexity, and we decide $\{\mathbf{s}_1^1, \mathbf{s}_2^1\}$ as the PMAP solution of $\{\mathbf{s}_1, \mathbf{s}_2\}$.

Furthermore, the probability of dimension reduction (PDR) is defined as

$$P_{cond} = \Pr\left(\min_{\mathbf{s}_1} \frac{1}{N_0} \parallel \mathbf{r} - (\mathbf{A}_1\mathbf{s}_1 + \mathbf{A}_2\mathbf{s}_2^1) \parallel^2 \leq \log \frac{\Pr(\mathbf{s}_2 = \mathbf{s}_2^1)}{\Pr(\mathbf{s}_2 = \mathbf{s}_2^2)}\right). \tag{3.9}$$

The lower bound of P_{cond} can be derived as

$$P_{cond} \geq \hat{P}_{cond} \triangleq 1 - e^{-L_T/2} \sum_{k=0}^{N-1} \frac{1}{k!} (\frac{L_T}{2})^k, \tag{3.10}$$

where $L_T = \log \frac{\Pr(\mathbf{s}_2 = \mathbf{s}_2^1)}{\Pr(\mathbf{s}_2 = \mathbf{s}_2^2)}$ (see [27] for more details). Clearly, the PDR is the probability that the computational complexity of an N dimensional detection problem is reduced to the computational complexity of N_1 dimensional and N_2 dimensional detection problems.

3.3.2 General Case

With the list length $Q = m$, where $m \in \{1, 2, \cdots, M-1\}$, a general case can be considered. Note that the case of $m = M$ will be explained later. With $Q = m$, the log - APP ratio can be given by

$$L(\mathbf{s}_2 \mid \mathbf{r}) = \log \frac{\Pr(\mathbf{s}_2 = \mathbf{s}_2^1 \mid \mathbf{r}) + \cdots + \Pr(\mathbf{s}_2 = \mathbf{s}_2^m \mid \mathbf{r})}{\max_{\mathbf{s}_2^n \neq \mathbf{s}_2^{1,2,\cdots,m}} \Pr(\mathbf{s}_2 = \mathbf{s}_2^n \mid \mathbf{r})}. \tag{3.11}$$

If $L(\mathbf{s}_2 \mid \mathbf{r}) \geq 0$, then we have $\Pr(\mathbf{s}_2 = \mathbf{s}_2^1 \mid \mathbf{r}) + \cdots + \Pr(\mathbf{s}_2 = \mathbf{s}_2^m \mid \mathbf{r}) \geq \max_{\mathbf{s}_2^n \neq \mathbf{s}_2^{1,2,\cdots,m}} \Pr(\mathbf{s}_2 = \mathbf{s}_2^n \mid \mathbf{r})$. Therefore, $\Pr(\mathbf{s}_2 = \mathbf{s}_2^{1,2,\cdots,m} \mid \mathbf{r}) = \Pr(\mathbf{s}_2 = \mathbf{s}_2^1 \mid \mathbf{r}) + \cdots + \Pr(\mathbf{s}_2 = \mathbf{s}_2^m \mid \mathbf{r})$ becomes the maximum, and the PMAP solution of $\mathbf{s}_2$ can be found from $\bar{\mathbf{s}}_2 \in \{\mathbf{s}_2^1, \cdots, \mathbf{s}_2^m\}$.

Using the max - log approximation [59] principle, we can have the modified

log - APP ratio as

$$\begin{aligned}\hat{L}(\mathbf{s}_2 \mid \mathbf{r}) \approx & \min_{\mathbf{s}_1}\left\{\frac{1}{N_0}\parallel \mathbf{r}-(\mathbf{A}_1\mathbf{s}_1+\mathbf{A}_2\mathbf{s}_2^{1,2,\cdots,m})\parallel^2\right. \\ & \left.+\log\frac{1}{\Pr(\mathbf{s}_2=\mathbf{s}_2^{1,2,\cdots,m})}\right\} \\ & -\min_{\mathbf{s}_1,\mathbf{s}_2^n\neq\mathbf{s}_2^{1,2,\cdots,m}}\left\{\frac{1}{N_0}\parallel \mathbf{r}-(\mathbf{A}_1\mathbf{s}_1+\mathbf{A}_2\mathbf{s}_2^n)\parallel^2\right. \\ & \left.+\log\frac{1}{\Pr(\mathbf{s}_2=\mathbf{s}_2^n)}\right\}.\end{aligned} \tag{3.12}$$

More details about the derivation can be found in [60, 61, 62]. If $\hat{L}(\mathbf{s}_2 \mid \mathbf{r}) \leq 0$, then $\{\mathbf{s}_2^1, \cdots, \mathbf{s}_2^m\}$ becomes the list of candidates for the PMAP solution of $\mathbf{s}_2$. Here, we suppose that

$$\min_{\mathbf{s}_1,\mathbf{s}_2}\frac{1}{N_0}\parallel \mathbf{r}-(\mathbf{A}_1\mathbf{s}_1+\mathbf{A}_2\mathbf{s}_2)\parallel^2 \geq C, \tag{3.13}$$

where $C \geq 0$ is a constant. Furthermore, we can show that

$$\min_{\mathbf{s}_2^n\neq\mathbf{s}_2^{1,2,\cdots,m}}\left\{\log\frac{1}{\Pr(\mathbf{s}_2=\mathbf{s}_2^n)}\right\} \geq \log\frac{1}{\Pr(\mathbf{s}_2=\mathbf{s}_2^{m+1})}. \tag{3.14}$$

If

$$\begin{aligned}\min_{\mathbf{s}_1}&\left\{\frac{1}{N_0}\parallel \mathbf{r}-(\mathbf{A}_1\mathbf{s}_1+\mathbf{A}_2\mathbf{s}_2^{1,2,\cdots,m})\parallel^2\right. \\ &\left.+\log\frac{1}{\Pr(\mathbf{s}_2=\mathbf{s}_2^{1,2,\cdots,m})}\right\} \leq C+\log\frac{1}{\Pr(\mathbf{s}_2=\mathbf{s}_2^{m+1})},\end{aligned} \tag{3.15}$$

we can have $\hat{L}(\mathbf{s}_2 \mid \mathbf{r}) \leq 0$ and the PMAP solution can be found. Let $C = 0$, the DRC can be derived as

$$\begin{aligned}\min_{\mathbf{s}_1}\frac{1}{N_0}\parallel \mathbf{r}-(\mathbf{A}_1\mathbf{s}_1+\mathbf{A}_2\mathbf{s}_2^k)\parallel^2 \leq \log\frac{\Pr(\mathbf{s}_2=\mathbf{s}_2^k)}{\Pr(\mathbf{s}_2=\mathbf{s}_2^{m+1})}, \\ k=1,2,\cdots,m.\end{aligned} \tag{3.16}$$

Note that if any condition in (3.16) is satisfied with the PMAP solution of $\mathbf{s}_2$, denoted by $\bar{\mathbf{s}}_2 = \mathbf{s}_2^{\hat{m}}$, where $\hat{m} \in \{1, 2, \cdots, m\}$, then the PMAP detection problem in (3.5) can be simplified as

$$\mathbf{s}_1^{\hat{m}} = \arg\min_{\mathbf{s}_1}\frac{1}{N_0}\parallel \mathbf{r}_2^{\hat{m}}-\mathbf{A}_1\mathbf{s}_1\parallel^2, \tag{3.17}$$

where $\mathbf{r}_2^{\hat{m}} = \mathbf{r} - \mathbf{A}_2\mathbf{s}_2^{\hat{m}}$. Thus, the N dimensional detection problem can be decomposed into N_1 dimensional and N_2 dimensional detection problems to reduce the complexity, and we decide $\{\mathbf{s}_1^{\hat{m}}, \mathbf{s}_2^{\hat{m}}\}$ as the PMAP solution. Furthermore, for more than one of these conditions in (3.16) satisfied, the candidate of $\mathbf{s}_2$ whose $\min_{\mathbf{s}_1} \frac{1}{N_0} \parallel \mathbf{r} - (\mathbf{A}_1\mathbf{s}_1 + \mathbf{A}_2\mathbf{s}_2) \parallel^2 + \log \frac{1}{\Pr(\mathbf{s}_2)}$ achieves the minimum value can be chosen as the PMAP solution.

Let

$$D_{\bar{m}} = \min_{\mathbf{s}_1} \frac{1}{N_0} \parallel \mathbf{r} - (\mathbf{A}_1\mathbf{s}_1 + \mathbf{A}_2\mathbf{s}_2^{\bar{m}}) \parallel^2, \tag{3.18}$$

and

$$L_{T\bar{m}} = \log \frac{\Pr(\mathbf{s}_2 = \mathbf{s}_2^{\bar{m}})}{\Pr(\mathbf{s}_2 = \mathbf{s}_2^{m+1})}, \tag{3.19}$$

where $\bar{m} \in \{1, 2, \cdots, m\}$. Therefore, the probability of each condition satisfied in (16) is $\Pr(D_{\bar{m}} \leq L_{T\bar{m}})$, and the PDR is

$$P_{cond} = \Pr\left((D_1 \leq L_{T1}) \cup \cdots \cup (D_m \leq L_{Tm})\right), \tag{3.20}$$

where $\cup$ denotes the union.

Let $P_{cond}^{S.I.}$ denote the PDR under the assumption that the DRCs are statistical independent. In addition, let $P_{cond}^{F.C.}$ denote the PDR for the case of fully correlated DRCs. Then, we have

$$P_{cond}^{S.I.} \geq P_{cond} \geq P_{cond}^{F.C.}. \tag{3.21}$$

Furthermore, the lower bound of $P_{cond}^{S.I.}$ and $P_{cond}^{F.C.}$ can be obtained as

$$\begin{aligned} P_{cond}^{S.I.} \geq \hat{P}_{cond}^{S.I.} &= 1 - \textstyle\prod_{j=1}^{m} \Pr\left(\frac{1}{N_0} \parallel \mathbf{n} \parallel^2 \geq L_{Tj}\right) \\ P_{cond}^{F.C.} \geq \hat{P}_{cond}^{F.C.} &= 1 - \Pr\left(\frac{1}{N_0} \parallel \mathbf{n} \parallel^2 \geq L_{Tj}\right). \end{aligned} \tag{3.22}$$

Since $\frac{1}{N_0} \parallel \mathbf{n} \parallel^2$ is a chi-square random variable with $2N$ degrees of freedom, we have

$$\begin{aligned} \hat{P}_{cond}^{S.I.} &= 1 - \textstyle\prod_{j=1}^{m} G(L_{Tj}, N) \\ \hat{P}_{cond}^{F.C.} &= 1 - G(L_{Tj}, N), \end{aligned} \tag{3.23}$$

where $G(L_{Tj}, N) = e^{-L_{Tj}/2} \sum_{k=0}^{N-1} \frac{1}{k!} \left(\frac{L_{Tj}}{2}\right)^k$, and $j \in \{1, 2, \cdots, m\}$. Note that if $m = M$, it can be shown that $L_{TM} = \log \frac{\Pr(\mathbf{s}_2 = \mathbf{s}_2^M)}{\Pr(\mathbf{s}_2 = \mathbf{s}_2^M)} = 0$, thus, $\hat{P}_{cond}^{S.I.} = \hat{P}_{cond}^{F.C.} = 1$. (That is, since all the candidates have been on the list, then the condition must be satisfied, which is obvious.)

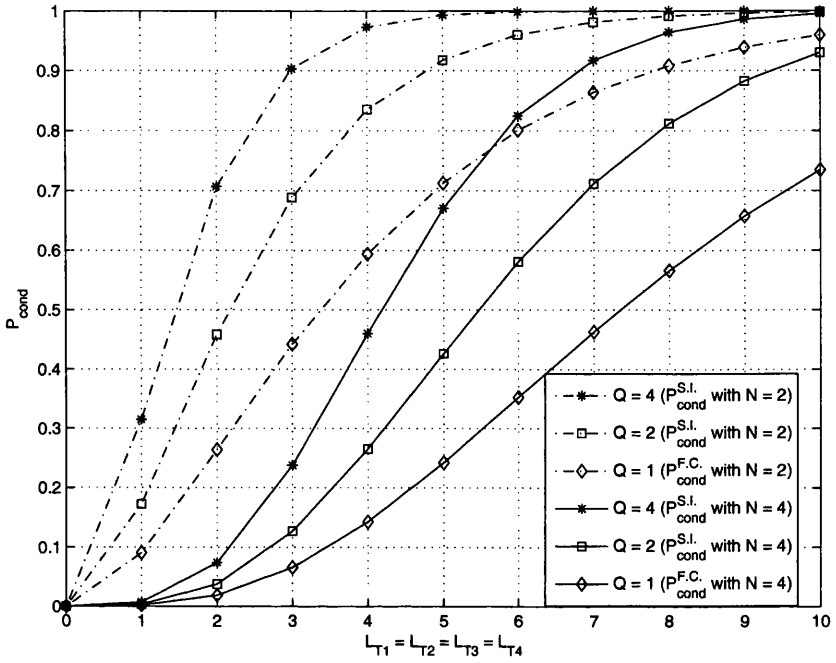

Figure 3.1: Bounds of P_{cond} for different list length with $N = 2$ and $N = 4$, separately.

Since $\hat{P}_{cond}^{S.I.}$ and $\hat{P}_{cond}^{F.C.}$ are the cumulative density functions (cdf), they increase with L_{T1} and L_{T2} and decrease with the number of receive antennas, N. The curves of $\hat{P}_{cond}^{S.I.}$ and $\hat{P}_{cond}^{F.C.}$ are showed in Fig. 3.1 with different list length Q and value of N. In these curves, we simply assume that $L_{T1} = L_{T2} = L_{T3} = L_{T4}$. According to Fig. 3.1, we can see that the PDR increases with the list length. It can also be showed that the probability decreases with the number of antennas.

3.3.3 Algorithm for the Partial MAP based List Detection

Using the S-Chase detection [14], we can propose a PMAP based list detection which is called the PMAP-list algorithm. The algorithm is summarized as follows.

1) Among the N data symbols in $\mathbf{s}_2$, we select N_2 symbols for $\mathbf{s}_2$. For convenience, let i_{n_2} denote the index of the n_2-th data symbols of $\mathbf{s}_2$, where $n_2 = 1, 2, \cdots, N_2$ and $i_{n_2} \in \{1, 2, \cdots, N\}$. According to [14], the index i_{n_2}

has the property that it corresponds to the index of $\mathbf{h}_j$ (the column vector of $\mathbf{H}$ and $j \in \{1, \cdots, N\}$), which has the n_2-th minimum or n_2-th maximum norm among all the columns, if $Q \leq \frac{3M}{4}$ or $Q > \frac{3M}{4}$, respectively.

2) After ordering the symbols, the QR factorization of the channel matrix $\mathbf{H}$ is carried out as $\mathbf{H\Pi} = \mathbf{QR}$, where the $N \times N$ matrix $\mathbf{\Pi}$ represents the permutation matrix according to the symbol ordering. Here, the n_2-th column of $\mathbf{\Pi}$ is the i_{n_2}-th column of the identity matrix. The final N_1 columns of $\mathbf{\Pi}$ are decided according to the sorted-QR decomposition [63], which orders the weaker symbols to be detected later.

3) Then, with the received signal vectors as (3.3), we find the APPs of $\mathbf{s}_2$ as follows:

   (a) for $j = 1$ to N

   (b) $d_j = \frac{1}{N_0} \parallel \mathbf{z} - \mathbf{B}\mathbf{s}_2^j \parallel^2$, $\mathbf{s}_2^j \in \beta^{N_2}$. Note that $\mathbf{s}_2^j$ is chosen with d_j being the j-th minimum among all the cases.

   (c) $\Pr(\mathbf{s}_2^j \mid \mathbf{z}) = c\exp(-\frac{1}{N_0} \parallel \mathbf{z} - \mathbf{B}\mathbf{s}_2^j \parallel^2)$, where c is the normalization constant.

   (d) end

4) The APRP of $\mathbf{s}_2$ is updated by using the resulting $\Pr(\mathbf{s}_2^j \mid \mathbf{z})$ in Step 3). With the APRP of $\mathbf{s}_2$, which is denoted by $\Pr(\mathbf{s}_2 = \mathbf{s}_2^j)$, the DRC can be verified as follows:

   (a) Let $m = 1$, the DRC in (3.16) is verified.

   (b) If the DRC is satisfied, the PMAP solution of $\mathbf{s}_2$, which is denoted by $\bar{\mathbf{s}}_2 = \mathbf{s}_2^{\hat{m}}$, where $\hat{m} \in \{1, 2, \cdots, m\}$, can be decided by choosing $\mathbf{s}_2$ that minimizes $\min_{\mathbf{s}_1} \frac{1}{N_0} \parallel \mathbf{r} - (\mathbf{A}_1\mathbf{s}_1 + \mathbf{A}_2\mathbf{s}_2^{\hat{m}}) \parallel^2 + \log \frac{1}{\Pr(\mathbf{s}_2 = \mathbf{s}_2^{\hat{m}})}$ among all the conditions in (3.16).

   (c) If the DRC is not satisfied, $m = m + 1$ and go back to Step (b). Note that the iterative method (called the IM-PMAP-list) is terminated until either the DRC satisfied or all of the candidates have been on the list.

5) From (3.17), the PMAP solution of$\{\mathbf{s}_1, \mathbf{s}_2\}$ is decided as $\{\mathbf{s}_1^{\hat{m}}, \mathbf{s}_2^{\hat{m}}\}$. The detected signals are re-ordered according to the original ordering.

To consider the computational complexity, let K denote the number of the elements in β, i.e., the size of the signal alphabet. The complexity of the ML detection that uses an exhaustive search is $O(K^N)$. The V-BLAST which uses the nulling and cancellation has a detection complexity of $O(NK)$ excluding the complexity associated with computing nulling filters' coefficients. The proposed PMAP-list algorithm has a detection complexity of $O(QK^{N_1} + K^{N_2})$, because $\mathbf{s}_1 \in \beta^{N_1}$ and $\mathbf{s}_2 \in \beta^{N_2}$. Since the S-Chase detector [14] chooses one symbol for the first sub-detector among the N received symbols, i.e., $N_2 = 1$, it has a detection complexity of $O(QK^{N-1} + K)$, because $\mathbf{s}_1 \in \beta^{N-1}$ and $\mathbf{s}_2 \in \beta$. The proposed PMAP-list detector has a comparable complexity to the S-Chase detector when $N_2 = 1$. It is noteworthy that the complexity can be lower if $N_1 = N_2$. Thus, if $N = 4$, then the complexity for the case of $N_1 = N_2 = 2$ is lower than that of $N_1 = 3$ and $N_2 = 1$. As shown in Table 3.1, when we list the empirical complexity of various detectors for each symbol vector detection, in terms of the average number of the floating point operation (flops), this can be confirmed[1]. Note that to compare with the sphere decoding, we also perform the sphere decoder as the sub-detector of the proposed approach in Table 3.1.

As shown above, the complexity of the list detector depends on the list length, Q. If Q approaches $M = K^{N_2}$, the complexity approaches that of the ML detector. Thus, it is desirable to have a small Q. As will be shown in Section 3.4, the list length of the proposed PMAP-list detector decreases with the SNR.

3.4 Simulation Results

In this section, we consider 16-QAM 2×2 and 16-QAM 4×4 MIMO systems for simulations. The elements of MIMO channels are generated as independent complex Gaussian random variables with mean zero and unit variance. The SNR is defined by the energy per bit to the noise power spectral density ratio, E_b/N_0.

[1]We simulate these systems using MATLAB-V5.3 on a PC. The MATLAB command "flops" is used to count the number of flops.

Table 3.1: The average complexity of various detection methods for 16-QAM 2×2 system and 16-QAM 4×4 system, separately.

Average flops ($\times 10^3$) for 16-QAM 2×2 system						
E_b/N_o(dB)	0.0	4.0	8.0	12.0	16.0	20.0
MMSE	0.240	0.240	0.240	0.240	0.240	0.240
V-BLAST	0.704	0.704	0.704	0.704	0.704	0.704
S-Chase, Q = 1, ML (exhaustive search) sub-detector	0.752	0.752	0.752	0.752	0.752	0.752
S-Chase + Partial MAP ML (exhaustive search) sub-detector	4.8719	3.6202	2.1472	1.3636	1.0822	1.0501
S-Chase + Partial MAP ML (sphere decoding) sub-detector	1.221	0.908	0.588	0.406	0.361	0.355
ML (sphere decoding)	0.614	0.598	0.568	0.556	0.551	0.549
ML (exhaustive search)	13.827	13.827	13.827	13.827	13.827	13.827
Average flops ($\times 10^3$) for 16-QAM 4×4 system						
E_b/N_o(dB)	0.0	4.0	8.0	12.0	16.0	20.0
MMSE	0.644	0.644	0.644	0.644	0.644	0.644
V-BLAST	2.0873	2.0873	2.0873	2.0873	2.0873	2.0873
S-Chase, $Q = 1$, ML (exhaustive search) sub-detector	565.9	565.9	565.9	565.9	565.9	565.9
S-Chase + Partial MAP ML (exhaustive search) sub-detector ($N_1 = 3, N_2 = 1$)	6291.8	4451.7	2429.1	1154.7	632.8	566.3
S-Chase + Partial MAP ML (exhaustive search) sub-detector ($N_1 = N_2 = 2$)	1061.6	502.64	187.47	75.687	48.767	45.545
S-Chase + Partial MAP ML (sphere decoding) sub-detector ($N_1 = 3, N_2 = 1$)	28.7475	19.9401	10.6409	5.1543	2.3321	2.2592
S-Chase + Partial MAP ML (sphere decoding) sub-detector ($N_1 = N_2 = 2$)	41.775	19.779	7.3768	2.9783	1.9190	1.7922
ML (sphere decoding)	3.8933	3.2906	2.9496	2.7760	2.7058	2.6756
ML (exhaustive search)	11140	11140	11140	11140	11140	11140

According to the simulation results, we perform the MMSE decoder, V-BLAST, S-Chase, sphere decoding, ML to compare with the proposed approach (for the detail of the MMSE, V-BLAST, and sphere decoding, see [64], chp. 10).

In Fig. 3.2, we show the BER simulation results for the 2×2 system, where $N_1 = N_2 = 1$. It is shown that the proposed PMAP-list detector outperforms the conventional list detector [13, 14]. Note that the proposed PMAP-list detector uses the approximation in (3.12). Due to this approximation, the performance is worse than that of the ML detection. Table 3.2 shows the average list length. We can observe that the list length decreases with E_b/N_0. Since the DRC can be satisfied with a shorter list length as E_b/N_0 increases, the list length can be shorter.

Moreover, in Fig. 3.2, the BER simulation results for the 4×4 MIMO system are also shown. We can see that the proposed PMAP-list detector has an insignificant performance degradation from the ML detector and the SNR loss is less 0.5 dB at a broad range of BER (up to BER $= 10^{-3}$). The performance of the proposed PMAP-list detector with $N_1 = N_2 = 2$ is better than that with $N_1 = 3$ and $N_2 = 1$. Since the first sub-detector is performed with $16^2 = 256$ candidates and 2-fold diversity gain when $N_2 = 2$, the reliability is better than that with 16

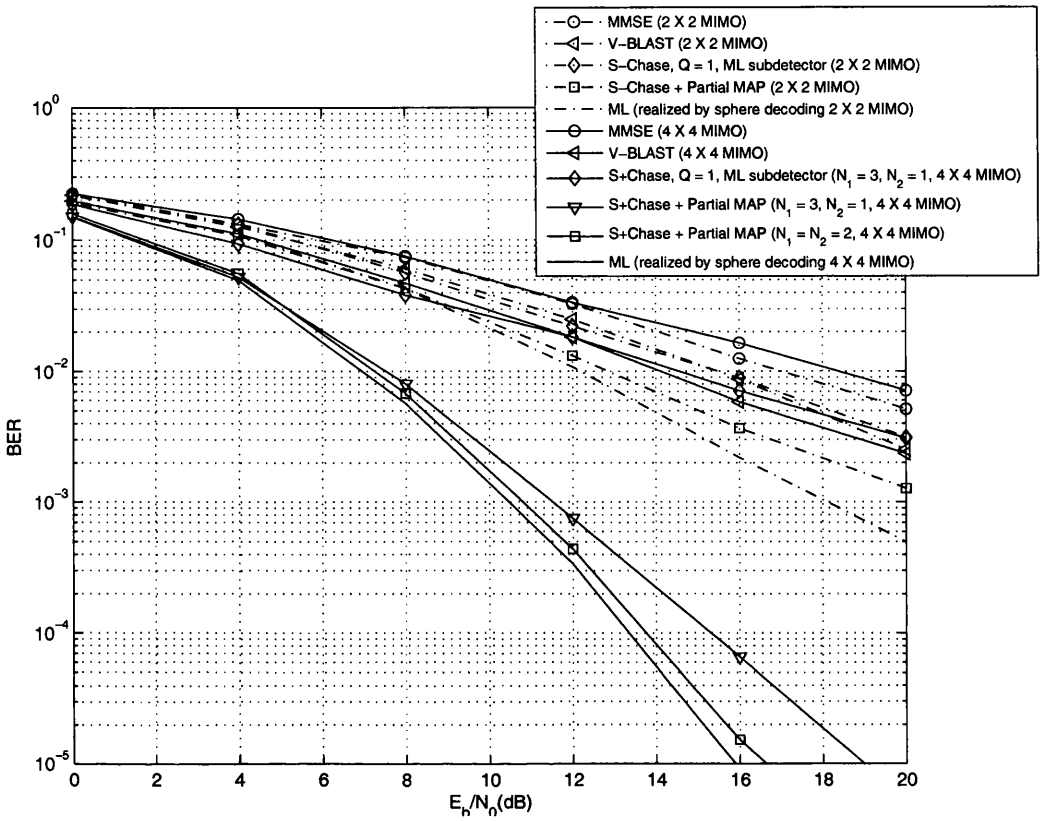

Figure 3.2: BER performance of various detection methods for 16-QAM 2×2 system (we have the partial MAP based S-Chase decoding with $N_1 = N_2 = 1$ and the S-Chase detector with list length $Q = 1$ and $N_1 = N_2 = 1$) and 16-QAM 4×4 system (we have the partial MAP based S-Chase decoding with $N_1 = 3, N_2 = 1$, and $N_1 = N_2 = 2$, and the S-Chase detector with list length $Q = 1$ and $N_1 = 3, N_2 = 1$).

candidates and 1-fold diversity gain when $N_2 = 1$. Thus, there would be less error propagation and the performance can be improved with a large N_2. The average list length for the 4×4 system is shown in Table 3.2. As E_b/N_0 increases, the average list length becomes shorter. This indicates that the proposed PMAP-list detector can be computationally efficient when the target BER is sufficiently low, say BER $= 10^{-4}$ for the case of $N_1 = N_2 = 2$, where the corresponding E_b/N_0 is 14dB.

Table 3.2: The average list length with different SNR and $N_1 = N_2$ obtained from the simulation with 16-QAM 2×2 and 4×4 MIMO systems, separately.

Average value of the list length						
E_b/N_o(dB)	0.0	4.0	8.0	12.0	16.0	20.0
2×2 MIMO	5.64598	4.00584	2.29326	1.29278	1.04493	1.01218
4×4 MIMO	23.3585	11.0593	4.1247	1.6653	1.073	1.0021

3.5 Conclusion

Since the complexity of the ML detection becomes prohibitively high for large MIMO systems, it is often impractical. We showed that the PMAP principle can be an effective means to reduce the computational complexity in conjunction with the list decoding for the MIMO detection. It was also shown that the PMAP principle based list decoding can perform better than the conventional list decoding. Furthermore, in terms of the performance and complexity, it is shown that the proposed approach with $N_1 = N_2 = 2$ outperforms the case of $N_1 = 3$ and $N_2 = 1$.

In order to improve the performance and reduce the complexity, we can consider the LR in conjunction with list detection. In the next chapter, we represent a column reordering strategy for the LR-based list detection for slow fading MIMO channels.

4

Error Probability based Column Reordering Criterion for Lattice Reduction based List MIMO Detection

4.1 Introduction

In MIMO systems, in order to achieve a good performance and a low complexity at the same time, LR-based [19, 20, 21, 22, 23, 24, 25, 26] and list-based [12, 13, 14, 15, 16, 17] MIMO detectors are well investigated. To further improve the performance and reduce the complexity, a LR-based list detection is proposed in [28] by decomposing a large MIMO detection problem into multiple small MIMO sub-detection problems, where the complexity grows linearly with its list length. It is shown that the LR-based list MIMO detection can provide a near ML performance with a sufficiently large list length. However, a good performance is not guaranteed with a small list length (low complexity). Thus, it is desired to develop a strategy to improve the performance of the LR-based list detection when a small list length is considered.

Noting that column swapping of channel matrices can result in different performance in the LR-based list detection, in this chapter, in order to obtain an

optimal order of columns in terms of the error probability of sub-detection, we propose column reordering criteria (CRC) for a given MIMO sub-detector employed. Through simulations, we show our proposed CRC can significantly improve the performance of LR-based list detection with a small list length (low complexity) for slow fading MIMO channels.

4.2 Lattice Reduction based List Detection

In this section, we briefly introduce the LR-based list detection [28]. Consider a MIMO system equipped with N transmit and N receive antennas (although the proposed approach is also valid when there are more receive antennas than transmit antennas, we assume they are the same for convenience). Let s_n denote the data symbol to be transmitted by the nth transmit antenna, $n = 1, 2, \ldots, N$. Note that $s_n \in \mathcal{S}$, where $\mathcal{S}$ denotes a common signal alphabet. Denote by y_n the received signal at the nth receive antenna. The received signal vector over a flat-fading MIMO channel with signal reordering is given by

$$\mathbf{y} = [y_1, \ldots, y_N]^{\mathrm{T}} = \mathbf{H}_{\mathcal{K}}\mathbf{s}_{\mathcal{K}} + \mathbf{n}, \tag{4.1}$$

where the $N \times N$ channel matrix $\mathbf{H}_{\mathcal{K}} = \left[\mathbf{h}_{k_{(1)}}, \ldots, \mathbf{h}_{k_{(N)}}\right]$, the transmit signal vector $\mathbf{s}_{\mathcal{K}} = \left[s_{k_{(1)}}, \ldots, s_{k_{(N)}}\right]^{\mathrm{T}}$, and the noise vector $\mathbf{n} = [n_1, \ldots, n_N]^{\mathrm{T}}$ which is a zero-mean CSCG random vector with $E[\mathbf{n}\mathbf{n}^{\mathrm{H}}] = N_0\mathbf{I}$. Here, the superscript T and H denote the transpose and Hermitian transpose, respectively. Note that $\mathbf{h}_{k_{(n)}}$ denotes the $k_{(n)}$th column vector of $\mathbf{H}_{\mathcal{K}}$ and the CRIS is denoted by $\mathcal{K} = \left\{k_{(1)}, \ldots, k_{(N)}\right\}$, which is a permutation of $\{1, 2, \ldots, N\}$. Throughout the chapter, we assume that the CSI is perfectly known at the receiver.

With the QR factorization $\mathbf{H}_{\mathcal{K}} = \mathbf{Q}_{\mathcal{K}}\mathbf{R}_{\mathcal{K}}$, where $N \times N$ matrices $\mathbf{Q}_{\mathcal{K}}$ and $\mathbf{R}_{\mathcal{K}}$ are unitary and upper triangular, respectively, from (4.1), we have $\mathbf{x} = \mathbf{Q}_{\mathcal{K}}^{\mathrm{H}}\mathbf{y} = \mathbf{R}_{\mathcal{K}}\mathbf{s}_{\mathcal{K}} + \mathbf{n}$. By defining two sub-CRIS's as $\mathcal{K}_1 = \left\{k_{(1)}, \ldots k_{(N-M)}\right\}$ and $\mathcal{K}_2 = \left\{k_{(N-M+1)}, \ldots k_{(N)}\right\}$, where $M < N$, we have $\mathbf{x} = \left[\mathbf{x}_1^{\mathrm{T}}\ \mathbf{x}_2^{\mathrm{T}}\right]^{\mathrm{T}}$, $\mathbf{s}_{\mathcal{K}} = \left[\mathbf{s}_{\mathcal{K}_1}^{\mathrm{T}}\ \mathbf{s}_{\mathcal{K}_2}^{\mathrm{T}}\right]^{\mathrm{T}}$, and $\mathbf{n} = \left[\mathbf{n}_1^{\mathrm{T}}\ \mathbf{n}_2^{\mathrm{T}}\right]^{\mathrm{T}}$ (i.e., $\mathbf{x}_2$ and $\mathbf{n}_2$ are $M \times 1$ sub-vectors of $\mathbf{x}$ and $\mathbf{n}$, respectively).

Then, $\mathbf{x}$ is rewritten as

$$\begin{bmatrix} \mathbf{x}_1 \\ \mathbf{x}_2 \end{bmatrix} = \begin{bmatrix} \mathbf{A}_{\mathcal{K}_1} & \mathbf{C} \\ \mathbf{0} & \mathbf{B}_{\mathcal{K}_2} \end{bmatrix} \begin{bmatrix} \mathbf{s}_{\mathcal{K}_1} \\ \mathbf{s}_{\mathcal{K}_2} \end{bmatrix} + \begin{bmatrix} \mathbf{n}_1 \\ \mathbf{n}_2 \end{bmatrix}. \tag{4.2}$$

From (4.2), a two-layer detection is carried out, namely the LR-based list detection [28], which is summarized as follows:

a) Perform a LR-based detector on $\mathbf{x}_2$ to obtain $\hat{\mathbf{u}}_2$, which is an estimated vector of $\mathbf{s}_{\mathcal{K}_2}$ in LR domain. Generate a list of candidate vectors $\mathcal{U}_2$ for $\hat{\mathbf{u}}_2$, by choosing the Q closest vectors to $\hat{\mathbf{u}}_2$, where $\mathcal{U}_2 = \left\{\hat{\mathbf{u}}_2^{(1)}, \hat{\mathbf{u}}_2^{(2)}, \ldots, \hat{\mathbf{u}}_2^{(Q)}\right\}$ and $\| \hat{\mathbf{u}}_2^{(1)} - \hat{\mathbf{u}}_2 \| \leq \| \hat{\mathbf{u}}_2^{(2)} - \hat{\mathbf{u}}_2 \| \leq \cdots \leq \| \hat{\mathbf{u}}_2^{(Q)} - \hat{\mathbf{u}}_2 \|$.

b) Denote by $\mathcal{S}_2$ the list of candidates for $\mathbf{s}_{\mathcal{K}_2}$, is mapped from $\mathcal{U}_2$, where $\mathcal{S}_2 = \left\{\hat{\mathbf{s}}_{\mathcal{K}_2}^{(1)}, \hat{\mathbf{s}}_{\mathcal{K}_2}^{(2)}, \ldots, \hat{\mathbf{s}}_{\mathcal{K}_2}^{(Q)}\right\}$ and $Q \leq |\mathcal{S}|^M$. Let $\mathbf{x}_1^{(q)} = \mathbf{x}_1 - \mathbf{C}\hat{\mathbf{s}}_{\mathcal{K}_2}^{(q)}$, $q = 1, 2, \ldots, Q$. LR-based detector is performed on $\mathbf{x}_1^{(q)}$ to estimate $\mathbf{s}_{\mathcal{K}_1}$ in the LR domain, the resulting vector is denoted by $\hat{\mathbf{u}}_1^{(q)}$.

c) Mapping $\hat{\mathbf{u}}_1^{(q)}$ to $\hat{\mathbf{s}}_{\mathcal{K}_1}^{(q)}$, let $\hat{\mathbf{s}}_{\mathcal{K}}^{(q)} = \left[\left(\hat{\mathbf{s}}_{\mathcal{K}_1}^{(q)}\right)^{\mathrm{T}} \left(\hat{\mathbf{s}}_{\mathcal{K}_2}^{(q)}\right)^{\mathrm{T}}\right]^{\mathrm{T}}$, the final hard decision is obtain by

$$\hat{\mathbf{s}}_{\mathcal{K}} = \arg \min_{\hat{\mathbf{s}}_{\mathcal{K}}^{(q)} \in \{\hat{\mathbf{s}}_{\mathcal{K}}^{(1)}, \ldots, \hat{\mathbf{s}}_{\mathcal{K}}^{(Q)}\}} \| \mathbf{x} - \mathbf{R}_{\mathcal{K}} \hat{\mathbf{s}}_{\mathcal{K}}^{(q)} \|^2 . \tag{4.3}$$

Since the list in *a*) is generate in LR domain, with the LR-based detection employed to detect $\mathbf{s}_{\mathcal{K}_2}$ and $\mathbf{s}_{\mathcal{K}_1}$ in two layers, a low complexity and good performance is guaranteed at the same time.

4.3 Error Probability based Column Reordering Criteria

Denote by $\bar{\mathbf{A}}_{\mathcal{K}_1}$ and $\bar{\mathbf{B}}_{\mathcal{K}_2}$ the lattice reduced matrices of $\mathbf{A}_{\mathcal{K}_1}$ and $\mathbf{B}_{\mathcal{K}_2}$, respectively. The performance of the LR-based list detection highly depends on: *i*) the list length Q; *ii*) the level of orthogonality of $\bar{\mathbf{A}}_{\mathcal{K}_1}$ and $\bar{\mathbf{B}}_{\mathcal{K}_2}$; *iii*) the performance of LR-based sub-detectors employed to detect $\mathbf{s}_{\mathcal{K}_1}$ and $\mathbf{s}_{\mathcal{K}_2}$ in terms of the error probability. Since the impact of Q (on performance and complexity) is

well discussed in [28], in this chapter, we aim to improve the performance of the LR-based list detection with a fixed Q. We note that for a channel matrix $\mathbf{H}_{\mathcal{K}}$, different $\mathcal{K}$ leads to different $\{\bar{\mathbf{A}}_{\mathcal{K}_1}, \bar{\mathbf{B}}_{\mathcal{K}_2}\}$, which results in different performance.

In order to obtain an optimal CRIS $\mathcal{K}$ to improve the performance, based on the well-known *Orthogonal Deficiency* (OD) [25], we first introduce a CRC (OD-CRC) to generate the most orthogonal $\{\bar{\mathbf{A}}_{\mathcal{K}_1}, \bar{\mathbf{B}}_{\mathcal{K}_2}\}$. Then, by taking account into an actual employed sub-detector, we propose an error probability (EP) based CRC or EP-CRC. We will compare the performance of the two CRC in simulations. Since the performance of LR-based list detection highly depends on the reliability of the detected $\mathbf{s}_{\mathcal{K}_2}$ (e.g., the error probability of the first layer detection plays a key role in overall performance), both OD-CRC and EP-CRC perform into two-layer.

4.3.1 OD-CRC

Letting $\bar{\mathcal{K}} = \{1, 2, \ldots, N\}$, the sub-CRIS $\mathcal{K}_2^{\mathrm{OD}}$ is obtained as

$$\mathcal{K}_2^{\mathrm{OD}} = \arg \min_{\mathcal{K}_2 \subset \bar{\mathcal{K}}} \mathcal{OD}(\bar{\mathbf{B}}_{\mathcal{K}_2}). \tag{4.4}$$

With $\bar{\mathcal{K}} \Leftarrow \bar{\mathcal{K}} \setminus \mathcal{K}_2^{\mathrm{OD}}$, the sub-CRIS $\mathcal{K}_1^{\mathrm{OD}}$ is given by

$$\mathcal{K}_1^{\mathrm{OD}} = \arg \min_{\mathcal{K}_1 \subset \bar{\mathcal{K}}} \mathcal{OD}(\bar{\mathbf{A}}_{\mathcal{K}_1}), \tag{4.5}$$

where " $\setminus$ " denotes the set minus and the OD function $\mathcal{OD}(\mathbf{D}) = 1 - \frac{\det(\mathbf{D}^{\mathrm{H}}\mathbf{D})}{\prod_{j=1}^{L}\|\mathbf{d}_j\|^2}$ [25] for matrix $\mathbf{D} = [\mathbf{d}_1, \ldots, \mathbf{d}_L]$. Here, $\det(\cdot)$ is the determinant. Take $\bar{\mathbf{B}}_{\mathcal{K}_2}$ as an example. Although a better performance of LR-based detection could be obtained with a more orthogonal $\bar{\mathbf{B}}_{\mathcal{K}_2}$, since the sub-matrix is nearly orthogonal as $\mathcal{OD}(\bar{\mathbf{B}}_{\mathcal{K}_2}) \approx 0$ for any $\mathcal{K}_2$ thanks to the LR, the use of OD-CRC may not improve the performance significantly.

4.3.2 Proposed Criterion: EP-CRC

By extending the vector selection criteria proposed in [41, 65], a two-layer selection strategy based EP-CRC can be proposed to minimize the error probability

for a given MIMO sub-detector employed. Suppose the LR-based MMSE sub-detector is used to detect both $\mathbf{s}_{\mathcal{K}_1}$ and $\mathbf{s}_{\mathcal{K}_2}$, in the first layer, the EP-CRC is carried out to obtain the sub-CRIS $\mathcal{K}_2^{\mathrm{EP}}$ as

$$\mathcal{K}_2^{\mathrm{EP}} = \arg \max_{\mathcal{K}_2 \subset \bar{\mathcal{K}}} \lambda_{\min} \left(\bar{\mathbf{B}}_{\mathcal{K}_2}^{\mathrm{H}} \bar{\mathbf{B}}_{\mathcal{K}_2} \right). \tag{4.6}$$

With $\bar{\mathcal{K}} \Leftarrow \bar{\mathcal{K}} \setminus \mathcal{K}_2^{\mathrm{EP}}$, in the second layer, the $\mathcal{K}_1^{\mathrm{EP}}$ is given by

$$\mathcal{K}_1^{\mathrm{EP}} = \arg \max_{\mathcal{K}_1 \subset \bar{\mathcal{K}}} \lambda_{\min} \left(\bar{\mathbf{A}}_{\mathcal{K}_1}^{\mathrm{H}} \bar{\mathbf{A}}_{\mathcal{K}_1} \right), \tag{4.7}$$

where $\lambda_{\min}(\cdot)$ denotes the minimum eigenvalue. This criterion is regarded as the ME, which is known to minimize the error probability for a given lattice reduced matrix. Note that the MD criterion [41, 65] can also be given for the LR-based MMSE-SIC sub-detector.

4.4 Simulation Results

We present simulation results with MIMO channels whose elements are generated as independent CSCG random variables with mean zero and unit variance. The SNR is defined as the energy per bit to the noise power spectral density ratio, E_b/N_o. We use 16-QAM for signaling with Gray mapping. Different MIMO detection methods are considered, namely **I**: MMSE detection, **II**: ML detection, **III**: LR-based MMSE detection [22], **IV**: LR-based list detection using LR-based MMSE sub-detection, **V**: OD-CRC employed for detection **IV**, **VI**: EP-CRC employed for detection **IV**.

In Fig. 4.1, in terms of BER versus SNR, we show simulation results of 6 different detectors on 4×4 MIMO systems. Here, we assume $M = 2$ and $Q = 4$ for detection **IV**, **V**, and **VI**. It shows that by using OD-CRC, the performance of detection **IV** cannot be improved. With our proposed EP-CRC, a more than 2 dB improvement is observed at BER $= 10^{-4}$ compared to that without CRC. Moreover, we can see that detection **VI** has a SNR loss of half dB at a range of BER $= 10^{-3}$ to 10^{-5} compared with the ML detection (i.e., detection **II**).

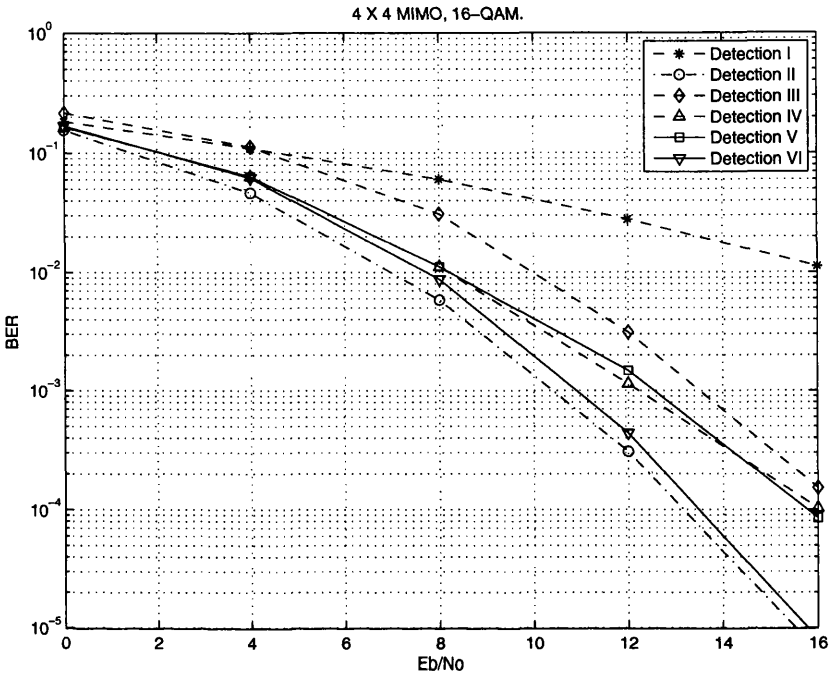

Figure 4.1: BER versus E_b/N_o of different MIMO detection for 16-QAM, $\{N, M, Q\} = \{4, 2, 4\}$.

Since the complexity for obtaining $\{\bar{\mathbf{A}}_{\mathcal{K}_1}, \bar{\mathbf{B}}_{\mathcal{K}_2}\}$ is well discussed in [28], here, we analysis the computational complexity for EP-CRC only. Denote by $C_{\text{ME,A}}$ and $C_{\text{ME,B}}$ the complexity of ME operation on $\bar{\mathbf{A}}_{\mathcal{K}_1}$ and $\bar{\mathbf{B}}_{\mathcal{K}_2}$, respectively. The overall complexity for EP-CRC is given by $C_{\text{EP-CRC}} = \prod_{u=0}^{M-1}(N-u)\mathcal{C}_{\text{ME,B}} + \prod_{v=1}^{N-M} v\mathcal{C}_{\text{ME,A}}$. Note that EP-CRC is only employed once for a channel matrix. For slow fading channels, since the coherence time is long, the extra computational complexity required for EP-CRC per each symbol detection would be negligible. Under the assumption that the channel is not varying in the duration of 1000 transmitted symbol vectors, with the same MIMO system used in simulations, we compare the computational complexity for each symbol vector detection by employing detection **VI** and other detection methods in terms of the average number of flops[1]. The flops per symbol vector of different detection

[1]We simulate these systems using MATLAB-V5.3 on a PC. The MATLAB command "flops" is used to count the number of flops.

methods are listed as follows: Detection **I**: 458, Detection **II**: 11140, Detection **III**: 467, Detection **IV**: 957, Detection **VI**: 979.

4.5 Conclusion

In this chapter, we proposed EP-CRC for LR-based list detection. We compared OD-CRC with our proposed EP-CRC. It showed that with our proposed EP-CRC, the performance of LR-based list detection is significantly improved. Furthermore, a near optimal performance can be achieved with a small list length by employing EP-CRC, where a low complexity is considered.

So far, we have developed two low complexity detection methods for MIMO systems with square or tall channel matrices. However, it is not straightforward to develop a detection method that can be adopted into underdetermined MIMO systems to achieve a good performance and a low complexity at the same time. For this sake, we propose a pre-voting cancellation based detection for such a system in the next chapter.

5

Pre-voting Cancellation based Detection for Underdetermined MIMO Systems

5.1 Introduction

In MIMO systems, the channel matrix is called fat, square, or tall matrix if the number of transmit antennas M is greater than, equal to, or smaller than the number of receive antennas N. According to [1], the MIMO channel capacity can be approximated as $C_{\text{MIMO}} \simeq \min(M, N)C_{\text{SISO}}$, where C_{SISO} denotes the channel capacity of single-input single-output channels. Thus, with regard to capacity, we may prefer a square channel matrix (i.e., $M = N$). However, if we need to employ a lower order modulation due to a limited receiver's complexity, we can consider a fat channel matrix (i.e., $M > N$), because the spectral efficiency per transmit antenna can be lower as $\frac{C_{\text{MIMO}}}{M} = \frac{N}{M}C_{\text{SISO}} < C_{\text{SISO}}$. For this reason, in this chapter, we focus on underdetermined MIMO systems[1].

For the detection in underdetermined MIMO systems, various techniques can be considered. Instead of exhaustive searching for all the possible decision vectors as in the ML detection, list-based detectors [5, 6, 7, 8, 9, 10, 11] create a list of candidate decision vectors and then choose the best candidate as their

[1]Throughout this chapter, it is assumed that different symbols transmitted by M transmit antennas are linear independent with others within a time slot.

final decision. In [12, 13, 14, 15, 16, 17], a family of list-based Chase detectors are proposed. Since the Chase detection cannot achieve a full receive diversity order, especially when underdetermined MIMO systems are considered, GSD approaches [29, 30, 31, 32, 33] were developed. In [34], two sub-optimal group detectors are introduced and a geometrical approach based detection for underdertermined MIMO systems is studied in [35]. To further reduce the complexity, a computationally efficient GSD-based detector with column reordering is proposed in [36], namely, "tree search decoder - column reordering" (TSD-CR). However, their complexity is still high. Moreover, the LR-based detector is only applicable to the case of tall or square channel matrices [22, 25]. Hence, we need to develop a detector that can be employed for fat channel matrices and has a near optimal performance with a reasonably low complexity, especially for a low order modulation.

To apply MIMO detectors to underdertermined MIMO systems, in this chapter, a PVC-based MIMO (PVC-MIMO) detection approach is proposed. The main idea of the proposed detector is to divide the transmitted symbols into two groups. First, one or more reference symbols are selected out of all the transmitted symbols as the pre-voting vector (the residual symbols from the post-voting vector) and all the possible candidate symbols for the pre-voting vector are considered (e.g. for 2 symbols are selected for the pre-voting vector and 4-QAM method is used, there are $4 \times 4 = 16$ possible candidate symbol vectors to be considered). Then, for each candidate pre-voting vector, its contribution (as the interference) is canceled from the received signal and the remaining symbol estimates are obtained by a sub-detector (which could be a linear detector or LR-based detector) operating on size-reduced square sub-channels. The final hard-decision symbol vector is obtained by taking the one that minimizes the Euclidean distance metric among the candidate vectors. Note that the size of pre-voting vectors is determined to generate square sub-channels (e.g., for a 2×4 channel matrix, 2 symbols are selected for the pre-voting vectors and the size of sub-channel matrix is 2×2 square matrix). With a LR-based detector for the sub-detection, theoretical and numerical results show that the proposed approach can achieve a full receive diversity order.

In [41], user selection criteria are considered for multiuser MIMO systems, where a single user is selected to transmit signals to a BS at a time. By viewing multiuser MIMO as virtual antennas in a single user MIMO system, the user selection problems can be regarded as the transmit antenna selection problems. In this chapter, we extend the selection criteria in [41] to support multiple antennas (transmit symbols) at a time for the PVC-MIMO detection where there are more transmit antennas than receive antennas. This extension of the antenna selection, namely the PVS, becomes a combinatorial problem. Using low complexity sub-optimal detectors (LR-based detectors or linear detectors) for the sub-detection, with an optimal PVS, it is also shown that a near ML performance can be achieved. For slow fading MIMO channels, through simulations, we show that the computational complexity of the proposed PVC-MIMO detection with PVS is lower than that of TSD-CR.

The rest of the chapter is organized as follows. The system model and our proposed pre-voting cancellation based MIMO detection are presented in Section 5.2. The optimal PVS is discussed in Section 5.3. The performance of the proposed PVC-MIMO detectors is analyzed in Section 5.4. Simulation results and some further discussions are presented in Section 5.5. Finally, we conclude this chapter in Section 5.6 with some remarks.

Throughout the chapter, complex-valued vectors and matrices are represented by bold letters. We use Round-Gothic symbols to represent real-valued vectors and matrices. For a matrix $\mathbf{A}$, $\mathbf{A}^{\mathrm{T}}$, $\mathbf{A}^{\mathrm{H}}$, and $\mathbf{A}^{\dagger}$ denote its transpose, Hermitian transpose, and pseudo-inverse, respectively. $E[\cdot]$ denotes the statistical expectation. In addition, for a vector or matrix, $\|\cdot\|$ denotes the 2-norm. $\lceil\beta\rfloor$ denotes the nearest integer to β. Denote by $\setminus$ the set minus, by $\mathbf{I}_n$ an $n \times n$ identity matrix, and by $\mathcal{K} = \{k_{(1)}, k_{(2)}, \dots\}$ the collection set of $k_{(1)}, k_{(2)}, \dots$. The (p,q)-th element of a matrix $\mathbf{R}$ is denoted by $[\mathbf{R}]_{p,q}$.

5.2 Joint Detection for Underdetermined MIMO Systems

We consider underdetermined MIMO systems with a receiver of limited complexity, where low order modulation is employed as mentioned earlier. This would be the case for downlink channels in cellular systems where the transmitter is a BS and the receiver is a mobile terminal which usually has a small number of receive antennas and a limited computing power for detection. In this section, we present the system model for this underdetermined MIMO system and introduce our PVC-MIMO detection after brief description of some existing approaches.

5.2.1 System Model

Consider a MIMO system with M transmit and N receive antennas. Let s_m denote the data symbol to be transmitted by the mth transmit antenna. Assume that a common signal alphabet, denoted by $\mathcal{S}$, is used for all s_m. That is, $s_m \in \mathcal{S}$, $m = 1, 2, \ldots, M$. Furthermore, let $\mathcal{S}^A$ and $|\mathcal{S}|$ represent the A-dimensional Cartesian product and cardinality of $\mathcal{S}$, respectively. Denote by y_n the received signal at the nth receive antenna, $n = 1, 2, \ldots, N$. Then, the received signal vector over a flat-fading MIMO channel is given by

$$\begin{aligned} \mathbf{y} &= [y_1, y_2, \ldots, y_N]^{\mathrm{T}} \\ &= \mathbf{H}\mathbf{s} + \mathbf{n}, \end{aligned} \tag{5.1}$$

where $\mathbf{s} = [s_1, s_2, \ldots, s_M]^{\mathrm{T}}$ is the transmit signal vector, and $\mathbf{n} = [n_1, n_2, \ldots, n_N]^{\mathrm{T}}$ is the noise vector which is assumed to be a zero-mean CSCG random vector with $E[\mathbf{n}\mathbf{n}^{\mathrm{H}}] = N_0\mathbf{I}$. Here, $\mathbf{H}$ is the channel matrix which can also be written as

$$\mathbf{H} = [\mathbf{h}_1, \mathbf{h}_2, \ldots, \mathbf{h}_M], \tag{5.2}$$

where $\mathbf{h}_m$ denotes the mth column vector of $\mathbf{H}$. Throughout this chapter, we assume that the CSI is perfectly known at the receiver. The impact of channel estimation error on the performance will be discussed in Subsection 5.5.2.

5.2.2 Existing Approaches

Taking the equation in (5.1) as a linear system, various numerical algorithms can be used to estimate or detect $\mathbf{s}$ when the system is overdetermined (i.e., $M \leq N$). In particular, in [19] and [22], the LR-based detectors, which can provide a good performance with a low computational complexity, have been proposed to detect $\mathbf{s}$. However, if the MIMO system is underdetermined (i.e., $M > N$), few approaches (including an exhaustive search for the ML detection, list-based detection, and GSD technique) could be applied to the MIMO detection.

In this subsection, we briefly review two existing approaches, namely, list-based Chase detection and GSD-based detection, which are comparable to our proposed PVC-MIMO detection. The PVC-MIMO will be introduced in the next subsection.

5.2.2.1 Chase Detection

By dividing the symbols to be detected into two layers, the list-based Chase detection [12, 13, 14, 15, 16, 17] is carried out. With the system model shown in (5.1), the sub-vector $\mathbf{s}_\mathcal{J}$ of sized $(M-N) \times 1$ to be detected in the first layer is selected from $\mathbf{s}$ as the one with the smallest MSE (i.e., equivalently the highest SNR) and a list of Q candidates for this sub-vector is constructed. In the second layer, the contribution from the detected sub-vector is treated as the interference and is canceled from the received signal. Then, the sub-detection is employed with the corresponding $N \times N$ sub-channel matrix to detect the residual $N \times 1$ sub-vector[1].

With the Chase detector, a low complexity implementation can be obtained with a small list length Q. The performance of the Chase detector in above highly depends on the reliability of detected $\mathbf{s}_\mathcal{J}$. Note that when $\mathbf{H}$ is square, a QR factorization-based SIC can be carried out to estimate $\mathbf{s}_\mathcal{J}$ without the impact of interference. However, for underdetermined MIMO systems, since a linear detector to obtain a list of candidate vectors for $\mathbf{s}_\mathcal{J}$ suffers from the interference, a good performance cannot be achieved with the Chase detector, which is studied by simulations in Section 5.5.

[1]For the details of the list-based Chase detection, please see Section 2.2

5.2.2.2 GSD-based detection

To apply the well known sphere decoding (SD) to underdetermined MIMO detection, the GSD-based detection is proposed which provides a near ML performance [29, 30, 31, 32, 33, 34, 35, 36]. By viewing $\mathcal{S}$ as a $2^{|\mathcal{S}|}$-PAM signal set, where a mapping strategy is considered, the GSD-based detection is carried out to detect $\mathbf{s}$ by solving the underdetermined integer least squares (UILS) problem as

$$\hat{\mathbf{s}}_r = \arg \min_{\mathbf{s}_r \in \mathcal{S}^{2M}} \| \mathbf{y}_r - \mathbf{H}_r \mathbf{s}_r \|^2, \tag{5.3}$$

where real-valued vectors $\mathbf{y}_r = [\mathsf{y}_1, \mathsf{y}_2, \ldots, \mathsf{y}_{2N}]^{\mathrm{T}}$, $\mathbf{s}_r = [\mathsf{s}_1, \mathsf{s}_2, \ldots, \mathsf{s}_{2M}]^{\mathrm{T}}$, and matrix $\mathbf{H}_r$ of $2N \times 2M$, are transformed from complex-valued $\mathbf{y}$, $\mathbf{s}$, and $\mathbf{H}$ in (5.1), respectively, by using the approach introduced in [36]. With the QR factorization of $\mathbf{H}_r$, we have $\mathbf{H}_r = \mathbf{Q}_r \mathbf{R}_r$, where real-valued $2N \times 2N$ $\mathbf{Q}_r$ and $2N \times 2M$ $\mathbf{R}_r$ are unitary and upper trapezoidal, respectively. Letting $\bar{\mathbf{y}}_r = \mathbf{Q}_r^{\mathrm{T}} \mathbf{y}_r$, we have $\bar{\mathbf{y}}_r = \left[\bar{\mathbf{y}}_{r(\mathcal{A})}^{\mathrm{T}} \;\; \bar{\mathsf{y}}_{2N}\right]^{\mathrm{T}}$, $\mathbf{R}_r = \begin{bmatrix} \mathbf{R}_{r(1)} & \mathbf{R}_{r(2)} \\ 0 \cdots 0 & \mathbf{r}_r^{\mathrm{T}} \end{bmatrix}$, and $\mathbf{s}_r = \left[\mathbf{s}_{r(\mathcal{A})}^{\mathrm{T}} \;\; \mathbf{s}_{r(\mathcal{B})}^{\mathrm{T}}\right]^{\mathrm{T}}$, where $\bar{\mathbf{y}}_{r(\mathcal{A})} = [\bar{\mathsf{y}}_1, \bar{\mathsf{y}}_2, \ldots, \bar{\mathsf{y}}_{2N-1}]^{\mathrm{T}}$, $\mathbf{r}_r = [\mathsf{r}_1, \mathsf{r}_2, \ldots, \mathsf{r}_{2M-2N+1}]^{\mathrm{T}}$, $\mathbf{s}_{r(\mathcal{A})} = [\mathsf{s}_1, \mathsf{s}_2, \ldots, \mathsf{s}_{2N-1}]^{\mathrm{T}}$, and $\mathbf{s}_{r(\mathcal{B})} = [\mathsf{s}_{2N}, \mathsf{s}_{2N+1}, \ldots, \mathsf{s}_{2M}]^{\mathrm{T}}$. Note that $M > N$. Then, the following two-layer detection is carried out to solve the problem in (5.3) as

$$\begin{aligned} \hat{\mathbf{s}}_r &= \arg \min_{\mathbf{s}_r \in \mathcal{S}^{2M}} \| \bar{\mathbf{y}}_r - \mathbf{R}_r \mathbf{s}_r \|^2 \\ &= \arg \min_{\mathbf{s}_{r(\mathcal{B})} \in \mathcal{S}^{2M-2N+1}} \Big\{ \left(\bar{\mathsf{y}}_{2N} - \mathbf{r}_r^{\mathrm{T}} \mathbf{s}_{r(\mathcal{B})}\right)^2 \\ &\quad + \arg \min_{\mathbf{s}_{r(\mathcal{A})} \in \mathcal{S}^{2N-1}} \| \left(\bar{\mathbf{y}}_{r(\mathcal{A})} - \mathbf{R}_{r(2)} \mathbf{s}_{r(\mathcal{B})}\right) - \mathbf{R}_{r(1)} \mathbf{s}_{r(\mathcal{A})} \|^2 \Big\}. \end{aligned} \tag{5.4}$$

To apply a GSD based detector, a radius λ is chosen such that

$$\| \bar{\mathbf{y}}_r - \mathbf{R}_r \mathbf{s}_r \|^2 < \lambda^2. \tag{5.5}$$

From (5.4) and (5.5), we can also show that

$$\left(\bar{\mathsf{y}}_{2N} - \mathbf{r}_r^{\mathrm{T}} \mathbf{s}_{r(\mathcal{B})}\right)^2 < \lambda^2. \tag{5.6}$$

With a fixed $\mathbf{s}_{r(\mathcal{B})}$, a conventional SD algorithm is carried out to solve the problem in (5.4). The initial idea of GSD is proposed in [29], which takes every

possible candidates of $\mathbf{s}_{r(\mathcal{B})}$ to obtain the final decision. Note that the exhaustive search leads to a high computational complexity. To reduce the complexity, various computationally efficient algorithms [30, 31, 32, 33] are proposed. Using a column reordering strategy, the TSD-CR is introduced in [36] to further reduce the complexity. Although the GSD-based detection can provide a near ML performance, its complexity is still high in some applications, which is studied through simulations in Section 5.5.

5.2.3 Proposed Approach: Pre-voting Cancellation based MIMO Detection

For underdetermined MIMO systems, since a low complexity and a good performance cannot be obtained by existed MIMO detectors (i.e., MMSE detector, ML detector, list-based detectors [12, 13, 14, 15, 16, 17], and GSD-based detectors [29, 30, 31, 32, 33, 36]) at the same time, in this subsection, we propose the PVC-MIMO detection.

Let $R = M - N$ and denote by $\mathcal{P} = \{p_1, p_2, \ldots, p_R\}$ the index set for the pre-voting signal vector (the selection of this vector will be discussed in Section 5.3), which is denoted by $\mathbf{s}_{\mathcal{P}} = [s_{p_1}, \ldots, s_{p_R}]^{\mathrm{T}}$. Then, (5.1) is rewritten as

$$\mathbf{y} = \mathbf{H}_{\mathcal{P}}\mathbf{s}_{\mathcal{P}} + \mathbf{H}_{\mathcal{Q}}\mathbf{s}_{\mathcal{Q}} + \mathbf{n}, \tag{5.7}$$

where $\mathbf{H}_{\mathcal{P}} = [\mathbf{h}_{p_1}, \ldots, \mathbf{h}_{p_R}]$ is a sub-matrix of $\mathbf{H}$ associated with $\mathbf{s}_{\mathcal{P}}$, $\mathbf{s}_{\mathcal{Q}} = [s_{q_1}, \ldots, s_{q_N}]^{\mathrm{T}}$ is the post-voting signal vector, and $\mathbf{H}_{\mathcal{Q}} = [\mathbf{h}_{q_1}, \ldots, \mathbf{h}_{q_N}]$ is a sub-matrix of $\mathbf{H}$ associated with $\mathbf{s}_{\mathcal{Q}}$. Here, the index set $\mathcal{Q}$ is given by $\mathcal{Q} = \{1, \ldots, M\} \setminus \mathcal{P}$. Note that $\mathbf{H}_{\mathcal{Q}}$ is square, and $\mathbf{s}_{\mathcal{P}} \in \mathcal{S}^R$ and $\mathbf{s}_{\mathcal{Q}} \in \mathcal{S}^N$.

Define the finite set of all the possible candidate vectors for $\mathbf{s}_{\mathcal{P}}$ as $\{\mathbf{s}_{\mathcal{P}}^1, \mathbf{s}_{\mathcal{P}}^2, \ldots, \mathbf{s}_{\mathcal{P}}^K\}$, where $K = |\mathcal{S}|^R$ [for example, $K = 4^2$ if the size of $\mathbf{s}_{\mathcal{P}}$ is 2×1 and 4-QAM is used]. Assuming that $\mathbf{s}_{\mathcal{P}} = \mathbf{s}_{\mathcal{P}}^k$, $k \in \{1, \ldots, K\}$, (5.7) is rewritten as

$$\mathbf{r}^k = \mathbf{H}_{\mathcal{Q}}\mathbf{s}_{\mathcal{Q}} + \mathbf{n}, \tag{5.8}$$

where $\mathbf{r}^k = \mathbf{y} - \mathbf{H}_{\mathcal{P}}\mathbf{s}_{\mathcal{P}}^k$. After the PVC in (5.8), we can apply any conventional MIMO detector that works for a square MIMO channel for the detection of $\mathbf{s}_{\mathcal{Q}}$.

For convenience, denote by $\hat{\mathbf{s}}_{\mathcal{Q}}^k$ the detected symbol vector of $\mathbf{s}_{\mathcal{Q}}$ (by any means) for given $\mathbf{s}_{\mathcal{P}} = \mathbf{s}_{\mathcal{P}}^k$. Let

$$\mathbf{s}^k = \begin{bmatrix} \mathbf{s}_{\mathcal{P}} \\ \hat{\mathbf{s}}_{\mathcal{Q}}^k \end{bmatrix}. \tag{5.9}$$

With K candidates of $\mathbf{s}^k$, i.e., $\{\mathbf{s}^1, \ldots, \mathbf{s}^K\}$, based on the ML detection principle, the solution of the PVC-MIMO detection is given by

$$\hat{\mathbf{s}} = \arg \min_{\mathbf{s}^k \in \{\mathbf{s}^1, \ldots, \mathbf{s}^K\}} \| \mathbf{y} - \mathbf{H}'\mathbf{s}^k \|^2, \tag{5.10}$$

where $k \in \{1, \ldots, K\}$ and $\mathbf{H}' = [\mathbf{H}_{\mathcal{P}}\ \mathbf{H}_{\mathcal{Q}}]$.

5.3 Selection for Pre-voting Vectors Depending on Sub-Detectors

In the PVC-MIMO detection, we note that different post-voting vector results in different $\mathbf{H}_{\mathcal{Q}}$ which may leads to different performance of sub-detection. In order to exploit the performance of the PVC-MIMO detection, in this section, we focus on the selection of the post-voting vector. For the sub-detection, we consider a few low complexity detectors including linear and LR-based detectors. Note that since a number of the sub-detection operations are to be repeatedly performed, the complexity of sub-detection should be low.

5.3.1 Selection Criterion with Linear Detector

As a linear detector, we consider the MMSE detector in this subsection. Under the assumption that of the pre-voting vector is correct, from (5.8), the output of the MMSE detector is given by

$$\hat{\mathbf{s}}_{\mathcal{Q}}^k = \mathbf{W}_{\text{mmse}}^{\text{H}} \mathbf{r}^k, \tag{5.11}$$

where $\mathbf{W}_{\text{mmse}}$ is the MMSE filter that is given by $\mathbf{W}_{\text{mmse}} = \left(\mathbf{H}_{\mathcal{Q}}\mathbf{H}_{\mathcal{Q}}^{\text{H}} + \frac{N_0}{E_s}\mathbf{I}_N\right)^{-1} \mathbf{H}_{\mathcal{Q}}$. Here, E_s represents the symbol energy with $\mathcal{S}$.

The detection performance depends on the channel matrix. For a given channel matrix, as discussed in [41, 66], we can have the ME selection criterion for the

selection of Ω. Since $\Omega \in \{1, \ldots, M\}$, the optimal set Ω can be found by using the ME criterion as

$$\Omega_{\mathrm{ME}} = \arg\max_{\Omega} \lambda_{\min}\left(\mathbf{H}_{\Omega}^{\mathrm{H}}\mathbf{H}_{\Omega}\right), \tag{5.12}$$

where $\lambda_{\min}(\mathbf{A})$ denotes the minimum eigenvalue of $\mathbf{A}$.

5.3.2 Selection Criteria with LR-based Linear and SIC Detectors

To determine Ω for the PVS, we consider the case where LR-based MIMO detectors, which can provide a near ML performance with low complexity [19, 22], are employed for the sub-detection.

Without loss of generality, we assume that the elements of $\mathbf{s}$ are complex integers [19, 22]. For the LR-based linear detection, from (5.8), the received signal vector can be rewritten as

$$\mathbf{r}^k = \mathbf{G}\mathbf{c} + \mathbf{n}, \tag{5.13}$$

where $\mathbf{G} = \mathbf{H}_{\Omega}\mathbf{U}^{-1}$ and $\mathbf{c} = \mathbf{U}\mathbf{s}_{\Omega}$, while $\mathbf{U}$ is an integer unimodular matrix and $\mathbf{G}$ is a LR matrix of a nearly orthogonal basis. The LR-based linear detection is carried out to detect $\mathbf{c}$ as $\hat{\mathbf{c}} = \lfloor \tilde{\mathbf{W}}\mathbf{r}^k \rceil$, where $\tilde{\mathbf{W}} = \mathbf{G}^{\dagger}$ for the ZF detector and $\tilde{\mathbf{W}} = \mathbf{G}^{\mathrm{H}}\left(\mathbf{G}\mathbf{G}^{\mathrm{H}} + \frac{N_0}{E_s}\mathbf{I}_N\right)^{-1}$ for the MMSE detection.

For the LR-based MMSE-SIC detector, $\mathbf{H}_{\Omega}$ is replaced by an extended channel matrix defined as $\mathbf{H}_{\mathrm{ex}} = \left[\mathbf{H}_{\Omega}^{\mathrm{T}} \sqrt{\frac{N_0}{E_s}}\mathbf{I}_N\right]^{\mathrm{T}}$, while $\mathbf{r}^k$ and $\mathbf{n}$ are replaced by $\mathbf{r}_{\mathrm{ex}} = \left[(\mathbf{r}^k)^{\mathrm{T}}\ \mathbf{0}\right]^{\mathrm{T}}$ and $\mathbf{n}_{\mathrm{ex}} = \left[\mathbf{n}^{\mathrm{T}}\ -\sqrt{\frac{N_0}{E_s}}\mathbf{s}_{\Omega}^{\mathrm{T}}\right]^{\mathrm{T}}$, respectively. Using the LR with $\mathbf{H}_{\mathrm{ex}}$, the lattice reduced matrix $\mathbf{G}_{\mathrm{ex}}$ can be found as $\mathbf{H}_{\mathrm{ex}} = \mathbf{G}_{\mathrm{ex}}\mathbf{U}_{\mathrm{ex}}$, where $\mathbf{U}_{\mathrm{ex}}$ is an integer unimodular matrix. The LR-based MMSE-SIC detection is carried out using the QR factorization of $\mathbf{G}_{\mathrm{ex}} = \mathbf{Q}\mathbf{R}$, where $\mathbf{R}$ is upper triangular. Multiplying $\mathbf{Q}^{\mathrm{H}}$ to $\mathbf{y}$ results in

$$\mathbf{Q}^{\mathrm{H}}\mathbf{r}_{\mathrm{ex}} = \mathbf{R}\bar{\mathbf{c}} + \bar{\mathbf{n}}, \tag{5.14}$$

where $\bar{\mathbf{c}} = \mathbf{U}_{\mathrm{ex}}\mathbf{s}_{\Omega}$ and $\bar{\mathbf{n}} = \mathbf{Q}^{\mathrm{H}}\mathbf{n}_{\mathrm{ex}}$. The SIC is performed with (5.8). With the upper triangular matrix $\mathbf{R}$, the last element of $\bar{\mathbf{c}}$, i.e., the Nth layer, is detected first. Then, in the detection of the $(N-1)$th layer, the contribution of the last

element of $\bar{\mathbf{c}}$ is canceled and the signal of the $(N-1)$th layer is detected. This operation is terminated when all the layers are detected.

With the LR-based MMSE and MMSE-SIC detectors performed on $\mathbf{H}_{\mathcal{Q}}$, where $\mathcal{Q} \in \{1, \ldots, M\}$, the optimal set $\mathcal{Q}$ can be found by using the ME and the MD selection criteria [41], which are shown as

$$\mathcal{Q}_{\mathrm{ME}} = \arg\max_{\mathcal{Q}} \lambda_{\min}\left(\mathbf{G}_{\mathcal{Q}}^{\mathrm{H}}\mathbf{G}_{\mathcal{Q}}\right) \tag{5.15}$$

and

$$\mathcal{Q}_{\mathrm{MD}} = \arg\min_{\mathcal{Q}} \left\{ \min_{r} \mid r_{r,r}^{(\mathcal{Q})} \mid \right\}, \tag{5.16}$$

respectively, where $\mathbf{G}_{\mathcal{Q}}$ is the lattice reduced basis from $\mathbf{H}_{\mathcal{Q}}$ and $r_{r,r}^{(\mathcal{Q})}$ denotes the (r,r)th element of $\mathbf{R}$ from $\mathbf{H}_{\mathcal{Q}}$ in (5.8).

5.4 Performance Analysis

In this section, we consider the diversity gain of the proposed PVC-MIMO detector through the error probability under the assumption that the elements of $\mathbf{H}$ are independent CSCG random variables with mean zero and unit variance, i.e., Rayleigh MIMO channels. We also discuss the complexity of the PVC-MIMO detection.

5.4.1 Diversity Analysis

In order to characterize the error probability of the PVC-MIMO detection, let $\mathbf{s}^o$ represent the original transmitted vectors, and $\mathbb{S} = \{\mathbf{s}^1, \ldots, \mathbf{s}^K\}$ represent the set of the candidate solutions provided by the PVC, where each $\mathbf{s}^k$ is generated from (5.9), i.e., $\mathbf{s}^k = \left[\mathbf{s}_{\mathcal{P}}^{k\mathrm{T}}\ \hat{\mathbf{s}}_{\mathcal{Q}}^{k\mathrm{T}}\right]^{\mathrm{T}}$, $k = 1, 2, \ldots, K$. Let $\hat{\mathbf{s}}$ represent the final decision of the detector selected from the candidate solutions in $\mathbb{S}$ obtained in (5.10). Then, we can define two error probabilities as follows:

Definition 1 *We define the probability that the transmitted symbol vector does not belong to the set of candidate solutions as* $P_{e,\mathrm{PV}} = \Pr\left(\mathbf{s}^o \notin \mathbb{S}\right) = 1 - \Pr\left(\mathbf{s}^o \in \mathbb{S}\right)$, *i.e.,* $\Pr\left(\mathbf{s}^o \in \mathbb{S}\right) = \Pr\left(\exists \mathbf{s}^{k'} \in \mathbb{S} : \mathbf{s}^{k'} = \mathbf{s}^o\right)$, $k' = 1, 2, \ldots, K$, *where the event of* $\{\exists x : f(x)\}$ *denotes there is at least one* x *such that a function of* x, $f(x)$, *is true.*

Definition 2 *We define the probability that the final decision is not the transmitted one provided that the transmitted vector belongs to the set of candidate solutions as* $P_{e,\mathrm{SEL}}$. *In other words,* $P_{e,\mathrm{SEL}}$ *is the probability that the final decision is not correct conditioned on* $\mathbf{s}^o \in \mathbb{S}$, *i.e.,* $P_{e,\mathrm{SEL}} = \Pr\left(\hat{\mathbf{s}} \neq \mathbf{s}^o \middle| \mathbf{s}^o \in \mathbb{S}\right)$.

Using these two probabilities, the error probability of the PVC-MIMO detection can be given by

$$P_e = 1 - (1 - P_{e,\mathrm{PV}})(1 - P_{e,\mathrm{SEL}}) = P_{e,\mathrm{PV}} + P_{e,\mathrm{SEL}} - P_{e,\mathrm{PV}} P_{e,\mathrm{SEL}}. \tag{5.17}$$

We will first discuss the error probability when a LR-based detector is employed for the sub-detection of PVC-MIMO without PVS. Since a LR-based detector can provide a full receive diversity [25, 67], the PVC-MIMO detection can provide a reasonably good performance even without PVS. Next, we will consider the error probability when a linear detector is employed. In this case, the PVS plays a crucial role in achieving a good performance.

5.4.1.1 Error Probability with LR-based Detectors

Let us consider the case where LR-based detectors are used for the sub-detection of PVC-MIMO *without* PVS.

A sufficient and necessary condition for $\mathbf{s}^o \in \mathbb{S}$ is given by $\{\exists \mathbf{s}^{k'} \in \mathbb{S} : \mathbf{s}^{k'} = \mathbf{s}^o\}$. In the proposed PVC approach, noting that $\mathbf{s}^k = \left[\mathbf{s}_{\mathcal{P}}^{k\mathrm{T}}\ \hat{\mathbf{s}}_{\mathcal{Q}}^{k\mathrm{T}}\right]^{\mathrm{T}}$ and $\mathbf{s}^o = \left[\mathbf{s}_{\mathcal{P}}^{o\mathrm{T}}\ \mathbf{s}_{\mathcal{Q}}^{o\mathrm{T}}\right]^{\mathrm{T}}$, we have $\Pr\left(\mathbf{s}^o \in \mathbb{S}\right) = \Pr\left(\exists \mathbf{s}^{k'} \in \mathbb{S} : \mathbf{s}_{\mathcal{P}}^{k'} = \mathbf{s}_{\mathcal{P}}^o, \hat{\mathbf{s}}_{\mathcal{Q}}^{k'} = \mathbf{s}_{\mathcal{Q}}^o\right)$. That is, we have $\mathbf{s}^o \in \mathbb{S}$ if and only if there exists a candidate solution $\mathbf{s}^{k'}$ ($\mathbf{s}^{k'} \in \mathbb{S}$ and $\mathbf{s}^{k'} = \left[\mathbf{s}_{\mathcal{P}}^{k'\mathrm{T}}\ \hat{\mathbf{s}}_{\mathcal{Q}}^{k'\mathrm{T}}\right]^{\mathrm{T}}$), where the selected $\mathbf{s}_{\mathcal{P}}$ by the PVC approach, i.e., $\mathbf{s}_{\mathcal{P}}^{k'}$ in $\mathbf{s}^{k'}$, satisfies $\mathbf{s}_{\mathcal{P}}^{k'} = \mathbf{s}_{\mathcal{P}}^o$, and the detected post-voting vector (see (5.8)) after this PVC, i.e., $\hat{\mathbf{s}}_{\mathcal{Q}}^{k'}$ in $\mathbf{s}^{k'}$, also satisfies $\hat{\mathbf{s}}_{\mathcal{Q}}^{k'} = \mathbf{s}_{\mathcal{Q}}^o$. Note that with the exhaustive search approach of PVC, we have $\Pr\left(\exists \mathbf{s}^{k'} \in \mathbb{S} : \mathbf{s}_{\mathcal{P}}^{k'} = \mathbf{s}_{\mathcal{P}}^o\right) = 1$. Hence, we have

$$\begin{aligned} P_{e,\mathrm{PV}} &= 1 - \Pr(\mathbf{s}^o \in \mathbb{S}) = 1 - \Pr\left(\exists \mathbf{s}^{k'} \in \mathbb{S} : \mathbf{s}_{\mathcal{P}}^{k'} = \mathbf{s}_{\mathcal{P}}^o, \hat{\mathbf{s}}_{\mathcal{Q}}^{k'} = \mathbf{s}_{\mathcal{Q}}^o\right) \\ &= 1 - \Pr\left(\hat{\mathbf{s}}_{\mathcal{Q}}^{k'} = \mathbf{s}_{\mathcal{Q}}^o \middle| \mathbf{s}_{\mathcal{P}}^{k'} = \mathbf{s}_{\mathcal{P}}^o\right) = E_{\mathbf{H}_{\mathcal{Q}}}\left[P_{e|\mathbf{H}_{\mathcal{Q}}}\right], \end{aligned} \tag{5.18}$$

where $P_{e|\mathbf{H}_{\mathcal{Q}}}$ denotes the error probability of the sub-detection that detects $\mathbf{s}_{\mathcal{Q}}$ for given $\mathbf{H}_{\mathcal{Q}}$. That is, $P_{e,\mathrm{PV}}$ in (5.18) is equivalent to the (average) error probability of the sub-detection performed on the square sub-matrix, $\mathbf{H}_{\mathcal{Q}}$.

Based on the principle of LR, we derive $P_{e,\mathrm{PV}}$ for LR-based linear detectors. LR-based detectors can achieve a full receive diversity with a relative low complexity by generating a *nearly* orthogonal basis for a given channel matrix [22] to mitigate the effect of (multiple antenna) interference. In the LLL-LR [18] algorithm, we transform $\mathbf{H}_\Omega$ into a new basis, e.g., denoted by $\mathbf{G}$ in (5.13). Here, we have $\mathcal{L}(\mathbf{G}) = \mathcal{L}(\mathbf{H}_\Omega) \Longleftrightarrow \mathbf{G} = \mathbf{H}_\Omega\mathbf{T}$, where $\mathbf{T}$ is an integer unimodular matrix and $\mathcal{L}(\mathbf{A})$ denotes a basis of lattice generated by $\mathbf{A}$. Then, $\mathbf{G}$ is called LLL-reduced with parameter δ if $\mathbf{G}$ is QR factorized as

$$\mathbf{G} = \mathbf{QR}, \tag{5.19}$$

where $\mathbf{Q}$ is unitary ($\mathbf{Q}^{\mathrm{T}}\mathbf{Q} = \mathbf{I}_N$), $\mathbf{R}$ is upper triangular, and the elements of $\mathbf{R}$ satisfy the following inequalities:

$$|\,[\mathbf{R}]_{\ell,\rho}\,| \leq \frac{1}{2}\,|\,[\mathbf{R}]_{\ell,\ell}\,| \quad \text{with} \quad 1 \leq \ell < \rho \leq N \tag{5.20}$$

and

$$\delta[\mathbf{R}]^2_{\rho-1,\rho-1} \leq [\mathbf{R}]^2_{\rho,\rho} + [\mathbf{R}]^2_{\rho-1,\rho} \quad \text{with} \quad \rho = 2,\ldots,N, \tag{5.21}$$

where δ is a given parameter $\left(\delta \in (\frac{1}{2}, 1)\right)$ [25].

From [25], the error probability of the LR-based MMSE detection is almost equivalent to that of the LR-based ZF detection. From (5.13), with the LR-based ZF detection, let $\mathbf{x} = \mathbf{G}^\dagger\mathbf{r}^k$. Then, it follows that

$$\mathbf{x} = \mathbf{U}\mathbf{s}_\Omega + \mathbf{G}^\dagger\mathbf{n}. \tag{5.22}$$

The estimation of $\mathbf{s}_\Omega$ can be expressed as

$$\hat{\mathbf{s}}_\Omega = \mathbf{U}^{-1}\lfloor\mathbf{x}\rceil = \mathbf{s}_\Omega + \mathbf{U}^{-1}\lfloor\mathbf{G}^\dagger\mathbf{n}\rceil. \tag{5.23}$$

Thus, the error probability of detecting $\mathbf{s}_\Omega$ for given $\mathbf{H}_\Omega$ is upper bounded by

$$P_{e|\mathbf{H}_\Omega} \leq 1 - \Pr\left(\lfloor\mathbf{G}^\dagger\mathbf{n}\rceil = \mathbf{0}\middle|\mathbf{H}_\Omega\right). \tag{5.24}$$

Let $\mathbf{G}^\dagger = [\mathbf{g}_1,\ldots,\mathbf{g}_N]^{\mathrm{T}}$, where $\mathbf{g}_i^{\mathrm{T}}$, $i = 1,2,\ldots,N$, denotes the ith row of $\mathbf{G}^\dagger$. Let $\mathbf{h}_{\mathrm{min}}$ represent the vector of the minimum non-zero norm of all the vectors in

the lattice generated by $\mathbf{H}_{\mathcal{Q}}$. Following the derivation in [25], it can be deduced that[1]

$$P_{e|\mathbf{H}_{\mathcal{Q}}} \leq \Pr\left(\max_{1\leq i\leq N} |\mathbf{g}_i^{\mathrm{T}}\mathbf{n}| \geq \frac{1}{2}\middle|\mathbf{H}_{\mathcal{Q}}\right) \leq \Pr\left(\|\mathbf{n}\| \geq \frac{1}{2}c_\delta\|\mathbf{h}_{\min}\|\middle|\mathbf{H}_{\mathcal{Q}}\right), \quad (5.25)$$

and

$$\begin{aligned} P_{e,\mathrm{PV}} = E_{\mathbf{H}_{\mathcal{Q}}}[P_{e|\mathbf{H}_{\mathcal{Q}}}] &\leq E_{\mathbf{H}_{\mathcal{Q}}}\left[\Pr\left(\|\mathbf{n}\|^2 \geq \frac{1}{2}c_\delta^2\|\mathbf{h}_{\min}\|^2\middle|\mathbf{H}_{\mathcal{Q}}\right)\right] \\ &= E_{\mathbf{n}}\left[\Pr\left(\|\mathbf{h}_{\min}\|^2 \leq \frac{\|\mathbf{n}\|^2}{c_\delta^2/2}\middle|\mathbf{n}\right)\right] \\ &= c_{NN}\left(\frac{2}{c_\delta^2}\right)^N \frac{(2N-1)!}{(N-1)!}\left(\frac{1}{N_0}\right)^{-N}, \end{aligned} \quad (5.26)$$

where c_{NN} and c_δ^2 are constants, and $c_\delta := 2^{\frac{N}{2}}\left(\frac{2}{2\delta-1}\right)^{-\frac{N(N+1)}{4}} < 1$. The upper bound on $P_{e,\mathrm{PV}}$ in (5.26) results from the N-th moment of Chi-square random variable, $||\mathbf{n}||^2$.

In addition, for LR-based SIC detection, it can be deduced from [67] that the bound of its error probability results from the same moment of $||\mathbf{n}||^2$ as the LR-based linear detection. Thus, for LR-based detectors, the upper bound on $P_{e,\mathrm{PV}}$ in (5.26) results from the N-th moment of $||\mathbf{n}||^2$.

Next, we consider $P_{e,\mathrm{SEL}}$. Noting that if the ML detector can choose the correct transmitted symbol vector, $\mathbf{s}$, among all the possible candidate vectors in their alphabet $\mathcal{S}$, the detection in (5.10) can also choose $\mathbf{s}$ (provided that $\mathbf{s} \in \mathbb{S}$ and $\mathbb{S} \subset \mathcal{S}$) and it is obvious to show that[2]

$$P_{e,\mathrm{SEL}} \leq P_{e,\mathrm{ML}}, \quad (5.27)$$

where $P_{e,\mathrm{ML}}$ is the error probability of the ML detection employed with an $N \times M$ MIMO system. It is well known that a full receive diversity gain is achieved by this ML detector, which is N [1]. That is, the upper bound on $P_{e,\mathrm{SEL}}$ can also be obtained from the N-th moment of Chi-square random variable, $||\mathbf{n}||^2$.

[1]For the details of the derivation in (5.25) and (5.26), please see Section IV-C in [25].

[2]Inequality (5.27) is correct if $\mathbf{s}^o \in \mathbb{S}$. Note that the definition of $P_{e,\mathrm{SEL}}$ is the selection error probability when there is one correct candidate in the set $\mathbb{S}$. We can use (5.27) to calculate $P_{e,\mathrm{SEL}}$, while the error probability if $\mathbf{s}^o$ is not in $\mathbb{S}$ is already calculated by $P_{e,\mathrm{PV}}$.

From (5.17), when the LR-based detectors are employed for the sub-detection, the error probability of the PVC-MIMO detection is given by

$$P_e = P_{e,\mathrm{PV}} + P_{e,\mathrm{SEL}} - P_{e,\mathrm{PV}}P_{e,\mathrm{SEL}} \leq P_{e,\mathrm{PV}} + P_{e,\mathrm{ML}} - P_{e,\mathrm{PV}}P_{e,\mathrm{SEL}} \leq P_{e,\mathrm{PV}} + P_{e,\mathrm{ML}}. \tag{5.28}$$

Since $P_{e,\mathrm{PV}}$, $P_{e,\mathrm{SEL}}$, and $P_{e,\mathrm{ML}}$ in (5.28) are tail probabilities of a Chi-square random variable with $2N$ degrees of freedom, $||\mathbf{n}||^2$, we can see that $P_e \approx c\left(\frac{1}{N_0}\right)^{-N}$ as $N_0 \to 0$, where c is a constant that is independent of N_0. Note that N is also the maximum receive diversity order for an underdetermined $N \times M$ MIMO system. Thus, a full receive diversity can be achieved by the proposed PVC-MIMO detection with LR-based sub-detectors.

5.4.1.2 Error Probability with Linear Detectors

If a linear detector (e.g., the MMSE detector introduced in Subsection 5.3.1) is used for the sub-detection, the ME criterion can be employed for PVS. Since a linear detector cannot exploit a full receive diversity, the diversity order of the PVC-MIMO detection is less than N. However, if the PVS is employed, the PVC-MIMO detection can achieve a higher diversity order.

It can be shown that for a given set Ω, the error probability of the linear sub-detection that detects $\mathbf{s}_\Omega$ for a given square sub-matrix $\mathbf{H}_\Omega$ is expressed as [41]

$$P_{e|\mathbf{H}_\Omega} \leq \frac{1}{2}\mathrm{erfc}\left(\sqrt{\frac{\lambda_{\min}(\mathbf{H}_\Omega^{\mathrm{H}}\mathbf{H}_\Omega)||\boldsymbol{\Delta}||^2}{4N_0}}\right). \tag{5.29}$$

where $\boldsymbol{\Delta} = \mathbf{s}_{\Omega(1)} - \mathbf{s}_{\Omega(2)}$ (suppose that $\mathbf{s}_{\Omega(1)}$ is transmitted, while $\mathbf{s}_{\Omega(2)}$ is erroneously detected), and $\mathrm{erfc}(x)$ is the complementary error function of x, i.e., $\mathrm{erfc}(x) = \frac{2}{\sqrt{\pi}}\int_x^{+\infty} e^{-z^2}dz$. Thus, under the ME selection criterion, the PEP for

detecting $\mathbf{s}_{\mathcal{Q}}$ becomes:

$$P\left(\mathbf{s}_{\mathcal{Q}(1)} \to \mathbf{s}_{\mathcal{Q}(2)}\right) = P_{e|\mathbf{H}_{\mathcal{Q}_{\mathrm{ME}}}} \leq \frac{1}{2}\mathrm{erfc}\left(\sqrt{\frac{\max_{\mathcal{Q}} \lambda_{\min}(\mathbf{H}_{\mathcal{Q}}^{\mathrm{H}}\mathbf{H}_{\mathcal{Q}})||\mathbf{\Delta}||^2}{4N_0}}\right)$$
$$= \frac{1}{2}\mathrm{erfc}\left(\sqrt{\frac{\sigma_h^2||\mathbf{\Delta}||^2 \max_{\mathcal{Q}} X_{\mathcal{Q}}}{4N_0}}\right)$$
$$= \frac{1}{2}\mathrm{erfc}\left(\sqrt{\frac{\sigma_h^2||\mathbf{\Delta}||^2 V}{4N_0}}\right), \tag{5.30}$$

where $X_{\mathcal{Q}} = \lambda_{\min}(\mathbf{H}_{\mathcal{Q}}^{\mathrm{H}}\mathbf{H}_{\mathcal{Q}})/\sigma_h^2$, $V = \max_{\mathcal{Q}} X_{\mathcal{Q}}$, and σ_h^2 is the variance of the elements in channel matrix $\mathbf{H}_{\mathcal{Q}}$.

Similar to (5.18), we have

$$P_{e,\mathrm{PV}} = 1 - \Pr\left(\exists \mathbf{s}^{k'} \in \mathbb{S} : \mathbf{s}_{\mathcal{P}}^{k'} = \mathbf{s}_{\mathcal{P}}^{o}, \hat{\mathbf{s}}_{\mathcal{Q}}^{k'} = \mathbf{s}_{\mathcal{Q}}^{o}\right)$$
$$= 1 - \Pr\left(\hat{\mathbf{s}}_{\mathcal{Q}}^{k'} = \mathbf{s}_{\mathcal{Q}}^{o} | \mathbf{s}_{\mathcal{P}}^{k'} = \mathbf{s}_{\mathcal{P}}^{o}\right) = E_{\mathbf{H}_{\mathcal{Q}}}\left[P_{e|\mathbf{H}_{\mathcal{Q}_{\mathrm{ME}}}}\right]. \tag{5.31}$$

Then according to (5.30), we can obtain that

$$P_{e,\mathrm{PV}} = E_{\mathbf{H}_{\mathcal{Q}}}\left[P_{e|\mathbf{H}_{\mathcal{Q}_{\mathrm{ME}}}}\right]$$
$$\leq E_V\left[\frac{1}{2}\mathrm{erfc}\left(\sqrt{\frac{\sigma_h^2||\mathbf{\Delta}||^2 V}{4N_0}}\right)\right]. \tag{5.32}$$

For the random matrix $\mathbf{H}_{\mathcal{Q}}$, the pdf of $X_{\mathcal{Q}}$ is given by [69]

$$f_x(x) = Ne^{-Nx}. \tag{5.33}$$

If all the possible sub-matrices $\mathbf{H}_{\mathcal{Q}}$ (after PVS), which are the candidate channel matrices for the sub-detection, are assumed to be independent[1], the pdf of V is

$$f_V(v) = LN(1 - e^{-Nv})^{L-1}e^{-Nv}$$
$$= LN^L v^{L-1} + o(v^{L-1+\epsilon}), (v \to 0^+), \tag{5.34}$$

[1]This assumption does not hold in practical situation (the last paragraph of this subsection addresses the practical situation).

where $\epsilon > 0$ and $L = C_M^N$ denotes the number of possible candidates for Ω (C_M^N is the number of combinations for selecting N items in M items).

The relation between the PEP in (5.30) and the pdf of variable V can be deduced by Wang and Giannakis [68]. Thus, according to [68], we can show that

$$\begin{aligned} P_{e,\mathrm{PV}} &\leq E_V\left[\frac{1}{2}\mathrm{erfc}\left(\sqrt{\frac{\sigma_h^2||\mathbf{\Delta}||^2 V}{4N_0}}\right)\right] \\ &\leq \int_0^{+\infty}\frac{1}{2}\mathrm{erfc}\left(\sqrt{\frac{\sigma_h^2||\mathbf{\Delta}||^2 v}{4N_0}}\right) f_V(v)dv \\ &= c_1\gamma_\Delta^{-L} + o(\gamma_\Delta^{-(L+1)}), \end{aligned} \tag{5.35}$$

where $\gamma_\Delta = \sigma_h^2||\mathbf{\Delta}||^2/N_0$ and $c_1 > 0$ is constant.

Note that for $M \geq N+1$, $C_M^N = \frac{M!}{(M-N)!N!} \geq \frac{M!}{(M-N)!N(N-1)\cdots 2}$ $\geq \frac{M!}{(M-N)!(M-1)(M-2)\cdots(M-N+1)} = \frac{M!}{(M-1)!} = M > N$, that is, $L > N$. In addition, (5.27) and (5.28) also hold for linear detectors. Hence, according to (5.35), a full diversity order N can be achieved by the proposed detectors when the ME criterion for index set Ω selection is employed.

In practice, different $\mathbf{H}_\Omega$'s are not independent (i.e., X_Ω are correlated for different Ω), and the minimum eigenvalues of $\mathbf{H}_\Omega^{\mathrm{H}}\mathbf{H}_\Omega$'s are correlated in the proposed detection after PVS. Thus, (5.34) may *not* be valid (but just an approximation) and a full diversity order N *cannot* be achieved. However, for a small sized matrix $\mathbf{H}_\Omega$, a near full diversity order may be achieved due to the low correlation of the minimum eigenvalues of different $\mathbf{H}_\Omega^{\mathrm{H}}\mathbf{H}_\Omega$'s. The numerical results shown in the following section also confirm this observation. That is, with the optimal PVS, the linear detector based PVC-MIMO detection can achieve a higher diversity; for a small matrix $\mathbf{H}_\Omega$ (e.g., a 2×2 matrix), a near-full receive diversity is achieved by the proposed detection.

5.4.2 Complexity Analysis

Denote by $\mathcal{C}_{\mathrm{Sub}}$ the complexity of the sub-detection with a square channel matrix of $N \times N$. Excluding the complexity of the PVS, the complexity of the PVC-

MIMO detection is given by

$$\mathcal{C}_{\text{PVC}} = K\mathcal{C}_{\text{Sub}}. \tag{5.36}$$

If an exhaustive search is employed to determine $\mathcal{Q}$ in (5.12), (5.15), or (5.16), because there are $\prod_{i=0}^{M-N-1}(M-i)$ possible index sets, the complexity for building $\mathcal{Q}$ is $\prod_{i=0}^{M-N-1}(M-i)\mathcal{C}_{\text{Sel}}$, where $\mathcal{C}_{\text{Sel}}$ denotes the computational complexity for each possible index set. For example, if the MD selection criterion is used when $M = 4$ and $N = 2$, we need $4 \times 3 = 12$ LRs of 2×2 complex-valued channel matrices and $\mathcal{C}_{\text{Sel}}$ becomes the complexity for each LR. We will list the complexity of $\mathcal{C}_{\text{Sel}}$ with different PVS's for their corresponding sub-detectors in Section 5.5, empirically using the average number of flops.

For a block fading channel, assume that the channel is not varying for a duration of W symbol vectors transmitted. Note that PVS is only performed once for a channel matrix. Then, including the complexity of PVS, the overall computational complexity of the PVC-MIMO detection per each symbol vector is given by

$$\mathcal{C}_{\text{PVC}} = \frac{\prod_{i=0}^{M-N-1}(M-i)\mathcal{C}_{\text{Sel}}}{W} + K\mathcal{C}_{\text{Sub}}. \tag{5.37}$$

For slow fading channels, where the coherence time is long, W will be large. In this case, the extra computational complexity required for PVS per each symbol detection would be negligible, where we have $\mathcal{C}_{\text{PVC}} \approx K\mathcal{C}_{\text{Sub}}$. In Section 5.5, we will compare the complexity of our proposed PVC-MIMO detectors to other MIMO detectors using flops.

5.5 Simulation Results and Discussions

5.5.1 Simulation Results

In this subsection, we present simulation results to compare our PVC-MIMO detectors with other detectors (including the MMSE (linear) detector, ML detector, the Chase detector [12, 13, 14, 15, 16, 17][1], and the TSD-CR [36] which provides

[1]Two scenarios are considered for the Chase detection: *i*) MMSE + Chase (MMSE sub-detector used in Chase detection); *ii*) LR-based MMSE-SIC + Chase (LR-based MMSE-SIC sub-detector used in Chase detection).

the ML performance) for underdetermined MIMO systems. Six combinations of the PVC-MIMO detectors are considered as follows: *a*) MMSE + PVC-MIMO (MMSE sub-detector used in PVC-MIMO); *b*) LR-based MMSE + PVC-MIMO (LR-based MMSE sub-detector used in PVC-MIMO); *c*) LR-based MMSE-SIC + PVC-MIMO (LR-based MMSE-SIC sub-detector used in PVC-MIMO); *d*) MMSE + PVC-MIMO + PVS (MMSE sub-detector used in PVC-MIMO with optimal PVS (ME criterion)); *e*) LR-based MMSE + PVC-MIMO + PVS (LR-based MMSE sub-detector used in PVC-MIMO with optimal PVS (ME criterion)); *f*) LR-based MMSE-SIC + PVC-MIMO + PVS (LR-based MMSE-SIC sub-detector used in PVC-MIMO with optimal PVS (MD criterion)). As we are interested in the case where the receiver's computational complexity is limited, we only consider the cases of $(M, N) \in \{(4,2),(4,3),(3,2)\}$[1]. Note that elements of MIMO channel matrices in simulations are generated as independent CSCG random variables with mean zero and unit variance. The SNR is defined as the energy per bit to the noise power spectral density ratio, E_b/N_0. We assume 4-QAM and 16-QAM are used for signaling with Gray mapping.

With 4-QAM modulation, in Figs. 5.1 and 5.2, for channel matrices of size 2×4 and 3×4, respectively, we show simulation results of BER for various detectors. In Figs. 5.3 and 5.4, with 16-QAM modulation, for channel matrices of size 2×3 and 3×4, respectively, simulation results of BER for various detectors are presented.

From the simulation results, it is shown that a full receive diversity can be achieved by employing the PVC-MIMO detection approach with LR-based sub-detectors. In Figs. 5.1 and 5.3, we can see that "LR-based MMSE/MMSE-SIC + PVC-MIMO" has a slight performance degradation from the ML detector and the SNR loss is a half dB at a broad range of BER. In all the simulation results, it is also shown that "LR-based MMSE/MMSE-SIC + PVC-MIMO + PVS" has negligible performance degradation compared to the ML performance. Furthermore, we note that "MMSE + Chase" and "LR-based MMSE-SIC + Chase" cannot provide a full diversity and good performance, especially when SNR is high.

[1]The case of a large $M - N$ is discussed in Subsection 5.5.2.

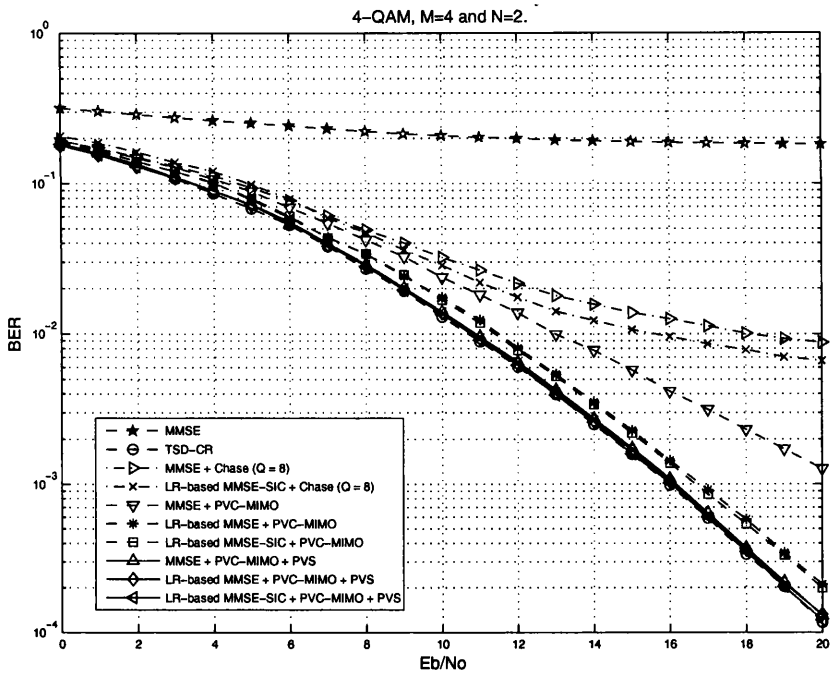

Figure 5.1: BER versus E_b/N_0 of different detectors represented in Subsection 5.5.1 for 4-QAM, $M = 4$, $N = 2$.

In Figs. 5.2 and 5.4, we can see "MMSE + PVC-MIMO + PVS" can provide a reasonably good performance. For a 2×2 sub-matrix, we can observe that "MMSE + PVC-MIMO + PVS" can provide a near ML performance from Figs. 5.1 and 5.3, where the sizes of channel matrices are 2×4 and 2×3, respectively. We note that the performance of "MMSE + PVC-MIMO + PVS" with $N = 2$ is better than that with $N = 3$. Since a low correlation of the minimum eigenvalue of $\mathbf{H}_{\mathcal{Q}}^{\mathrm{H}}\mathbf{H}_{\mathcal{Q}}$ is obtained by employing a reduced-sized channel matrix $\mathbf{H}_{\mathcal{Q}}$, a less error propagation is expected. This confirms that the PVC-MIMO detection with MMSE sub-detector could be effective when N is sufficiently small.

In Table 5.1, we list the complexity of $\mathcal{C}_{\mathrm{Sel}}$ for different detectors (i.e., "MMSE + PVC-MIMO + PVS", "LR-based MMSE + PVC-MIMO + PVS", and "LR-based MMSE-SIC + PVC-MIMO + PVS") by using flops[1], for the case of $N = 2$

[1]We simulate these systems using MATLAB-V5.3 on a PC. The MATLAB command "flops" is used to count the number of flops.

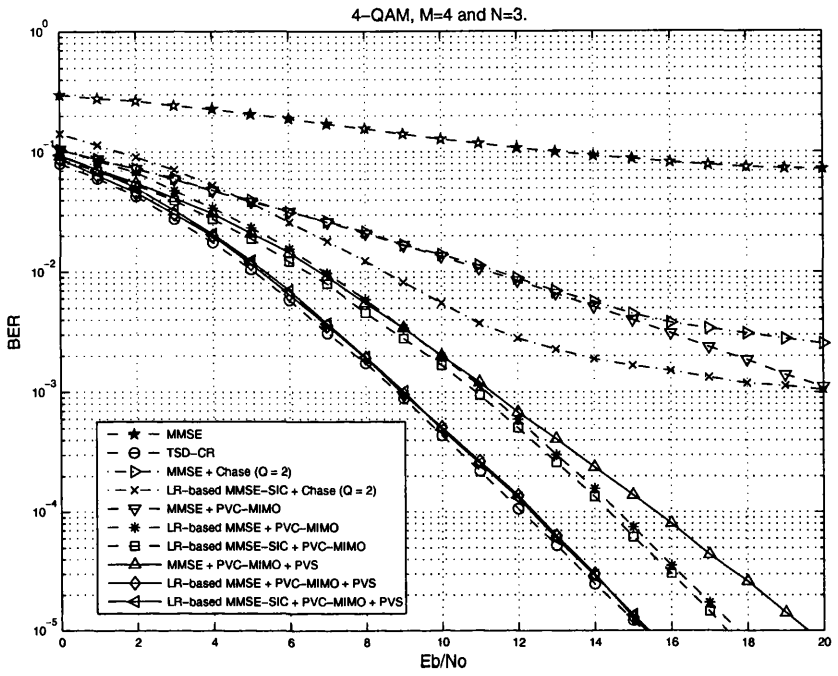

Figure 5.2: BER versus E_b/N_0 of different detectors represented in Subsection 5.5.1 for 4-QAM, $M = 4$, $N = 3$.

and $N = 3$, respectively. Since the computation for both LR and eigenvalue is considered in "LR-based MMSE + PVC-MIMO + PVS", the highest complexity is required.

Since the TSD-CR approach [36] can be applied to underdetermined MIMO systems with a reasonable low complexity and optimal performance, it is worthy to compare its complexity with our proposed schemes. In Table 5.2, we compare the complexity of our proposed PVC-MIMO detectors to other MIMO detectors including the ML detector (using an exhaustive search), MMSE detector, TSD-CR, and Chase detectors by using flops with $W = 1000$, where slow fading channels are considered[1]. Note that for PVC-MIMO and TSD-CR, the PVS and Householder QR decomposition of channel matrix with minimum column pivoting are carried out once for 1000 symbol vectors transmitted, respectively, to make this comparison fair. The flops listed in Table 5.2 are obtained with $E_b/N_0 = 20$

[1]The complexity of PVC-MIMO with fast fading channels is discussed in Subsection 5.5.2

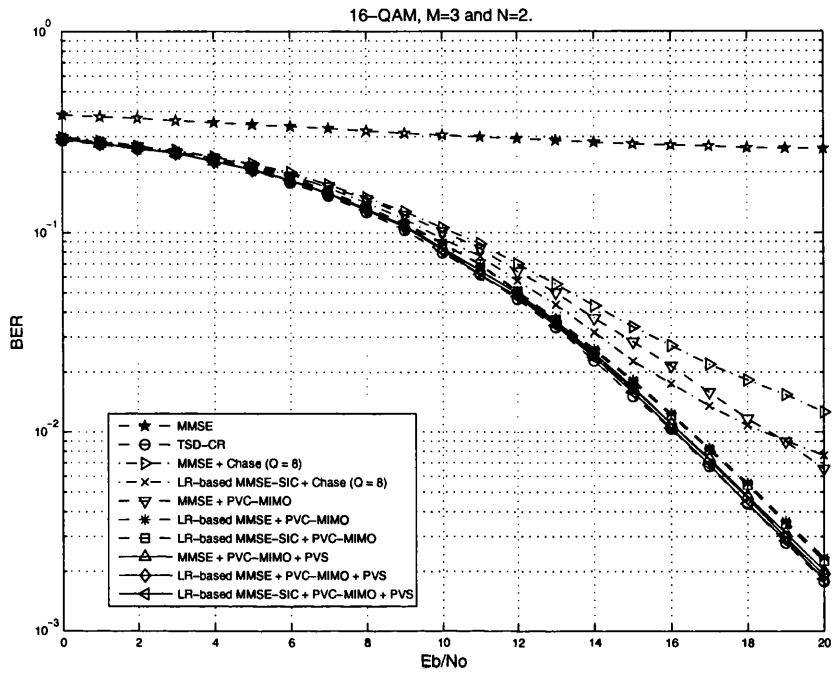

Figure 5.3: BER versus E_b/N_0 of different detectors represented in Subsection 5.5.1 for 4-QAM, $M = 3$, $N = 2$.

dB.

Although the MMSE and Chase detectors have a low complexity, they do not suit for underdetermined MIMO systems. It is shown that the computational complexity of the proposed PVC-MIMO detectors with optimal PVS for the case of $\{M, N\} = \{3, 2\}$, $\{M, N\} = \{4, 2\}$, and $\{M, N\} = \{4, 3\}$ with 4-QAM is significantly lower than that of ML and TSD-CR. It is also shown that with 16-QAM, the proposed detectors can also provide a relatively lower complexity for the case of $\{M, N\} = \{3, 2\}$ and $\{M, N\} = \{4, 3\}$. In addition, for different PVC-MIMO detectors in the same MIMO system, "MMSE + PVC-MIMO + PVS" has the lowest computational complexity among the PVC-MIMO detectors, since no LR is used in PVS and sub-detection.

Overall, "LR-based MMSE-SIC + PVC-MIMO + PVS" is shown to be very attractive, because its performance is close to that of the ML detection and its complexity is low (the complexity is almost the same as that of "MMSE + PVC-

Table 5.1: Complexity comparison of $\mathcal{C}_{\text{Sel}}$ for different detectors listed in Subsection 5.5.1.

Average flops of $\mathcal{C}_{\text{Sel}}$		
Detector	$N = 2$	$N = 3$
MMSE + PVC-MIMO + PVS	258	1608
LR-based MMSE + PVC-MIMO + PVS	678	3070
LR-based MMSE-SIC + PVC-MIMO + PVS	473	1587

Table 5.2: Complexity comparison of different detectors listed in Subsection 5.5.1.

Average flops for each symbol vector detection					
	4-QAM			16-QAM	
System	$\{M,N\}=\{3,2\}$	$\{M,N\}=\{4,2\}$	$\{M,N\}=\{4,3\}$	$\{M,N\}=\{3,2\}$	$\{M,N\}=\{4,3\}$
MMSE	78	109	112	302	411
ML	4484	22021	32773	286724	8388613
TSD-CR	753	1296	1226	3467	5546
MMSE + Chase	168	623	239	1671	2479
LR-based MMSE-SIC + Chase	170	626	255	1673	2490
MMSE + PVC-MIMO + PVS	193	770	325	3056	4645
LR-based MMSE + PVC-MIMO + PVS	201	783	377	3074	4697
LR-based MMSE-SIC + PVC-MIMO + PVS	197	778	356	3060	4666

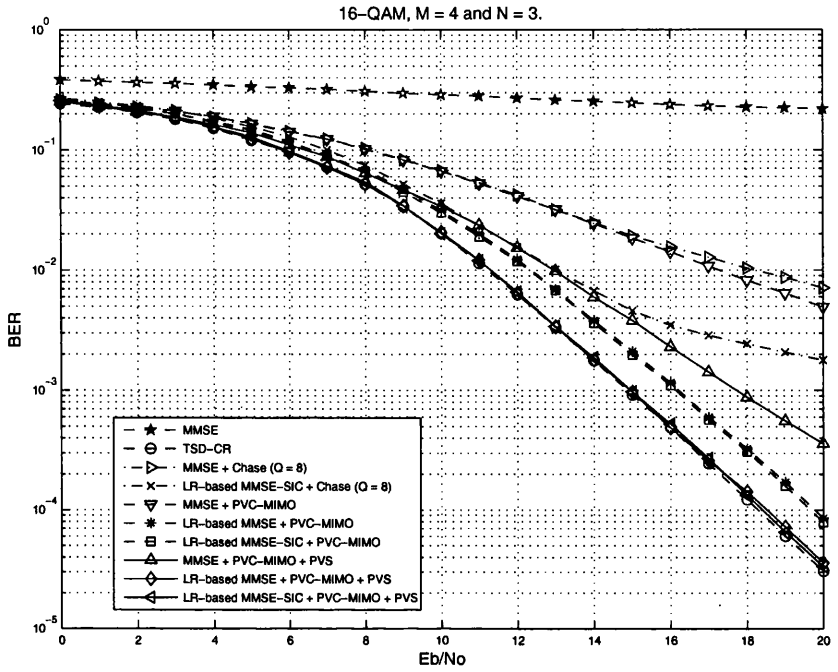

Figure 5.4: BER versus E_b/N_0 of different detectors represented in Subsection 5.5.1 for 4-QAM, $M = 4$, $N = 3$.

MIMO + PVS", which is the lowest). From this, we can see that the combination of LR detector and optimal PVS is the key ingredient to build low complexity, but near ML performance, detection schemes for underdetermined MIMO systems.

5.5.2 Discussion

In Subsection 5.5.1, we have discussed the computational complexity of PVC-MIMO detection with slow fading MIMO channels where $M - N$ is small (e.g., 1 or 2). In this subsection, we discuss the complexity of the PVC-MIMO detection for fast fading channels and a large $M - N$. Furthermore, the impact of channel estimation errors is considered.

5.5.2.1 Fast Fading Channels

Previously, we have analyzed the complexity of the PVC-MIMO detection with PVS for slow fading MIMO channels, where W is large (e.g., $W = 1000$). Note that fast fading channels lead to a small W. With the overall complexity per each symbol vector of the PVC-MIMO detection in (5.37), $\mathcal{C}_{\text{PVC}}$ would be high due to the weight of $\mathcal{C}_{\text{Sel}}$ is high when W is small (i.e., the complexity of $\mathcal{C}_{\text{Sel}}$ is given in Table 5.1). Therefore, the PVC-MIMO detection with PVS could have a high complexity with a small W.

For the case of $W = 10$, where channel varies every 10 symbol vectors transmitted (i.e., reasonably fast fading channels), with $\{N, M\} = \{2, 3\}$ and $\{N, M\} = \{2, 4\}$, the average computational complexity per each symbol vector for PVS of "LR-based MMSE-SIC + PVC-MIMO + PVS" is 155 and 310, respectively, in terms of flops. In this case, compared to existing approaches (in Table 5.2), the complexity of the PVC-MIMO with PVS is still low.

5.5.2.2 Large $M - N$

Since there are underdetermined MIMO systems with a large $M - N$, it is worthy to discuss the complexity of PVC-MIMO detection employed in such MIMO systems. Consider a low order modulation (4-QAM), by using the same method that obtains the flops in Table 5.2, we compare the computational complexity of "LR-based MMSE-SIC + PVC-MIMO + PVS" and TSD-CR [36] for the cases of $\{M, N\} = \{5, 2\}$ and $\{6, 2\}$, respectively, in terms of flops. For "LR-based MMSE-SIC + PVC-MIMO + PVS", the flops of $\{M, N\} = \{5, 2\}$ and $\{6, 2\}$ are 3106 and 12263, respectively. For TSD-CR, the flops of $\{M, N\} = \{5, 2\}$ and $\{6, 2\}$ are 5010 and 19564, respectively. It shows that the PVC-MIMO detection has a lower complexity than TSD-CR with a large $M - N$ and a low order modulation.

We note that the PVC-MIMO detection is not suitable for the case of a large $M - N$ and a high order modulation (16-QAM or 64-QAM) due to the exhaustive cancellation of pre-voting vectors. However, it is noteworthy that the GSD-based detection (e.g., TSD-CR) has also high complexity [29, 30, 31, 32, 33, 34, 35, 36].

5.5.2.3 Imperfect CSI Estimation

In practice, the channel matrix has to be estimated and there could be estimation errors. Consider an $N \times M$ channel matrix $\mathbf{H}$ represented in (5.1), whose elements are generated as independent CSCG random variables with mean zero and unit variance, with an imperfect CSI estimation, the estimated channel matrix is given by $\hat{\mathbf{H}} = \mathbf{H} + \mathbf{E}$. Here, an $N \times M$ matrix $\mathbf{E}$ represents errors in the CSI estimation, whose elements are generated as independent zero-mean CSCG random variables with variance v_e^2.

With $\{N, M\} = \{2, 4\}$ and 4-QAM modulation, in Fig. 5.5, we present simulation results of BER for TSD-CR and "LR-based MMSE-SIC + PVC-MIMO + PVS" with different CSI errors, where $v_e = 0$, 0.02, and 0.05. Fig. 5.5 shows that the performance of TSD-CR and "LR-based MMSE-SIC + PVC-MIMO + PVS" degrades when v_e increases in general. Nevertheless, it shows that our proposed PVC-MIMO detection with PVS (i.e., "LR-based MMSE-SIC + PVC-MIMO + PVS") has a negligible performance gap from the ML performance (i.e., TSD-CR) with CSI estimation errors.

5.6 Conclusion

For underdetermined MIMO systems where a lower order modulation scheme can be employed, we considered low complexity MIMO detection approaches based on PVC in this chapter. It was shown that if a LR-based detector is used for the sub-detection, the PVC-MIMO detection can achieve a full receive diversity order. We confirmed this through simulations. It was also shown that the complexity of the proposed PVC-MIMO detectors is low and comparable to that of the MMSE detector when 4-QAM is used. Therefore, the proposed detection approach can be employed for underdetermined MIMO systems where the receiver's computational complexity is limited such as mobile terminals.

An extension of MIMO systems is multiuser MIMO systems, where the user selection plays a key role to exploit the diversity. In the next chapter, we consider the user selection for multiuser MIMO systems with an actual employed MIMO detector.

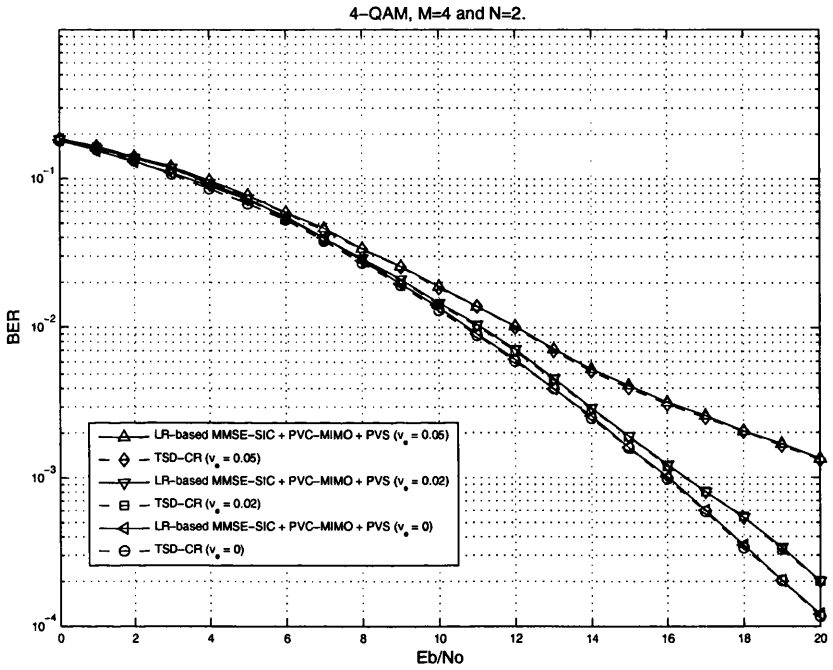

Figure 5.5: BER versus E_b/N_0 of "TSD-CR" and "LR-based MMSE-SIC + PVC-MIMO + PVS" represented in Subsection 5.5.1 for $v_e = \{0, 0.02, 0.05\}$ with 4-QAM, $M = 4$, $N = 2$.

6

Greedy User Selection using a Lattice Reduction Updating Method for Multiuser MIMO Systems

6.1 Introduction

In wireless communications, the spectral efficiency can be improved by exploiting the space domain when antenna arrays are used. In particular, space division multiple access (SDMA) [70, 71, 72] can be adopted with various beamforming techniques. If both transmitter and receiver are equipped with multiple antennas, the resulting channel becomes MIMO channels, which can provide a rich spatial diversity gain. Instead of performing an exhaustive search, tree search techniques (e.g., SD-based detection [10, 73, 74]) which can provide the optimal performance in some cases are developed with a reduced complexity. Furthermore, using the properties of lattice, the LR-based low complexity detectors [19, 20, 21, 22, 23, 24, 25, 26, 75] are proposed which can provide a full receive diversity gain.

Due to users' different locations and channel conditions, it is possible to exploit another diversity gain in a multiuser system, where the throughput can be maximized by choosing the user of the strongest channel gain at a time. The resulting diversity gain is called the multiuser diversity gain [38]. Multiuser systems

can be extended to the case of MIMO systems [37], where the multiuser MIMO user selection plays a key role in increasing the throughput of downlink channels [40]. It is noteworthy that by viewing multiuser MIMO as virtual antennas in a single user MIMO system, various antenna selection techniques can be applied to user selection [53, 54, 76]. A mutual information based criterion is proposed in [53] to select the antenna subset that maximizes the mutual information. In [54], a geometrical-based criterion is developed with a LR-based linear detector to minimum the error probability. In general, user selection problems are combinatorial problems and the complexity required to solve the problems could be prohibitively high for a large multiuser MIMO system. Thus, low complexity suboptimal selection strategies are considered in [39, 77, 78, 79, 80, 81, 82, 83, 84] at the expense of degraded performance. In [39, 77, 78, 79], a single antenna is selected at a time to maximize the throughput based on greedy selection schemes.

Although the achievable rate or related SNR can be used for the user selection criterion, it would be more practical to use a certain performance measure that is directly related to the performance of the actual detector or decoder employed. Therefore, it is desirable to derive a user selection criterion that can maximize the performance of the actual MIMO detector employed in a multiuser MIMO system. In [41], for the user selection in uplink channels of a cellular system, where a single user is selected to transmit signals to a BS at a time, the error probability is used for the user selection criteria to choose the user who has the smallest error probability for given MIMO detectors. Various user selection criteria are derived with the ML detector as well as other low complexity suboptimal detectors. It is shown that a near optimal performance with a full diversity gain (i.e., multiuser diversity and multiple antenna diversity) can be achieved using those user selection criteria proposed in [41] with LR-based detectors.

In this chapter, we extend the user selection in [41] to support multiple users at a time. This extension of the user selection (i.e., multiple user selection) is not straightforward as the multiple user selection problem becomes a combinatorial problem. If an exhaustive search is used for multiple user selection when a LR-based MIMO detector is employed, LR needs to be performed for all the possible channel matrices composited by a group of sub-channel matrices of the selected users, which results in a highly computational complexity as the number of user

combinations is large. Therefore, we propose a greedy user selection in uplink channels for the complexity reduction when a LR-based detector is used. Moreover, to further reduce the computational complexity, an iterative LR updating algorithm is investigated.

From a theoretical analysis in this chapter, we show that with the combinatorial user selection, the LR-based detection can achieve the same diversity as the ML detector. Through simulations, we compare the performance obtained by our proposed selection criteria (i.e., combinatorial and greedy ones) to other existing approaches. With the LR-based detection employed, simulation results confirm that our combinatorial user selection can provide the best performance, while the performance of the greedy user selection scheme could approach that of the combinatorial one as the correlation between possible composite channel matrices decreases. It also shows that our proposed greedy user selection provides a better performance and a significantly reduced complexity compared to other approaches.

This chapter is organized as follows. In Section 6.2, a system model for multiuser MIMO is presented. Various user selection criteria are discussed in Section 6.3 for given multiuser MIMO system. The proposed greedy user selection approach is derived in Section 6.4 with an iterative LR updating algorithm. We present performance analysis and simulation results in Section 6.5. Finally, we conclude this chapter with some remarks in Section 6.6.

Throughout the chapter, vectors and matrices are represented by bold letters. For a matrix $\mathbf{A}$, $\mathbf{A}^{\mathrm{T}}$, $\mathbf{A}^{\mathrm{H}}$, and $\mathbf{A}^{*}$ denote its transpose, Hermitian transpose, and conjugate, respectively. $\mathbf{A}(a:b, c:d)$ denotes the submatrix of $\mathbf{A}$ with the elements obtained from rows $a, \ldots, b$ and columns $c, \ldots, d$. Furthermore, $\mathbf{A}(:, n)$ and $\mathbf{A}(n, :)$ denote the n-th column and n-th row vectors, respectively. $\Re(z)$ and $\Im(z)$ denote the real and complex parts of a complex number z, respectively. In addition, for a vector or matrix, $\| \cdot \|$ denotes the 2-norm. $\lfloor \beta \rfloor$ represents the closest integer which is smaller than β, while $\lceil \beta \rfloor$ denotes the nearest integer to β. Denote by $\setminus$ the set minus, by $\mathbf{I}_n$ an $n \times n$ identity matrix, and by $\mathcal{K} = \{k_{(1)}, k_{(2)}, \ldots\}$ the collection set of $k_{(1)}, k_{(2)}, \ldots$.

6.2 System Model

Consider the multiuser MIMO system with K users in uplink channels, where each user is equipped with P transmit antennas and the BS is equipped with N receive antennas. Each user has an $N \times P$ channel matrix and a $P \times L$ signal matrix, which are denoted by $\mathbf{H}_k$ and $\mathbf{S}_k$, respectively, where $k \in \{1, 2, \ldots, K\}$. Here, L is number of symbols transmitted by a user. It is assumed that all the users share a common uplink channel and M users can access the channel at a time, where $M \leq \lfloor \frac{N}{P} \rfloor$[1]. The channel is assumed to be a quasi-static block flat-fading channel with its channel matrix is not varying over a time slot duration of L symbols. Here, a set of the M users who can access the channel could be updated[2] for every time slot interval. Note that this selection problem can also be regarded as that with virtual antennas in a single user MIMO system, where MP antennas are selected out of KP available antennas. Let $k_{(m)}$ be the mth selected user's index. For convenience, define the set of the selected users' indices as $\mathcal{K} = \{k_{(1)}, k_{(2)}, \ldots, k_{(M)}\}$. Then, over a slot duration, the received signal at the BS is given by

$$\mathbf{Y}_{\mathcal{K}} = \mathbf{H}_{\mathcal{K}}\mathbf{S}_{\mathcal{K}} + \mathbf{N}, \tag{6.1}$$

where $\mathbf{H}_{\mathcal{K}}$, $\mathbf{S}_{\mathcal{K}}$, and $\mathbf{N}$ are the $N \times MP$ composite channel matrix, the $MP \times L$ transmitted signal matrix, and the $N \times L$ background noise matrix, respectively. We assume that each column vector of $\mathbf{N}$ is an independent zero-mean CSCG random vector with $E[\mathbf{n}_l \mathbf{n}_l^{\mathrm{H}}] = N_0\mathbf{I}$, where $\mathbf{n}_l$ denotes the l-th column vector of $\mathbf{N}$. Note that $\mathbf{H}_{\mathcal{K}} = \left[\mathbf{H}_{k_{(1)}}, \ldots, \mathbf{H}_{k_{(M)}}\right]$ and $\mathbf{S}_{\mathcal{K}} = \left[\mathbf{S}_{k_{(1)}}^{\mathrm{T}}, \ldots, \mathbf{S}_{k_{(M)}}^{\mathrm{T}}\right]^{\mathrm{T}}$.

Throughout this chapter, we assume that the CSI is perfectly known at the receiver. Furthermore, the following assumptions are used to derive user selection methods.

[1]Note that if an ML or linear detector is employed to detect signal, there could be more transmit antennas than receive antennas in multiuser MIMO systems, which results in $M > \lfloor \frac{N}{P} \rfloor$. However, consider that the LR-based detection is used as the detection method, in this chapter, we have $M \leq \lfloor \frac{N}{P} \rfloor$.

[2]In this chapter, we only consider channel conditions to select users. However, this could be extended to include transmit optimization [85, 86], traffic conditions, and users' priorities [87, 88], which are beyond the scope of the chapter.

A1) The elements of $\mathbf{S}_{\mathcal{K}}$ have a common signal alphabet, denoted by $\mathcal{S}$, and $\mathcal{S} \subset \mathbb{Z} + j\mathbb{Z}$, where $\mathbb{Z}$ denotes the set of integer numbers and $j = \sqrt{-1}$. Furthermore, let $\mathcal{S}^A$ represent the A-dimensional Cartesian product of $\mathcal{S}$.

A2) The transmitted signals are uncoded. This implies that the user selection criteria in this chapter are based on uncoded BER. For uncoded signals, we can assume $L = 1$ (Note that this assumption is used to simplify the derivation of user selection criteria, while the length of slot can be any number). Thus, $\mathbf{Y}_{\mathcal{K}}$, $\mathbf{S}_{\mathcal{K}}$, and $\mathbf{N}$ are vectors and will be denoted by $\mathbf{y}_{\mathcal{K}}$, $\mathbf{s}_{\mathcal{K}}$, and $\mathbf{n}$, respectively.

6.3 User Selection Criteria

To maximize the performance, if $M = 1$, the user who can have the minimum BER is chosen for a given MIMO detector. In [41], a few user selection criteria are derived depending on the types of actually employed MIMO detectors. It has been shown that the user selection criteria with the LR-based MMSE-SIC detector [2, 22] can provide a good performance with a reasonably low complexity, compared to that with the ML detector. Note that only one user is selected (i.e., $M = 1$) in [41]. To extend the user selection criteria to the case of $M > 1$, in this and next sections, we consider the combinatorial and greedy user selection criteria.

6.3.1 ML and MMSE Selection Criteria

For convenience, we omit the user index set $\mathcal{K}$. The estimated symbol vectors from the ML and MMSE detectors are given by

$$\hat{\mathbf{s}}_{\text{ml}} = \arg \min_{\mathbf{s} \in \mathcal{S}^{MP}} \| \mathbf{y} - \mathbf{H}\mathbf{s} \|^2 \tag{6.2}$$

and

$$\hat{\mathbf{s}}_{\text{mmse}} = \mathbf{W}_{\text{mmse}}^{\text{H}} \mathbf{y}, \tag{6.3}$$

respectively, where $\mathbf{W}_{\text{mmse}}$ is the MMSE filter that is given by $\mathbf{W}_{\text{mmse}} = \left(\mathbf{H}\mathbf{H}^{\text{H}} + \frac{N_0}{E_s}\mathbf{I}_N\right)^{-1} \mathbf{H}$. Here, E_s represents the symbol energy. The

detection performance depends on the channel matrix. For a given channel matrix, as discussed in [41], we can apply the MDist and the ME criteria for user selection.

For a given $M > 1$, the set of the users who can access the channel can be found using the MDist or ME user selection criterion as follows:

$$\mathcal{K}_{\text{MDist}} = \arg\max_{\mathcal{K}} \mathcal{D}\left(\mathbf{H}_{\mathcal{K}}\right) \tag{6.4}$$

or

$$\mathcal{K}_{\text{ME}} = \arg\max_{\mathcal{K}} \lambda_{\min}\left(\mathbf{H}_{\mathcal{K}}^{\text{H}}\mathbf{H}_{\mathcal{K}}\right), \tag{6.5}$$

respectively, where $\mathcal{D}(\mathbf{H}_{\mathcal{K}})$ denotes the length of the shortest non-zero vector of the lattice generated by $\mathbf{H}_{\mathcal{K}}$ and $\lambda_{\min}(\mathbf{A})$ denotes the minimum eigenvalue of $\mathbf{A}$. If the ML detector is employed, the MDist user selection criterion can be used to choose the M users who can have the lowest BER, while the ME criterion is to choose the M users who have the highest worst SNR (i.e., max-min SNR). Note that if $P = M = 1$, both the criteria choose the user of the highest SNR. The two criteria shown in (6.4) and (6.5) can be used with any MIMO detector, although the MDist criterion has been derived to maximize the performance with the ML detector and the ME criterion suits for the MMSE detector.

6.3.2 LR-based MMSE and MMSE-SIC Selection Criteria

In this subsection, the user selection criteria with LR-based detectors in [41] are extended to the case of $M > 1$. Although the LR can be performed with a complex-valued $\mathbf{H}$ as in [23, 24, 25] or a real-valued one converted from $\mathbf{H}$ as in [19] and [22], there is no performance difference as shown in [23]. In general, since the LR with a complex-valued $\mathbf{H}$ is suitable for performance analysis and deriving numerical algorithms, in this chapter, as in [23], we consider the LR with a complex-valued $\mathbf{H}$.

For the LR-based MMSE detection, from (6.1), with omitting the user index set $\mathcal{K}$, the received signal vector can be rewritten as

$$\mathbf{y} = \mathbf{G}\mathbf{c} + \mathbf{n}, \tag{6.6}$$

where $\mathbf{G} = \mathbf{H}\mathbf{U}^{-1}$ and $\mathbf{c} = \mathbf{U}\mathbf{s}$. Here, $\mathbf{U}$ is an integer unimodular matrix and $\mathbf{G}$ is a lattice basis reduced (LBR) matrix which has a nearly orthogonal basis. The LR-based MMSE detection is carried out to detect $\mathbf{c}$ as $\hat{\mathbf{c}} = \lceil \mathbf{W}_{\text{mmse}}^{\text{H}}\mathbf{y} \rfloor$, where $\mathbf{W}_{\text{mmse}} = \left(\mathbf{G}\mathbf{G}^{\text{H}} + \frac{N_0}{E_s}\mathbf{I}_N\right)^{-1}\mathbf{G}$.

For the LR-based MMSE-SIC detection, $\mathbf{H}$ is replaced by an extended channel matrix defined as $\mathbf{H}_{\text{ex}} = \left[\mathbf{H}^{\text{T}} \sqrt{\frac{N_0}{E_s}}\mathbf{I}_N\right]^{\text{T}}$, while $\mathbf{y}$ and $\mathbf{n}$ are replaced by $\mathbf{y}_{\text{ex}} = \left[\mathbf{y}^{\text{T}}\ \mathbf{0}^{\text{T}}\right]^{\text{T}}$ and $\mathbf{n}_{\text{ex}} = \left[\mathbf{n}^{\text{T}} - \sqrt{\frac{N_0}{E_s}}\mathbf{s}^{\text{T}}\right]^{\text{T}}$, respectively. Through LR with $\mathbf{H}_{\text{ex}}$, the LBR matrix $\mathbf{G}_{\text{ex}}$ can be found as $\mathbf{H}_{\text{ex}} = \mathbf{G}_{\text{ex}}\mathbf{U}_{\text{ex}}$, where $\mathbf{U}_{\text{ex}}$ is an integer unimodular matrix. The LR-based MMSE-SIC detection is carried out with the QR factorization of $\mathbf{G}_{\text{ex}} = \mathbf{Q}_{\text{ex}}\mathbf{R}_{\text{ex}}$, where $\mathbf{Q}_{\text{ex}}$ is unitary and $\mathbf{R}_{\text{ex}}$ is upper triangular. Multiplying $\mathbf{Q}_{\text{ex}}^{\text{H}}$ to $\mathbf{y}_{\text{ex}}$ results in

$$\mathbf{Q}_{\text{ex}}^{\text{H}}\mathbf{y}_{\text{ex}} = \mathbf{R}_{\text{ex}}\tilde{\mathbf{c}} + \tilde{\mathbf{n}}, \tag{6.7}$$

where $\tilde{\mathbf{c}} = \mathbf{U}_{\text{ex}}\mathbf{s}$ and $\tilde{\mathbf{n}} = \mathbf{Q}_{\text{ex}}^{\text{H}}\mathbf{n}_{\text{ex}}$. With the upper triangular matrix $\mathbf{R}_{\text{ex}}$, the element of the last row, i.e., the MP-th layer, is detected first. Then, in the second last row, its contribution is canceled and the signal of the $(MP-1)$th layer is detected. This operation is terminated until all the layers are processed. The MD criterion derived in [41] with $M = 1$ for the LR-based MMSE-SIC detection can be extended to the case with $M > 1$ as follows:

$$\mathcal{K}_{\text{MD}} = \arg\max_{\mathcal{K}} \left\{ \min_{q} \mid r_{q,q}^{(\mathcal{K})} \mid \right\} \tag{6.8}$$

and the ME criterion for the LR-based MMSE detection can also be modified as

$$\mathcal{K}_{\text{ME}} = \arg\max_{\mathcal{K}} \lambda_{\min}\left(\mathbf{G}_{\mathcal{K}}^{\text{H}}\mathbf{G}_{\mathcal{K}}\right), \tag{6.9}$$

where $r_{q,q}^{(\mathcal{K})}$ denotes the (q,q)-th element of $\mathbf{R}_{\text{ex}}$ in (6.7). The user selection based on (6.4), (6.5), (6.8), and (6.9) is called the combinatorial user selection as the users can be selected by combinatorial (or exhaustive) search.

6.4 LR-based Greedy User Selection using an Updating Method

The computational complexity of the user selection under the criteria derived in Section 6.3 grows rapidly with M or K as they are all combinatorial optimization

problems. Thus, it is desirable to derive low complexity approaches for the user selection. In this section, we propose low complexity greedy approaches for the user selection. Note that we focus on the greedy user selection with a LR-based MIMO detector only as its performance is comparable to that of the ML detector and, more importantly, we can derive a computationally efficient LR updating method in conjunction with greedy user selection.

6.4.1 LR-based Greedy User Selection

The user selection approaches in Section 6.3 have the complexity that becomes prohibitively high as M or K increases, because there are $U = \prod_{i=0}^{M-1}(K-i)$ possible user index sets[1]. For each user index set, a LR of an $N \times MP$ complex channel matrix is to be performed. For example, when $K = 10$, $M = N = 4$ and $P = 1$, $10 \times 9 \times 8 \times 7 = 5040$ LRs of 4×4 complex-valued channel matrices should be carried out.

To reduce the computational complexity in the user selection, we consider a greedy approach when a LR-based MIMO detector is employed. The resulting approach is called the LR-based greedy (LRG) user selection, which is of course suboptimal. The LRG user selection algorithm is summarized as follows:

1) Let $m = 1$ and $\bar{\mathcal{K}} = \{1, \ldots, K\}$. In order to select the first user, we can use any criterion. For example, if the ME criterion is used, we have

$$k_{(1)} = \arg\max_{k \in \bar{\mathcal{K}}} \lambda_{\min}\left(\mathbf{G}_k^{\mathrm{H}} \mathbf{G}_k\right), \tag{6.10}$$

where $\mathbf{G}_k$ represents the LBR matrix of $\mathbf{H}_k$ or $\mathbf{H}_{\mathrm{ex},k} = \left[\mathbf{H}_k^{\mathrm{T}} \ \sqrt{\frac{N_0}{E_s}}\mathbf{I}_N\right]^{\mathrm{T}}$ (for the LR-based MMSE detector). Once the first user is chosen, we update $\bar{\mathcal{K}}$ as $\bar{\mathcal{K}} \Leftarrow \bar{\mathcal{K}} \setminus \{k_{(1)}\}$. In addition, we let $\mathbf{H}_{(1)} = \mathbf{H}_{k_{(1)}}$.

[1]For the LR-based combinatorial user selection schemes, we note that different order of user index leads to different decision, which results in different performance. In order to maximize the performance with the combinatorial user selection, the order of user index is considered in this chapter.

2) Let $m \Leftarrow m+1$ and $\mathbf{H}_{(m),k} = \left[\mathbf{H}_{(m-1)}\ \mathbf{H}_k\right]$, $k \in \bar{\mathcal{K}}$. The mth user can be chosen if the ME criterion is used as

$$k_{(m)} = \arg\max_{k\in\bar{\mathcal{K}}} \lambda_{\min}\left(\mathbf{G}^{\mathrm{H}}_{(m),k}\mathbf{G}_{(m),k}\right), \tag{6.11}$$

where $\mathbf{G}_{(m),k}$ is the LBR matrix of $\mathbf{H}_{(m),k}$ or $\mathbf{H}_{\mathrm{ex},(m),k} = \left[\mathbf{H}^{\mathrm{T}}_{(m),k}\ \sqrt{\frac{N_0}{E_s}}\mathbf{I}_N\right]^{\mathrm{T}}$. Once the mth user is found, we update as follows:

$$\begin{aligned} &\text{add } k_{(m)} \text{ to the index set of the selected users, } \mathcal{K}, \\ &\bar{\mathcal{K}} \Leftarrow \bar{\mathcal{K}} \setminus k_{(m)}, \\ &\mathbf{H}_{(m)} = \mathbf{H}_{(m),k_{(m)}}. \end{aligned} \tag{6.12}$$

3) If $m = M$, stop. Otherwise, go to 2).

Note that in this algorithm, the $N \times mP$ complex-valued matrix $\mathbf{H}_{(m)}$ denotes the channel matrix for the first m selected users, while the $N \times P$ complex-valued matrix $\mathbf{H}_{k_{(m)}}$ represents the channel matrix for the selected user in the mth selection with the index $k_{(m)}$, where $k_{(m)} \in \bar{\mathcal{K}}$ and $\bar{\mathcal{K}} = \{1,\ldots,K\} \setminus \{k_{(1)},\ldots,k_{(m-1)}\}$.

In the LRG user selection, the number of required LR operations is $\sum_{i=1}^{M}(K-i+1)$ and the matrix size for LR in selecting the mth user is $N \times mP$. Using the upper bound on the average complexity of LR studied in [23, 51, 52], we can show that the complexity of LRG is upper-bounded as $\sum_{i=1}^{M}(K-i+1)O\left((iP)^3 N\log(iP)\right)$ (Note that when $P=1$, no LR is required for the first user selection, where the complexity of LRG reduces to $\sum_{i=2}^{M}(K-i+1)O\left((iP)^3 N\log(iP)\right)$). On the other hand, the number of required LR operations in the combinatorial user selection according to (6.8) or (6.9) is $\prod_{i=1}^{M}(K-i+1)$ and the matrix size for LR is always $N \times MP$, which leads to its complexity that is upper-bounded as $\prod_{i=1}^{M}(K-i+1)O\left((MP)^3 N\log(MP)\right)$. This shows a significant computational complexity reduction. However, since the LRG user selection does not jointly select M users, there will be performance loss.

Note that the ME criterion is used in above for illustration purposes. The MD criterion can also be used for the LRG user selection with the LR-based MMSE-SIC detector.

6.4.2 A Complexity Efficient Method for LR Updating

We note that in the LRG user selection, the LR operation is repeatedly performed for each updated channel matrix. For instance, at the mth user selection, a LR is carried out with the complex-valued channel matrix $\mathbf{H}_{(m)} = \left[\mathbf{H}_{(m-1)}\ \mathbf{H}_k\right]$ as shown in (6.11), where $\mathbf{H}_k$ contains P newly added column vectors and the other $(m-1)P$ column vectors in $\mathbf{H}_{(m)}$ are already chosen and LBR. Instead of performing a new LR on all of the mP column vectors in $\mathbf{H}_{(m)}$, by utilizing the established $(m-1)P$ LBR vectors, we can derive a computationally efficient LR updating method with new P column vectors, which is referred to as the Updated Basis LR (UBLR) in this chapter. The resulting user selection scheme is referred to as the UBLR-based greedy (UBLRG)[1] user selection.

The UBLR algorithm is based on the CLLL algorithm [23, 24, 25]. Suppose that LR is performed by the CLLL algorithm in order to transform a given basis (a complex-valued channel matrix $N \times mP$ $\mathbf{H}_{(m)}$) into a new $N \times mP$ basis $\mathbf{G}_{(m)}$ consisting of nearly orthogonal basis vectors (i.e., $\mathcal{L}(\mathbf{G}_{(m)}) = \mathcal{L}(\mathbf{H}_{(m)}) \Longleftrightarrow \mathbf{G}_{(m)} = \mathbf{H}_{(m)}\mathbf{U}_{(m)}$, where $\mathbf{U}_{(m)}$ is unimodular). A basis $\mathbf{G}_{(m)}$ is called a reduced basis of a lattice with parameter δ if $\mathbf{G}_{(m)}$ is QR factorized as $\mathbf{G}_{(m)} = \mathbf{Q}_{(m)}\mathbf{R}_{(m)}$, where $\mathbf{Q}_{(m)}$ is unitary, $\mathbf{R}_{(m)}$ is upper triangular, and the elements of $\mathbf{R}_{(m)}$ satisfy the following inequalities [25]:

$$| \Re([\mathbf{R}]_{\ell,\rho}) | \leq \frac{1}{2} | [\mathbf{R}]_{\ell,\ell} | \quad \text{and} \quad | \Im([\mathbf{R}]_{\ell,\rho}) | \leq \frac{1}{2} | [\mathbf{R}]_{\ell,\ell} | \quad \text{for} \quad 1 \leq \ell < \rho \leq mP \tag{6.13}$$

and

$$\delta |[\mathbf{R}]_{\rho-1,\rho-1}|^2 \leq |[\mathbf{R}]_{\rho,\rho}|^2 + |[\mathbf{R}]_{\rho-1,\rho}|^2 \quad \text{for} \quad \rho = 2, \ldots, mP. \tag{6.14}$$

Here, $[\mathbf{R}]_{p,q}$ denotes the (p,q)-th element of $\mathbf{R}_{(m)}$. The parameter δ is closely related to the quality of the reduced basis. In this chapter, we assume $\delta = 3/4$[2] which is usually chosen for complexity and performance trade-off. For the

[1] Since the performance of the LRG and UBLRG user selection schemes are the same (in fact, UBLRG is a computationally efficient version of LRG), we now only consider UBLRG and assume that LRG and UBLRG are interchangeable.

[2] Here, δ is a factor selected to achieve a good quality-complexity trade-off [18]. We note that δ can be chose from $(\frac{1}{4}, 1)$ and $(\frac{1}{2}, 1)$ for the real and complex LLL algorithms, respectively [25].

UNIVERSITY OF WALES SWANSEA LIBRARY

initialization, let $\mathcal{A}'_{(m)} = \{\mathbf{Q}'_{(m)}, \mathbf{R}'_{(m)}, \mathbf{U}'_{(m)}\}$, where the QR factorization $\mathbf{H}_{(m)} = \mathbf{Q}'_{(m)}\mathbf{R}'_{(m)}$ and $\mathbf{U}'_{(m)} = \mathbf{I}_{mP}$. With $\{\mathbf{Q}_{(m)}, \mathbf{R}_{(m)}, \mathbf{U}_{(m)}\} = \{\mathbf{Q}'_{(m)}, \mathbf{R}'_{(m)}, \mathbf{U}'_{(m)}\}$ and $\rho = 2$, a version of CLLL algorithm is summarized as follows (note that since CLLL is used in UBLR, in Table 6.1, CLLL becomes part of UBLR).

a) To fulfill (6.13), a size-reduction is performed with the 1^{st} to ρ^{th} columns of $\mathbf{R}_{(m)}$ and $\mathbf{U}_{(m)}$ (see rows (15)-(21) in Table 6.1).

b) As the basis of $\mathbf{R}_{(m)}$ is size-reduced according to (6.13), let $\rho \Leftarrow \rho + 1$ and go to step a) if (6.14) is fulfilled. Swap the $(\rho-1)^{\text{th}}$ and ρ^{th} columns in $\mathbf{R}_{(m)}$ and $\mathbf{U}_{(m)}$ if (14) is not satisfied and update $\{\mathbf{R}_{(m)}, \mathbf{Q}_{(m)}\}$. Let $\rho \Leftarrow \max(\rho - 1, 2)$ and go to step a) (see rows (22)-(32) in Table 6.1).

c) The algorithm is terminated if $\rho = mP$. The output of the CLLL reduced matrix $\mathbf{G}_{(m)}$ is given by the updated $\mathcal{A}_{(m)} = \{\mathbf{Q}_{(m)}, \mathbf{R}_{(m)}, \mathbf{U}_{(m)}\}$, i.e., $\mathbf{G}_{(m)} = \mathbf{Q}_{(m)}\mathbf{R}_{(m)} = \mathbf{H}_{(m)}\mathbf{U}_{(m)}$.

In our LRG user selection, at the mth user selection, the channel matrix of size $N \times P(m-1)$ (denoted by $\mathbf{H}_{(m-1)}$) is obtained from the previous user selections. Under the assumption that the CLLL has been performed with $\mathbf{H}_{(m-1)}$ and its CLLL reduced matrix $\mathbf{G}_{(m-1)}$ is available, we have $\mathbf{H}_{(m)} = \left[\mathbf{H}_{(m-1)}\ \mathbf{H}_{k_{(m)}}\right]$ which is the channel matrix for the first m selected users.

The UBLR algorithm is carried out to transform $\mathbf{H}_{(m)}$ into a reduced basis $\mathbf{G}_{(m)}$ by utilizing a given set of already available matrices $\mathcal{A}_{(m-1)} = \{\mathbf{Q}_{(m-1)}, \mathbf{R}_{(m-1)}, \mathbf{U}_{(m-1)}\}$ associated with the CLLL reduced matrix $\mathbf{G}_{(m-1)}$ in the previous $m-1$ users selection, where $\mathbf{G}_{(m-1)} = \mathbf{Q}_{(m-1)}\mathbf{R}_{(m-1)} = \mathbf{H}_{(m-1)}\mathbf{U}_{(m-1)}$. The unimodular matrix $\mathbf{U}_{(m-1)}$ is employed to represent the column swaps in the CLLL, while $\mathbf{R}_{(m-1)}$ satisfies (6.13) and (6.14). The transformation algorithm for generating $\mathbf{G}_{(m)}$ in UBLR is summarized as follows.

Instead of starting the size-reduction of $\mathbf{R}'_{(m)}$ with the first two columns (the 1^{st} to ρ^{th} columns, where $\rho = 2$ in a)), UBLR reduces the iteration by starting the size-reduction with $\rho = (m-1)P+1$. In this case, the iteration of size-reduction from that with $\rho = 2$ to that with $\rho = (m-1)P+1$ need to be obtained by updating $\mathcal{A}'_{(m)}$ from $\mathcal{A}_{(m-1)}$.

Table 6.1: The UBLR (based on the CLLL) algorithm at the mth user selection

INPUT: $\{\mathcal{A}_{(m-1)}, \mathcal{B}_{(m-1)}, \mathbf{H}_{(m-1)}, \mathbf{H}_{k_{(m)}}\}$.

OUTPUT: $\{\mathcal{A}_{(m)}, \mathcal{B}_{(m)}\}$.

(1) $\mathbf{H}_{(m)} \leftarrow \left[\mathbf{H}_{(m-1)}\ \mathbf{H}_{k_{(m)}}\right]$

(2) $\omega \leftarrow \text{size}(\mathbf{H}_{(m-1)}, 2)$

(3) $\zeta \leftarrow \text{size}(\mathbf{H}_{(m)}, 2)$

(4) $[\mathbf{Q}_{(m)}\ \mathbf{R}_{(m)}] \leftarrow \text{qr}(\mathbf{H}_{(m)})$

(5) $\mathbf{U}_{(m)} \leftarrow \mathbf{I}_{\zeta}$

(6) $\mathbf{U}_{(m)}(1:\omega, 1:\omega) \leftarrow \mathbf{U}_{(m-1)}$

(7) $\mathbf{Q}_{(m)} \leftarrow \mathbf{Q}_{(m-1)}$

(8) $\mathbf{R}_{(m)}(:, 1:\omega) \leftarrow \mathbf{R}_{(m-1)}$

(9) for $\ell = 1 : \eta_{(m-1)}$

(10) $\quad \mathbf{R}_{(m)}\left(\gamma_{(m-1,\ell)} - 1 : \gamma_{(m-1,\ell)}, \omega + 1 : \zeta\right)$
$\quad\quad \leftarrow \mathbf{\Theta}_{(m-1,\ell)}\mathbf{R}_{(m)}\left(\gamma_{(m-1,\ell)} - 1 : \gamma_{(m-1,\ell)}, \omega + 1 : \zeta\right)$

(11) end for

(14) $\rho \leftarrow \omega + 1$

(13) $\eta_{(m)} \leftarrow 0$

(14) while $\rho \leq \zeta$

(15) $\quad$ for $\ell = 1 : \rho - 1$

(16) $\quad\quad \mu \leftarrow \lceil \mathbf{R}_{(m)}(\rho - \ell, \rho) / \mathbf{R}_{(m)}(\rho - \ell, \rho - \ell) \rfloor$

(17) $\quad\quad$ if $\mu \neq 0$

(18) $\quad\quad\quad \mathbf{R}_{(m)}(1 : \rho - \ell, \rho) \leftarrow \mathbf{R}_{(m)}(1 : \rho - \ell, \rho) - \mu\mathbf{R}_{(m)}(1 : \rho - \ell, \rho - \ell)$

(19) $\quad\quad\quad \mathbf{U}_{(m)}(:, \rho) \leftarrow \mathbf{U}_{(m)}(:, \rho) - \mu\mathbf{U}_{(m)}(:, \rho - \ell)$

(20) $\quad\quad$ end if

(21) $\quad$ end for

(22) $\quad$ if $\delta|(\mathbf{R}_{(m)}(\rho - 1, \rho - 1))|^2 > |\mathbf{R}_{(m)}(\rho, \rho)|^2 + |\mathbf{R}_{(m)}(\rho - 1, \rho)|^2$

(23) $\quad\quad \eta_{(m)} \leftarrow \eta_{(m)} + 1$

(24) $\quad\quad$ Swap the $(\rho - 1)$-th and ρth columns in $\mathbf{R}_{(m)}$ and $\mathbf{U}_{(m)}$

(25) $\quad\quad \mathbf{\Theta}_{(m,\eta_{(m)})} = \begin{bmatrix} \alpha^* & \beta \\ -\beta & \alpha \end{bmatrix}$ with $\alpha = \frac{\mathbf{R}_{(m)}(\rho-1,\rho-1)}{\|\mathbf{R}_{(m)}(\rho-1:\rho,\rho-1)\|}$, $\beta = \frac{\mathbf{R}_{(m)}(\rho,\rho-1)}{\|\mathbf{R}_{(m)}(\rho-1:\rho,\rho-1)\|}$

(26) $\quad\quad \gamma_{(m,\eta_{(m)})} \leftarrow \rho$

(27) $\quad\quad \mathbf{R}_{(m)}(\rho-1:\rho,\rho-1:\zeta) \leftarrow \mathbf{\Theta}_{(m,\eta_{(m)})}\mathbf{R}_{(m)}(\rho-1:\rho,\rho-1:\zeta)$

(28) $\quad\quad \mathbf{Q}_{(m)}(:,\rho-1:\rho) \leftarrow \mathbf{Q}_{(m)}(:,\rho-1:\rho)\mathbf{\Theta}^{\mathrm{T}}_{(m,\eta_{(m)})}$

(29) $\quad\quad \rho \leftarrow \max\{\rho-1,2\}$

(30) $\quad$ else

(31) $\quad\quad \rho \leftarrow \rho+1$

(32) $\quad$ end if

(33) end while

Since $\mathbf{R}'_{(m-1)}$ of size $N \times P(m-1)$ and $\mathbf{R}'_{(m)}$ of size $N \times Pm$ are upper triangular, it is straightforward to obtain that $\mathbf{R}'_{(m-1)} = \mathbf{R}'_{(m)}(:,1:P(m-1))$, which results in that the size reduction and column swapping performed on the first $P(m-1)$ columns of $\mathbf{R}'_{(m)}$ are the same as those on $\mathbf{R}'_{(m-1)}$. Using $\mathbf{R}_{(m-1)}$, let $\mathcal{A}_{(m)} = \mathcal{A}'_{(m)}$ and $\mathbf{R}_{(m)}(:,1:P(m-1)) = \mathbf{R}_{(m-1)}$. Then, we have the 1^{st} to $P(m-1)$-th column vectors of $\mathbf{R}_{(m)}$ satisfying (6.13) and (6.14). From this, we can see that CLLL is partially performed on $\mathbf{R}_{(m)}$ by employing UBLR. Similarly, with $\mathbf{Q}_{(m)} = \mathbf{Q}_{(m-1)}$ and $\mathbf{U}_{(m)}(1:P(m-1),1:P(m-1)) = \mathbf{U}_{(m-1)}$, $\{\mathbf{Q}_{(m)},\mathbf{U}_{(m)}\}$ can be updated with low computational complexity from $\{\mathbf{Q}_{(m-1)},\mathbf{U}_{(m-1)}\}$. Thus, from $\mathcal{A}_{(m-1)}$, UBLR is carried out to update the elements in $\mathcal{A}_{(m)}$ as shown in rows (6)-(8) in Table 6.1.

In addition, we note that, in row (8) of Table 6.1, we do not consider updating $\mathbf{R}_{(m)}(1:P(m-1),P(m-1)+1:Pm)$ in $\mathcal{A}_{(m)}$. It can be observed that when we perform a CLLL on $\mathbf{H}_{(m)}$ with the same operations of the CLLL for previous user selections, $\mathbf{R}_{(m)}(1:P(m-1),P(m-1)+1:Pm)$ will also be influenced. Hence, extra processing is necessary to recover $\mathbf{R}_{(m)}(1:P(m-1),P(m-1)+1:Pm)$ in $\mathcal{A}_{(m)}$. To this end, we define that $\mathcal{B}_{(m-1)} = \{\mathbf{\Theta}_{(m-1)},\gamma_{(m-1)},\eta_{(m-1)}\}$, where $\mathbf{\Theta}_{(m-1)} = \{\mathbf{\Theta}_{(m-1,1)},\cdots,\mathbf{\Theta}_{(m-1,\eta)}\}$, $\gamma_{(m-1)} = \{\gamma_{(m-1,1)},\cdots,\gamma_{(m-1,\eta)}\}$, and $\eta_{(m-1)} = \eta$. The operations of swapping and updating $\mathbf{R}_{(m-1)}$ and $\mathbf{Q}_{(m-1)}$ are kept in $\eta_{(m-1)}$, $\gamma_{(m-1)}$, and $\mathbf{\Theta}_{(m-1,\eta)}$, where $\eta_{(m-1)}$ keeps the number of swapping times, $\gamma_{(m-1)}$ keeps those columns involved in the swaps, and $\mathbf{\Theta}_{(m-1,\eta)}$ keeps the operations of column swaps. From the CLLL (see row (27) in Table 6.1), we note that $\mathbf{R}_{(m)}(1:P(m-1),P(m-1)+1:Pm)$ is generated by a transformation with $\mathbf{\Theta}_{(m)}$. Thus, using the information kept in $\mathcal{B}_{(m-1)}$, we can generate $\mathbf{R}_{(m)}(1:$

$P(m-1), P(m-1)+1 : Pm)$ as shown in rows (9)-(11) of Table 6.1.

With an updated $\mathcal{A}_{(m)}$, one CLLL can be carried out to generate the reduced basis $\mathbf{G}_{(m)}$. The calculation of this new basis generation starts with $\rho = (m-1)P+1$. Hence, the computational complexity of UBLR is evidently reduced as compared to employing one CLLL starting with $\rho = 2$. Note that since UBLR and CLLL generate the same LBR $\mathbf{G}_{(m)}$, they provide the same performance. In Section 6.5, this performance of UBLRG is validated by simulations.

The UBLR algorithm of the mth user selection is summarized in Table 6.1. The inputs of the algorithm of the mth user selection are $\{\mathcal{A}_{(m-1)}, \mathcal{B}_{(m-1)}, \mathbf{H}_{(m-1)}, \mathbf{H}_{k_{(m)}}\}$, while the outputs are $\{\mathcal{A}_{(m)}, \mathcal{B}_{(m)}\}$. Note that for the first user selection, with its channel matrix $\mathbf{H}_{k_{(1)}}$ as the input, instead of using the UBLR, one CLLL is carried out to generate $\{\mathcal{A}_{(1)}, \mathcal{B}_{(1)}\}$ as the output. Since the outputs of the mth user selection are regarded as the inputs at the $(m+1)$-th user selection, the algorithm is recursively carried out from $m = 2$. The algorithm is terminated if $m = M$.

The complexity of CLLL and UBLR algorithms highly depends on the number of column swaps, which is denoted by the output parameter η. In Table 6.2, the average value of η per iteration is shown when the CLLL-based MMSE-SIC detector is used with the proposed LRG and UBLRG user selection. It is assumed that $K = 10$ and $N = 8$ for the two possible cases of $(M, P) = (8, 1)$ and $(M, P) = (4, 2)$. Based on these results, we can observe that the complexity is significantly reduced if UBLR is employed. We also note that with the LRG, the complexity for the case of $(M, P) = (8, 1)$ is higher than that of $(M, P) = (4, 2)$ as expected (a large M implies a higher complexity). We can also show that the complexity of UBLRG is upper-bounded as $(K-M+1)O\left((MP)^3 N \log(MP)\right) + \sum_{i=1}^{M-1} O\left((iP)^3 N \log(iP)\right)$. Compared to the complexity of LRG which is upper-bounded as $\sum_{i=1}^{M}(K-i+1)O\left((iP)^3 N \log(iP)\right)$, the UBLRG scheme has a lower complexity, especially when large K and M are considered.

By using the real-valued LLL algorithm which is proposed as the LLL-LR in [22], UBLR can also be performed with a real-valued channel matrix. Since its derivation is straightforward, we do not discuss it any further. However, the simulation results in Section 6.5 show that the approaches using the real-valued LLL provide the same performance as the CLLL-based approaches. As shown

Table 6.2: The average value of η in the LRG and UBLRG user selection with the CLLL based MMSE-SIC detector is used.

Average value of η								
Number of columns in $\mathbf{H}_{\mathcal{K}}$	2	3	4	5	6	7	8	Sum
LRG[1]	0.2909	0.9029	1.8022	3.0633	4.7711	7.2925	12.1228	30.2457
UBLRG[1]	0.2904	0.5851	0.8940	1.2708	1.7653	2.5620	4.7728	12.1404
LRG[2]	0.2926	n/a	1.7977	n/a	4.7663	n/a	12.0856	18.9422
UBLRG[2]	0.2879	n/a	1.4952	n/a	3.0191	n/a	7.3761	12.1783

Note that the superscript [1] denotes the case of $K = 10$, $N = 8$, $(M, P) = (8, 1)$ and the superscript [2] denotes the case of $K = 10$, $N = 8$, $(M, P) = (4, 2)$, respectively.

in Table 6.3, the computational complexity can also be reduced if our UBLR algorithm is used with the LLL-LR.

Note that although the users are selected using a greedy method, we need to detect all the signals from the selected users jointly for a reasonably good performance[1]. As shown in [19, 22, 23, 24], the joint detection can be efficiently carried out by a LR-based detector.

6.5 Diversity Analysis and Numerical Results

In this section, we consider the diversity gain of the combinatorial user selection approaches with various detectors, such as the ML, MMSE, and LR-based SIC detectors, in Section 6.3. We derive lower bounds on the diversity gain of them. Since the diversity gain analysis of the proposed greedy user selection approach is difficult, we rely on simulations, from which we can show that our proposed LRG/UBLRG user selection approach has a similar diversity gain and comparable performance to the combinatorial one. Throughout this section, we assume that the elements of the channel matrix $\mathbf{H}_{\mathcal{K}}$ are independent zero-mean CSCG random variables with variance σ_h^2.

[1]As shown by simulation results in Subsection 6.5.2, the performance degradation due to the greedy user selection is not significant as long as joint detection is performed.

6.5.1 Diversity Gain Analysis from Error Probability

Through the following diversity gain analysis, we can see the impact of the type of MIMO detectors on the performance of multiuser systems.

6.5.1.1 Diversity Gain of Combinatorial User Selection with ML and MMSE Detectors

Using the PEP, we can show the diversity order from multiple receive antennas as well as multiple user selection.

Theorem 3 *The average PEP of the ML detector with the M selected users under the MDist user selection criterion in Section 6.3, denoted by P_e^{ml}, is upper-bounded as*

$$P_e^{\text{ml}} \leq c_1 \left(\frac{\|\sigma_h^2 \mathbf{d}\|^2}{N_0}\right)^{-N\lfloor \frac{K}{M} \rfloor} + o\left(\left(\frac{\|\sigma_h^2 \mathbf{d}\|^2}{N_0}\right)^{-N\lfloor \frac{K}{M} \rfloor + 1}\right), \tag{6.15}$$

where $c_1 > 0$ is constant, and $\mathbf{d} = \mathbf{s}_{(1)} - \mathbf{s}_{(2)}$ (here, $\mathbf{s}_{(i)} \in \mathcal{S}^{MP}$ and $\mathbf{s}_{(1)} \neq \mathbf{s}_{(2)}$).

See Appendix A.

This theorem shows that a full receive diversity gain of N together with a partial multiuser diversity gain of at least $\lfloor \frac{K}{M} \rfloor$ can be achieved by the ML detectors under the MDist user selection criterion. This result is derived under the fact that there are at least $\lfloor \frac{K}{M} \rfloor$ statistically independent alternative combinations of the composite channel matrix $\mathbf{H}_{\mathcal{K}}$ for M users. Hence, this result is a lower bound on the diversity gain. In fact, there are more combinations for $\mathbf{H}_{\mathcal{K}}$, which are not independent, that can increase the multiuser diversity gain. By simulations, we will further demonstrate the impact of the combinations of M selected users that are not independent.

Theorem 4 *The average PEP of the MMSE detector with the selected M users under the ME user selection criterion in Section 6.3, denoted by P_e^{mmse}, is upper-bounded as*

$$P_e^{\text{mmse}} \leq c_2 \left(\frac{\sigma_h^2 \|\mathbf{d}\|^2}{N_0}\right)^{-(N-P+1)\lfloor \frac{K}{M} \rfloor} + o\left(\left(\frac{\sigma_h^2 \|\mathbf{d}\|^2}{N_0}\right)^{-(N-P+1)\lfloor \frac{K}{M} \rfloor + 1}\right), \tag{6.16}$$

where $c_2 > 0$ is constant.

See Appendix B.

This theorem shows that for the MMSE detector, the ME user selection criterion may not be able to exploit a full receive diversity.

6.5.1.2 Diversity Gain of Combinatorial User Selection with LR-based Detector

Theorem 5 *The average PEP of the LR-based SIC detector with the selected M users under the MD user selection criterion in Section 6.3, denoted by P_e^{lr}, is upper-bounded as*

$$P_e^{\text{lr}} \leq c_3 \left(\frac{\|\sigma_h^2 \mathbf{d}\|^2}{N_0}\right)^{-N\lfloor \frac{K}{M} \rfloor} + o\left(\left(\frac{\|\sigma_h^2 \mathbf{d}\|^2}{N_0}\right)^{-N\lfloor \frac{K}{M} \rfloor + 1}\right), \tag{6.17}$$

where $c_3 > 0$ is constant.

See Appendix C.

This theorem shows that a full receive diversity gain of N together with the same partial multiuser diversity gain, $\lfloor \frac{K}{M} \rfloor$, as with the ML detector, can be achieved by the LR-based detector under the MD user selection criterion.

From these results, we can see that the LR-based detector is as good as the ML detector with respect to the diversity gains. These results are the extension of the performance analysis results in [41] for $M > 1$ and the consistent with the diversity gain results derived in [41] when we set $M = 1$ for the single-user case, for all the ML, MMSE detectors and the LR-based detector. That is, when $M = 1$, the diversity gain lower bounds of the proposed user selection criteria for the ML, MMSE detectors and the LR-based detector are NK, $(N - P + 1)K$, and NK, respectively.

6.5.2 Numerical Results

In this subsection, we present simulation results with MIMO channels of $\sigma_h^2 = 1$. The SNR is defined by the energy per bit to the noise power spectral density ratio, E_b/N_0. 16-QAM is used for signaling with Gray mapping. Note that LLL and CLLL denote the real-valued LLL-LR and the complex-valued LLL-LR, respectively (where they provide the same performance). Nine multiuser MIMO

systems are considered, namely **I**: MMSE detection under ME criterion, **II**: ML detection under MDist criterion, **III**: LR-based MMSE-SIC detection under MMI criterion [53], **IV**: LR-based MMSE-SIC detection[1] under ODR criterion [54], **V**: LR-based MMSE-SIC detection under semi-orthogonal user group (SUS) selection criterion [39], **VI**: LR-based MMSE-SIC detection under incremental selection criterion [78], **VII**: LR-based MMSE-SIC detection under fast antenna selection criterion [79], **VIII**: LR-based MMSE-SIC detection under LLL/CLLL-based MD criterion, **IX**: our proposed LR-based MMSE-SIC detection under LLL/CLLL-based UBLRG criterion. Since the LLL and CLLL-based user selection schemes provide the same performance, in BER simulations, we use the same notation (i.e., Systems **VIII** and **IX**) to represent the system using LLL or CLLL-based selection approach (but, as shown in Table 6.3, the complexity can be different depending on the use of LLL or CLLL).

In Figs. 6.1 and 6.2, the BER results of the multiuser MIMO systems are shown for the cases of $(M, P) = (4, 1)$ and $(M, P) = (2, 2)$, respectively. We assume that $K = 5$ and $N = 4$. From the diversity gain analysis in Subsection 6.5.1, we expect that the user selection methods with $(M, P) = (2, 2)$ in Fig. 6.2 outperform those with $(M, P) = (4, 1)$ in Fig. 6.1. From the curve of System **II** with $(M, P) = (2, 2)$ in Fig. 6.2, it is shown that when BER drops from 10^{-5} to 10^{-6}, SNR increases by approximately 1.2 dB. Thus, an estimate of the diversity gain from the simulation becomes $G \approx 8.3$, which is larger than the lower bound, $G_{low} = N\lfloor \frac{K}{M} \rfloor = 8$, derived from the theoretical analysis. Similarly, for the system with $(M, P) = (4, 1)$ in Fig. 6.1, when BER drops from 10^{-5} to 10^{-6}, SNR increases by approximately 1.7 dB, which results in $G \approx 5.9$, which is larger than the lower bound $G_{low} = 4$. Moreover, it is shown that the user selection approach with the LR-based detector has the same diversity gain as that with the ML detector, while the approach with the MMSE detector has a lower diversity gain as expected in Subsection 6.5.1. In general, we can show that System **IX** can provide a reasonably good performance, which outperforms that of Systems **III**, **V-VII** and approaches that of System **VIII**. Note that compared to System **IV**,

[1] Although the ODR criterion is developed for the LR-based linear detection, there are some performance gain by employing it with the LR-based MMSE-SIC detection. In order to make the comparison fair, we use the same detection method in Systems **III-IX**.

the proposed System **IX** provides a similar performance, however, its complexity is lower by a factor of thousands as shown in Table 6.3. Although the proposed System **IX** has a slight performance improvement compared to Systems **V-VII**, as shown in Fig. 6.3, the BER gain of the proposed method can be significant with a large K.

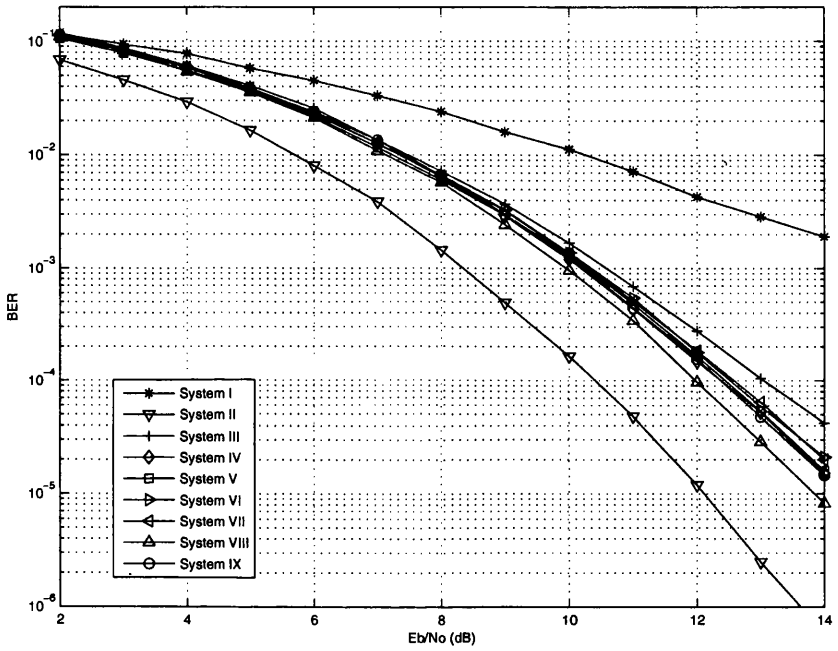

Figure 6.1: BER versus E_b/N_0 of the multiuser MIMO systems represented in Subsection 6.5.2 for the case of $(M, P) = (4, 1)$ (16-QAM, $K = 5$, $N = 4$).

In Figs. 6.3 and 6.4, we show the performance for different values of K when $E_b/N_0 = 12$ dB and $N = 4$ for the two possible cases of $(M, P) = (4, 1)$ and $(M, P) = (2, 2)$, respectively. It is shown that the performance can be improved as K increases in general. More importantly, we can observe in Fig. 6.3 that with a large K (e.g., $K = 8$), the proposed System **IX** can provide a much lower BER compared to Systems **V-VII** where throughput or capacity based selection criteria are considered.

In Table 6.3, we show the empirical result of the average number of flops for different multiuser MIMO systems to see the computational complexity. We

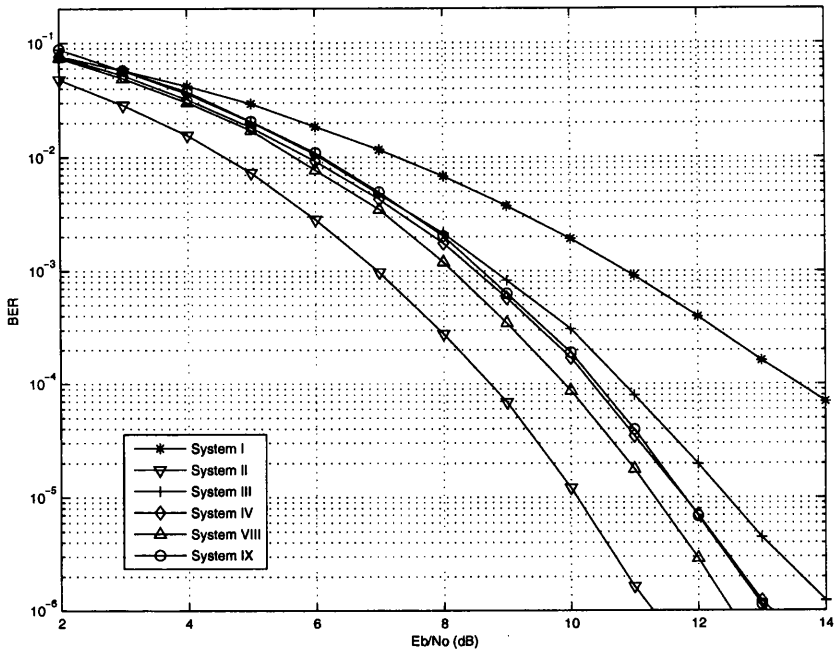

Figure 6.2: BER versus E_b/N_0 of the multiuser MIMO systems represented in Subsection 6.5.2 for the case of $(M, P) = (2, 2)$ (16-QAM, $K = 5$, $N = 4$).

simulate these systems using MATLAB-V5.3 on a PC. The MATLAB command "flops" is used to count the number of flops. We can observe that System **IX** can reduce the complexity by a factor of thousands compared to Systems **IV** and **VIII**. Although the throughput-based greedy user selection methods (i.e., Systems **V**-**VII**) provide lower computational complexity, their performance is worse than the proposed approaches' performance, especially when a large K is considered (which has been illustrated in Fig. 6.3). It is also shown that System **VIII** with LLL-based user selection scheme has the highest computational complexity as a real-valued LR-based combinatorial approach is used for user selection. With the combinatorial user selection, the computational complexity for the case of $(M, P) = (4, 1)$ is higher than that of $(M, P) = (2, 2)$, while a larger K can also lead to a higher complexity (from the comparison of the cases of $K = 10$ and $K = 15$). Since CLLL provides the same performance with a nearly half computational complexity of LLL [23], in Table 6.3, it is shown that

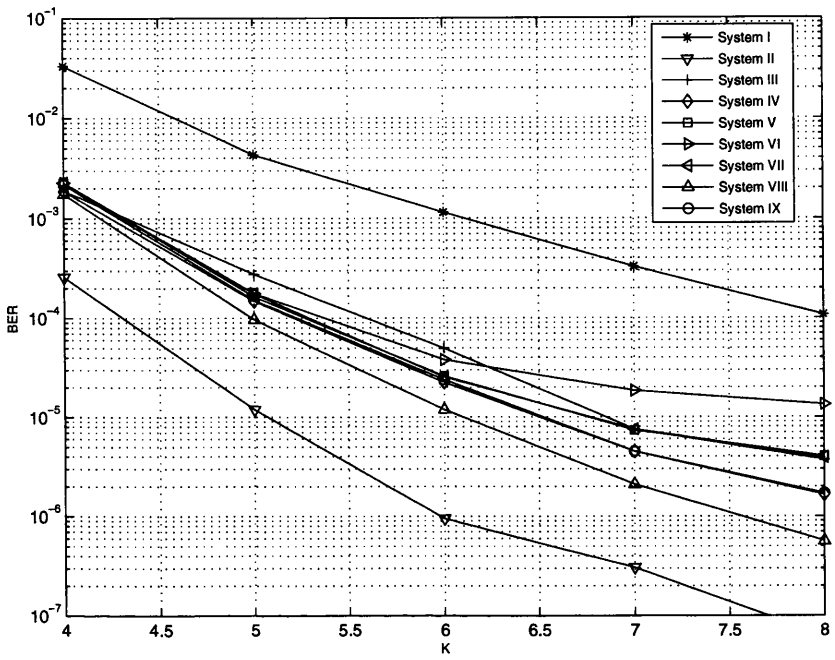

Figure 6.3: BER versus K of the multiuser MIMO systems represented in Subsection 6.5.2 for the case of $(M, P) = (4, 1)$ (16-QAM, $E_b/N_0 = 12$ dB, $N = 4$).

the CLLL-based approaches are more effective in terms of complexity.

Overall, System **IX** with CLLL-based detection is shown to be very attractive, because its performance is close to that of System **VIII** with a much lower complexity. Furthermore, it is noteworthy that if we target on a low BER, error probability based selection criteria become more suitable than capacity or throughput based selection criteria. From this, we can see that our proposed UBLRG approaches with LR-based detection is a key ingredient to build an error probability based low complexity criterion for multiuser MIMO user selection.

6.6 Conclusion

In multiuser systems, in order to fully exploit the performance in terms of the BER, error probability based user selection methods have been considered. If the user selection is based on a fully exhaustive search (i.e., the combinatorial

Table 6.3: The average complexity of multiuser MIMO systems represented in Subsection 6.5.2.

Average flops ($\times 10^5$) for 16-QAM, $N = 4$.				
	$K = 10$		$K = 15$	
System	$M = 4$, $P = 1$	$M = P = 2$	$M = 4$, $P = 1$	$M = P = 2$
I	339.02	3.6355	1780.1	8.2817
II	457.92	6.2495	2579.8	14.404
III	42.386	0.7569	275.51	1.7661
IV	459.84	6.3923	2688.5	14.975
V	0.1830	N/A	0.3005	N/A
VI	0.0739	N/A	0.1008	N/A
VII	0.0234	N/A	0.0309	N/A
VIII^1	589.12	8.0217	3413.1	18.600
VIII^2	405.51	5.4223	2335.3	12.711
IX^1	1.0129	1.0825	1.5474	1.6368
IX^2	0.6051	0.7189	0.9273	1.0834

Note that the superscript ^{1} and ^{2} denote the cases of LLL-based and CLLL-based user selection schemes used, respectively.

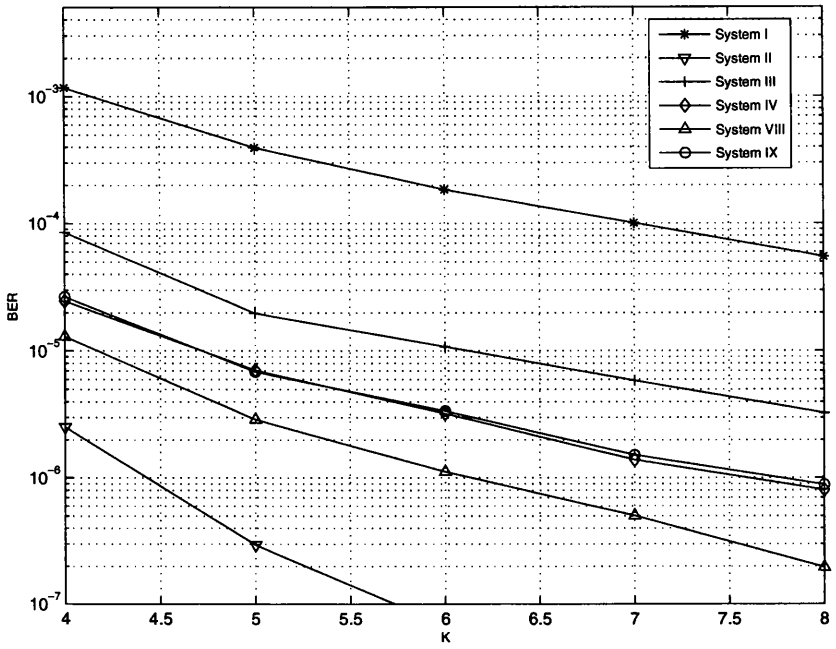

Figure 6.4: BER versus K of the multiuser MIMO systems represented in Subsection 6.5.2 for the case of $(M, P) = (2, 2)$ (16-QAM, $E_b/N_0 = 12$ dB, $N = 4$).

user selection), the complexity becomes prohibitively high. To avoid this heavy computational burden, in this chapter, we proposed an error probability based greedy user selection approach, called the LRG user selection, in conjunction with the UBLR algorithm which is a computationally efficient approach for LRG. With a combinatorial user selection, we showed that the LR-based detector is as good as the ML detector in terms of the diversity gains by the theoretical analysis and simulation results. From simulation results, it was also shown that the LR-based detection with our proposed UBLRG approaches can achieve a similar diversity gain and have a comparable performance to that based on a combinatorial approach.

7

Conclusion and Future Work

In this chapter, we conclude the main contributions of this thesis and present some possible extension for the future work.

7.1 Conclusion of Contributions

In this thesis, we first reviewed and explained the well-known and recently proposed MIMO detection schemes, including the list and LR based detection. The user selection for multiuser MIMO systems is introduced as an extension of MIMO systems. Then, we proposed a computationally efficient PMAP-based list MIMO detection. It showed that the proposed approach with $N_1 = N_2 = 2$ provides a near ML performance with a reasonably low complexity (around 3 times of the MMSE detector) when SNR $\geq$ 16 dB. For slow fading MIMO channels, we developed the CRC for the LR-based list detection to further improve the performance. It showed that with our proposed CRC, the performance of LR-based list detection was significantly improved. It can provide a near ML performance with a sufficiently low complexity (around 2 times of the MMSE detector) when slow fading MIMO channels are considered. After that, we investigated a complexity efficient PVC-MIMO detection with optimal PVS for underdetermined MIMO systems. We showed that the proposed MIMO detection schemes can exploit a near ML performance with a full receive diversity gain. It was also shown that the complexity of PVC-MIMO detection is low and comparable to that of the MMSE detection (around 3 times of the MMSE detector) when 4-QAM is used.

Finally, we extend the MIMO systems to multiuser MIMO systems and proposed a low complexity greedy user selection with an iterative LR updating algorithm when a LR-based MIMO detector is used. It showed that the proposed selection scheme can provide a comparable performance to the combinatorial ones (around 0.5-dB SNR loss at a broad range of BER) with a similar diversity gain (i.e., multiple antenna diversity and multiuser diversity). More importantly, it was shown that our proposed scheme can reduce the complexity by a factor of thousands compared to the combinatorial schemes.

7.2 Future Work

In this thesis, we only consider channel conditions to select users for multiuser MIMO systems. However, user selection is part of transmission optimization. It is possible to formulate more complicated optimization problem to further improve the performance. For example, the power allocation [85, 86], traffic conditions, and users' priorities [87, 88] in conjunction with user selection can be considered. While the performance can be improved in this case, there should be more control information to users, which makes the resulting system more complicated. Therefore, we treat it as an extension of this work with some practical approach for associated power allocation, traffic conditions, and users' priorities.

Appendix A

Proof of Theorem 3

With the selected M users by the combinatorial user selection approach under the MDist criterion, suppose that we jointly detect M users' signals with the $N \times MP$ channel matrix $\mathbf{H}_{\mathcal{K}}$ using the ML detector. The PEP in detecting M users' signals has the following upper bound:

$$\Pr\left(\mathbf{s}_{(1)} \to \mathbf{s}_{(2)}\right) \leq \operatorname{erfc}\left(\sqrt{\frac{\|\mathbf{H}_{\mathcal{K}}\bar{\mathbf{d}}\|^2}{2N_0}}\right), \tag{A.1}$$

where

$$\bar{\mathbf{d}} = \arg \min_{\mathbf{d}\in\mathcal{D},\mathbf{d}\neq\mathbf{0}} \|\mathbf{H}_{\mathcal{K}}\mathbf{d}\|^2,$$

$$\mathbb{D} = \left\{\mathbf{d} = \mathbf{s} - \mathbf{s}' \mid \mathbf{s} \neq \mathbf{s}' \in \mathcal{S}^{MP}\right\} \subset \mathbb{Z}^{MP} + j\mathbb{Z}^{MP}, \tag{A.2}$$

and $\operatorname{erfc}(x)$ is the complementary error function of x, i.e., $\operatorname{erfc}(x) = \frac{2}{\sqrt{\pi}} \int_x^{+\infty} e^{-z^2} dz$.

Let $\mathcal{D}(\mathbf{H}_{\mathcal{K}})$ denote the length of the shortest non-zero vector of the lattice generated by $\mathbf{H}_{\mathcal{K}}$. Then, we have

$$\Pr\left(\mathbf{s}_{(1)} \to \mathbf{s}_{(2)}\right) \leq \operatorname{erfc}\left(\sqrt{\frac{\mathcal{D}^2(\mathbf{H}_{\mathcal{K}})}{2N_0}}\right), \tag{A.3}$$

where

$$\mathcal{D}(\mathbf{H}_{\mathcal{K}}) = \|\mathbf{H}_{\mathcal{K}}\bar{\mathbf{d}}\|. \tag{A.4}$$

For the case that the MDist criterion (as shown in (6.4)) is employed, we have

$$\Pr\left(\mathbf{s}_{(1)} \to \mathbf{s}_{(2)}\right) \leq \operatorname{erfc}\left(\sqrt{\frac{\max_{\mathcal{K}} \mathcal{D}^2(\mathbf{H}_{\mathcal{K}})}{2N_0}}\right), \tag{A.5}$$

Note that

$$\max_{\mathcal{K}} \mathcal{D}^2(\mathbf{H}_{\mathcal{K}}) = \max_{\mathcal{K}} \min_{\mathbf{d}\in\mathbb{D},\mathbf{d}\neq\mathbf{0}} \mathbf{d}^{\mathrm{H}}\mathbf{H}_{\mathcal{K}}^{\mathrm{H}}\mathbf{H}_{\mathcal{K}}\mathbf{d}, \tag{A.6}$$

Let $\mathbf{w}_{\mathcal{K}} = \mathbf{H}_{\mathcal{K}}\mathbf{d}$. Note that $\mathbf{w}_{\mathcal{K}}$ is a zero-mean CSCG random vector and

$$E\left[\mathbf{w}_{\mathcal{K}}\mathbf{w}_{\mathcal{K}}^{\mathrm{H}}\right] = \sigma_h^2\|\mathbf{d}\|^2\mathbf{I}. \tag{A.7}$$

We can show that $X_{\mathcal{K}} = ||\mathbf{w}_{\mathcal{K}}||^2$ is a chi-square random variable with $2N$ degrees of freedom and its pdf is

$$f_X(x_{\mathcal{K}}) = \frac{1}{(\sigma_h^2\|\mathbf{d}\|^2)^N(N-1)!} x_{\mathcal{K}}^{N-1} e^{-x_{\mathcal{K}}/(\sigma_h^2\|\mathbf{d}\|^2)}. \tag{A.8}$$

The cumulative distribution function (cdf) is

$$F_X(x_{\mathcal{K}}) = 1 - e^{x_{\mathcal{K}}/(\sigma_h^2\|\mathbf{d}\|^2)} \sum_{q=0}^{N-1} \frac{(x_{\mathcal{K}}/(\sigma_h^2\|\mathbf{d}\|^2))^q}{q!}. \tag{A.9}$$

To obtain an upper bound on the error probability, we note that the number of alternative combinations of the channel matrices, which are statistically independent with each other, for selecting $\mathbf{H}_{\mathcal{K}}$ with the MDist selection in (6.4) is at least $\lfloor \frac{K}{M} \rfloor$. Let $\mathbf{H}_{\mathcal{K}_1}, \mathbf{H}_{\mathcal{K}_2}, \ldots, \mathbf{H}_{\mathcal{K}_{\lfloor \frac{K}{M} \rfloor}}$ represent such $\lfloor \frac{K}{M} \rfloor$ independent alternative combinations of the channel vectors. Then, there are at least $\lfloor \frac{K}{M} \rfloor$ of $\mathbf{w}_{\mathcal{K}}$, i.e., $\mathbf{w}_{\mathcal{K}_1}, \mathbf{w}_{\mathcal{K}_2}, \ldots, \mathbf{w}_{\mathcal{K}_{\lfloor \frac{K}{M} \rfloor}}$, which are independent. Let $V = \max\left\{X_1, X_2, \ldots, X_{\lfloor \frac{K}{M} \rfloor}\right\}$, where $X_m = ||\mathbf{w}_{\mathcal{K}_m}||^2$. Using order statistics, the pdf of V is given by

$$f_V(v) = K F_X^{\lfloor \frac{K}{M} \rfloor - 1}(v) f_X(v) = c_1' v^{N\lfloor \frac{K}{M} \rfloor - 1} + o(v^{N\lfloor \frac{K}{M} \rfloor - 1 + \epsilon}), \tag{A.10}$$

where $c_1' > 0$ is a constant, and $\epsilon > 0$. Thus, according to [68], we have

$$\begin{aligned} P_e^{\mathrm{ml}} &\leq \sum_{\mathbf{d}\in\mathcal{D},\mathbf{d}\neq\mathbf{0}} E_V\left[\operatorname{erfc}\left(\sqrt{\frac{\max_{\mathcal{K}} \mathbf{d}^{\mathrm{H}}\mathbf{H}_{\mathcal{K}}^{\mathrm{H}}\mathbf{H}_{\mathcal{K}}\mathbf{d}}{2N_0}}\right)\right] \\ &= c_1\left(\frac{\|\sigma_h^2\mathbf{d}\|^2}{N_0}\right)^{-N\lfloor \frac{K}{M} \rfloor} + o\left(\left(\frac{\|\sigma_h^2\mathbf{d}\|^2}{N_0}\right)^{-N\lfloor \frac{K}{M} \rfloor + 1}\right), \end{aligned} \tag{A.11}$$

where $c_1 > 0$ is a constant (c_1' and c_1 are proportional to each other[1]). This completes the proof.

[1]For the details of the connection between c_1' and c_1, please see the derivation in [68].

Appendix B

Proof of Theorem 4

It can be shown that under the ME criterion, for a given $\mathbf{H}_{\mathcal{K}}$, an upper bound on the error probability in detecting M users' signals is expressed as [41]

$$\begin{aligned} P_e^{\text{mmse}} &\leq \text{erfc}\left(\sqrt{\frac{\max_{\mathcal{K}} \lambda_{\min}(\mathbf{H}_{\mathcal{K}}^{\text{H}}\mathbf{H}_{\mathcal{K}})||\mathbf{d}||^2}{2N_0}}\right) \\ &= \text{erfc}\left(\sqrt{\frac{\sigma_h^2||\mathbf{d}||^2 \max_{\mathcal{K}} \tilde{X}_{\mathcal{K}}}{2N_0}}\right) \\ &= \text{erfc}\left(\sqrt{\frac{\sigma_h^2||\mathbf{d}||^2 V}{2N_0}}\right), \end{aligned} \tag{B.1}$$

where $\tilde{X}_{\mathcal{K}} = \lambda_{\min}(\mathbf{H}_{\mathcal{K}}^{\text{H}}\mathbf{H}_{\mathcal{K}})/\sigma_h^2$ and $V = \max_{\mathcal{K}} \tilde{X}_{\mathcal{K}}$.

According to [68], using the pdf of V (with the same derivation for the ML case in the last subsection), it can be deduced that

$$\begin{aligned} P_e^{\text{mmse}} &= E_{\mathbf{H}_{\mathcal{K}}}[\Pr\left(\mathbf{s}_{(1)} \rightarrow \mathbf{s}_{(2)}\right)] \\ &\leq E_V\left[\text{erfc}\left(\sqrt{\frac{\sigma_h^2||\mathbf{d}||^2 V}{2N_0}}\right)\right]. \end{aligned} \tag{B.2}$$

For independent alternative combinations of the channel matrices $\mathbf{H}_{\mathcal{K}_1}, \mathbf{H}_{\mathcal{K}_2}, \ldots, \mathbf{H}_{\mathcal{K}_{\lfloor \frac{K}{M} \rfloor}}$, similar to the proof of Theorem 3, we can follow the deriva-

tions in [68] and [69] and obtain that

$$\begin{aligned} P_e^{\text{mmse}} &\leq E_V\left[\text{erfc}\left(\sqrt{\frac{\sigma_h^2||\mathbf{d}||^2V}{2N_0}}\right)\right] \\ &\leq \int_0^{+\infty} \text{erfc}\left(\sqrt{\frac{\sigma_h^2||\mathbf{d}||^2v}{2N_0}}\right) f_V(v)dv \\ &= c_2\left(\frac{\sigma_h^2\|\mathbf{d}\|^2}{N_0}\right)^{-(N-P+1)\lfloor\frac{K}{M}\rfloor} + o\left(\left(\frac{\sigma_h^2\|\mathbf{d}\|^2}{N_0}\right)^{-(N-P+1)\lfloor\frac{K}{M}\rfloor+1}\right), \quad \text{(B.3)} \end{aligned}$$

where $c_2 > 0$ is constant. This completes the proof.

Appendix C

Proof of Theorem 5

In the LR algorithm, we transform the given channel matrix, e.g., $\mathbf{H}$, into a new basis, e.g., denoted by $\mathbf{G}$. Here, we have $\mathcal{L}(\mathbf{G}) = \mathcal{L}(\mathbf{H}) \Longleftrightarrow \mathbf{G} = \mathbf{HT}$, where $\mathbf{T}$ is an integer unimodular matrix and $\mathcal{L}(\mathbf{A})$ denotes the lattice generated by $\mathbf{A}$. Then, $\mathbf{G}$ is called LLL-reduced with parameter δ if $\mathbf{G}$ is QR factorized as $\mathbf{G} = \mathbf{QR}$ where $\mathbf{Q}$ is unitary, $\mathbf{R}$ is upper triangular, and the elements of $\mathbf{R}$ satisfies satisfies (6.13) and (6.14) with $m = M$. We rewrite (6.14) as

$$\delta \mid r_{\rho,\rho} \mid^2 \leq \mid r_{\rho,\rho+1} \mid^2 + \mid r_{\rho+1,\rho+1} \mid^2, \quad \rho = 1, 2, \ldots, MP - 1. \tag{C.1}$$

Then, we can obtain the following inequalities:

$$\mid r_{\rho+1,\rho+1} \mid^2 \geq \beta^{-1} \mid r_{\rho,\rho} \mid^2, \tag{C.2}$$

where $\beta = (\delta - \frac{1}{4})^{-1} > \frac{4}{3}$, and

$$\min_{\rho} \mid r_{\rho,\rho} \mid^2 \geq \beta^{-MP+1} \mid r_{1,1} \mid^2 . \tag{C.3}$$

Since $\mathbf{G} = \mathbf{QR}$, we have $\mid r_{1,1} \mid^2 = \|\mathbf{g}_1\|^2$ and

$$\|\mathbf{g}_1\|^2 \geq \min_{\mathbf{d} \in \mathcal{D}, \mathbf{d} \neq \mathbf{0}} \|\mathbf{Hd}\|^2 = \mathcal{V}^2(\mathbf{H}). \tag{C.4}$$

Thus, we have

$$\min_{\rho} \mid r_{\rho,\rho} \mid^2 \geq \beta^{-MP+1} \mathcal{V}^2(\mathbf{H}). \tag{C.5}$$

In the proposed user selection for selecting M users with the LR-based SIC detectors, (C.5) becomes

$$\min_{\rho} \mid r_{\rho,\rho} \mid^2 \geq \beta^{-MP+1} \mathcal{V}^2(\mathbf{H}_{\mathcal{K}}), \tag{C.6}$$

where $\mathcal{K}$ is the index set of the selected users.

Note that the LR-based SIC detection is performed with (6.7). Let n_ρ denote the ρth element of $\tilde{\mathbf{n}}$ in (6.7). Then, the LR-based SIC detection does not have error across all the layers if we have $\frac{|n_\rho|}{|r_{\rho,\rho}|} < \frac{1}{2}$ or $|n_\rho|^2 < \frac{|r_{\rho,\rho}|^2}{4}$ for all ρ. The probability of no error can be lower bounded as [89] (see pp. 292)

$$\Pr(\text{no error}) \geq \prod_{\rho=1}^{MP} \Pr\left(|n_\rho| < \frac{|r_{\rho,\rho}|^2}{4}\right). \tag{C.7}$$

Since $|n_\rho|^2$ is a chi-square random variable with 2 degrees of freedom (or an exponential random variable), we have

$$\Pr\left(|n_\rho| < \frac{|r_{\rho,\rho}|^2}{4}\right) = 1 - \exp\left(-\frac{|r_{\rho,\rho}|^2}{4N_0}\right). \tag{C.8}$$

Thus, the error probability of the LR-based SIC detector can be given by

$$\begin{aligned} \Pr(\text{error}) &\leq 1 - \prod_{\rho=1}^{MP} \left(1 - \exp\left(-\frac{|r_{\rho,\rho}|^2}{4N_0}\right)\right) \\ &\simeq \sum_{\rho=1}^{MP} \exp\left(-\frac{|r_{\rho,\rho}|^2}{4N_0}\right) \text{ as } N_0 \to 0. \end{aligned} \tag{C.9}$$

In the MD user selection criterion, the M users whose composite channel matrix (i.e., $\mathbf{H}_{\mathcal{K}}$) has the maximum $\min_\rho |r_{\rho,\rho}|$ are selected. Thus, the following approximation becomes accurate as $N_0 \to 0$ (or high SNR):

$$\sum_{\rho=1}^{MP} \exp\left(-\frac{|r_{\rho,\rho}|^2}{4N_0}\right) \simeq \exp\left(-\min_q \frac{|r_{\rho,\rho}|^2}{4N_0}\right); \tag{C.10}$$

$$\Pr(\text{error}) \simeq \exp\left(-\min_q \frac{|r_{\rho,\rho}|^2}{4N_0}\right). \tag{C.11}$$

Substituting (C.6) into (C.11), we have

$$\begin{aligned} \Pr(\text{error}) &\leq \exp\left(-\beta^{-MP+1} \mathcal{S}^2(\mathbf{H}_{\mathcal{K}})\right) \\ &\leq \sum_{\mathbf{d} \in \mathcal{D}, \mathbf{d} \neq 0} \exp\left(-\beta^{-MP+1} \frac{\max_{\mathcal{K}} \mathbf{d}^H \mathbf{H}_{\mathcal{K}}^H \mathbf{H}_{\mathcal{K}} \mathbf{d}}{2N_0}\right). \end{aligned} \tag{C.12}$$

Then, with the same approach used in the proof of Theorem 3, we can show that the upper bound on the average PEP is

$$P_e^{\text{lr}} \leq c_3 \left(\frac{\|\sigma_h^2 \mathbf{d}\|^2}{N_0} \right)^{-N\lfloor \frac{K}{M} \rfloor} + o\left(\left(\frac{\|\sigma_h^2 \mathbf{d}\|^2}{N_0} \right)^{-N\lfloor \frac{K}{M} \rfloor + 1} \right), \tag{C.13}$$

where $c_3 > 0$ is constant. This completes the proof.

Bibliography

[1] D. Tse and P. Vishwanath *Fundamentals of Wireless Communications*, Cambridge University Press, 2005. 1, 12, 66, 78

[2] P. W. Wolniansky, G. J. Foschini, G. D. Golden, and R. A. Valenzuela, "V-BLAST: An architecture for realizing very high data rates over the rich-scattering wireless channel," in *Proc. International Symposium on Signals, Systems, and Electronics (ISSSE),* Pisa, Italy, Sep. 1998. 1, 96

[3] L. Zheng and D. Tse, "Diversity and multiplexing: A fundamental tradeoff in multiple-antenna channels," *IEEE Transactions on Inform. Theory*, vol. 49, pp. 1073-1096, May 2003. 1, 12

[4] G. J. Foschini, G. D. Golden, R. A. Valenzuela, and P. W. Wolniansky, "Simplified processing for high spectral efficiency wireless communications employing multi-element arrays," in *IEEE J. Select. Areas Commun.*, vol. 17, pp. 1841-1852, Nov. 1999. 2

[5] A. B. Reid, A. J. Grant, and P. D. Alexander "List detection for multi-access channels," in *Proc. IEEE Globecom.*, vol. 2, pp. 1083-1087, Nov. 2002. 2, 17, 46, 48, 66

[6] H. Y. Fan, R. D. Murch, and W. H. Mow "Near maximum likelihood detection schemes for wireless MIMO systems" *IEEE Trans. on Wireless Communications* , vol. 3, no. 5, pp. 1427-1430, Sep. 2004. 2, 17, 46, 48, 66

[7] Y. Li and Z. Q. Luo "Parallel detection for V-BLAST system" in *Proc. IEEE ICC,* vol. 1, pp. 340-344, 2002. 2, 17, 46, 48, 66

[8] C. Windpassinger, L. H. J. Lampe, and R. F .H. Fischer "From lattice-reduction-aided detection towards maximum-likelihood detection in MIMO systems," in *Proc. IEEE Information Theory Workshop*, pp. 144-148, Mar. 2003. 2, 17, 46, 48, 66

[9] E. Agrell, T. Eriksson, A. Vardy, and K. Zeger, "Closest point search in lattices," *IEEE Trans. Inform. Theory*, vol. 48, no. 8, pp. 2201-2214, Aug. 2002. 2, 17, 46, 66

[10] B. Hassibi and H. Vikalo, "On the sphere-decoding algorithm I. Expected complexity," *IEEE Trans. Signal Processing*, vol. 53, no. 8, pp. 2806-2818, Aug. 2005. 2, 17, 46, 66, 92

[11] A. B. Reid, A. J. Grant, and P. D. Alexander, "List detection for the K-symmetric multiple-access channel," *IEEE Trans. Inform. Theory*, vol. 51, pp. 2930-2936, Aug. 2005. 2, 17, 46, 66

[12] D. Chase, "A class of algorithms for decoding block codes with channel measurement information," *IEEE Trans. on Information Theory*, vol. 18, pp. 170- 182, Jan. 1972. 3, 18, 47, 59, 67, 70, 72, 82

[13] D. W. Waters and J. R. Barry, "The Chase family of detection algorithms for multiple-input multiple-output channels," in *Proc. IEEE Globecom.*, vol. 4, pp. 2635- 2639, 29 Nov.-3 Dec. 2004. 3, 18, 19, 21, 22, 23, 47, 56, 59, 67, 70, 72, 82

[14] D. W. Waters and J. R. Barry, "The sorted-QR Chase detector for multiple-input multiple-output channels,"in *Proc. IEEE WCNC*, vol. 1, pp. 538- 543, 13-17 Mar. 2005. 3, 18, 20, 21, 47, 53, 55, 56, 59, 67, 70, 72, 82

[15] D. W. Waters, and J. R. Barry, "Partial decision-feedback detection for multiple-input multiple-output channels," in *Proc. IEEE ICC,* vol. 5, pp. 2668- 2672, 20-24 Jun. 2004. 3, 18, 47, 59, 67, 70, 72, 82

[16] D. J. Love, S. Hosur, A. Batra, and R. W. Heath, Jr., "Space-time Chase decoding," *IEEE Trans. Wireless Commun*, vol. 4, no. 5, pp. 2035-2039, Sept. 2005. 3, 18, 47, 59, 67, 70, 72, 82

[17] L. Bai and J. Choi, "Partial MAP-based list detection for MIMO systems," *IEEE Trans. Vehicular Tech.*, pp. 2544-2548, June 2009. 3, 18, 47, 59, 67, 70, 72, 82

[18] A. K. Lenstra, H. W. Lenstra, and L. Lovasz, "Factoring polynomials with rational coefficients," in *Math. Ann.*, vol. 261, pp. 515-534, 1982. 3, 26, 30, 31, 77, 101

[19] H. Yao and G. W. Wornell, "Lattice-reduction-aided detectors for MIMO communication systems," in *Proc. IEEE Global Telecommunications Conf.*, pp. 424-428, Nov. 2002. 3, 26, 28, 29, 36, 59, 70, 74, 92, 97, 106

[20] E. Viterbo and J. Boutros, "A universal lattice code decoder for fading channels," *IEEE Trans. Inform. Theory*, vol. 45, no. 5, pp. 1639-1642, July 1999. 3, 26, 29, 59, 92

[21] E. Agrell, T. Eriksson, A. Vardy, and K. Zeger, "Closest point search in lattices," *IEEE Trans. on Information Theory*, vol. 48, no. 8, pp. 2201-2214, Aug. 2002. 3, 26, 29, 59, 92

[22] D. Wubben, R. Bohnke, V. Kuhn, and K. D. Kammeyer, "Near-maximum-likelihood detection of MIMO systems using MMSE-based lattice reduction," in *Proc. IEEE International Conf. Communications,* pp. 798-802, June 2004. 3, 26, 28, 29, 31, 59, 63, 67, 70, 74, 77, 92, 96, 97, 105, 106

[23] Y. H. Gan, C. Ling, and W. H. Mow, "Complex lattice reduction algorithm for low-complexity full-diversity MIMO detection," *IEEE Trans. on Signal Proc.*, vol. 57, pp. 2701-2710, July 2009. 3, 26, 28, 29, 30, 32, 33, 36, 37, 59, 92, 97, 100, 101, 106, 111

[24] W. H. Mow, " Universal lattice decoding: a review and some recent results," *in Proc. IEEE International Conf. on Communications,* vol. 5, pp. 2842-2846, Paris, France, 20-24 June, 2004. 3, 26, 28, 29, 59, 92, 97, 101, 106

[25] X. Ma and W. Zhang, "Performance analysis for MIMO systems with lattice-reduction aided linear equalization," *IEEE Trans. on Communications* vol.

56, pp. 309-318, Feb. 2008. 3, 26, 28, 29, 31, 32, 33, 34, 35, 59, 62, 67, 76, 77, 78, 92, 97, 101

[26] A. M. M. Taherzadeh and A. K. Khandani, "LLL lattice-basis reduction achieves maximum diversity in MIMO systems," *in Proc. IEEE International Symposium on Information Theory (ISIT)*, Adelaide, Australia, 4-9 Sept. 2005. 3, 26, 29, 59, 92

[27] J. Choi "On the partial MAP detection with applications to MIMO channels" *IEEE Trans. on Signal Processing*, vol. 53, pp. 158- 167, Jan. 2005. 3, 46, 47, 48, 49, 50

[28] J. Choi and H. Nguyen, "SIC-based detection with list and lattice reduction for MIMO channels," *IEEE Trans. on Vehicular Tech.*, vol. 58, No. 7, pp, 3786-3790, Sep. 2009. 3, 59, 60, 61, 62, 64

[29] M. O. Damen, K. Abed-Meraim, and J. C. Belfiore, "Generalized sphere decoder for asymmetrical space-time communication architecture" *IEEE Electronics Letters*, vol. 36, pp. 166-167, 2000. 4, 67, 71, 72, 89

[30] M. Damen, H. El Gamal, and G. Caire, "On maximum-likelihood detection and the search for the closest lattice point" *IEEE Trans. Inform. Theory,* vol. 49, pp. 2389-2402, Oct. 2003. 4, 67, 71, 72, 89

[31] T. Cui and C. Tellambura, "An efficient generalized sphere decoder for rank-deficient MIMO systems," *IEEE Vehicular Tech. Conf.*, 2004. 4, 67, 71, 72, 89

[32] Z. Yang, C. Liu, and J. He, "A new approach for fast generalized sphere decoding in MIMO systems," *IEEE Signal Processing Letter,* Vol.12, No.1, Jan. 2005. 4, 67, 71, 72, 89

[33] P. Wang and T. Le-Ngoc, "A low-complexity generalized sphere decoding approach for underdetermined MIMO systems," *IEEE International Conference on Communications*, vol. 9, pp. 4266-4271, June 2006. 4, 67, 71, 72, 89

[34] A. Kapur and M. K. Varanasi, "Multiuser detection for overloaded CDMA systems" *IEEE Trans. Inform. Theory*, pp. 1728-1742, July 2003. 4, 67, 71, 89

[35] K. K. Wong and A. Paulraj, "Efficient near maximum-likelihood detection for underdetermined MIMO antenna systems using a geometrical approach" *EURASIP Journal on Wireless Communications and Networking*, Oct. 2007. 4, 67, 71, 89

[36] X. W. Chang and X. Yang, "An efficient tree search decoder with column reordering for underdetermined MIMO systems" *IEEE Globecom*, pp. 4375-4379, 2007. 4, 67, 71, 72, 82, 85, 89

[37] M. Bengtsson, "From single link MIMO to multi-user MIMO," *Proc. IEEE ICASSP*, 2004. 4, 38, 93

[38] R. Knopp and P. Humblet, "Information capacity and power control in single-cell multiuser communications," in *Proc. IEEE Int. Computer Conf, (ICC'95)*, Seattle, WA, June 1995. 4, 38, 92

[39] T. Yoo, N. Jindal, and A. Goldsmith, "Multi-antenna broadcast channels with limited feedback and user selection," *IEEE J. Sel. Areas Commun.*, vol. 25, no. 7, pp. 1478-1491, Sept. 2007. 4, 38, 41, 93, 109

[40] G. Dimic and N. Sidiropoulos, "On downlink beamforming with greedy user selection: Performance analysis and a simple new algorithm," *IEEE Trans. Signal Process.*, vol. 53, no. 10, pp. 3857-3868, Oct. 2005. 4, 38, 41, 93

[41] J. Choi and F. Adachi, "User selection criteria for multiuser systems with optimal and suboptimal LR-based detectors," *IEEE Trans. on Signal Proc.* (accepted). 4, 5, 36, 41, 42, 43, 44, 62, 63, 68, 73, 75, 79, 93, 96, 97, 98, 108, 120

[42] G. J. Foschini, "Layered space-time architecture for wireless communications in a fading environment when using multiple-element antenna,," *Bell Lab. Tech. J.*, vol. 1, pp. 41-59, Autumn 1996. 14

[43] G. J. Foschini, D. Chizhik, M. J. Gans, C. Papadias, and R. A. Valenzuela,"Analysis and performance of some basic space-time architectures," *IEEE J. Select. Areas Commun.*, vol. 21, pp. 303-320, Apr. 2003. 14, 16

[44] P. W. Wolniansky, G. J. Foschini, G. D. Golden, and R. A. Valenzuela, "V-BLAST: an architecture for realizing very high data rates over the rich-scattering wireless channel" in *Proc. ISSSE*, pp. 295-300, Sep. 1998. 16, 46

[45] W. Zha and S. Blostein, "Modified decorrelating decision-feedback detection of BLAST space-time system," in *Proc. IEEE Int. Conf. Communications,* vol. 1, pp. 335- 339, May 2002. 22

[46] H. Zhu, Z. Lei, and F. Chin, "An improved square-root algorithm for BLAST," *IEEE Trans. Signal Process.,* vol. 11, pp. 772-775, Sep. 2004. 22

[47] D. W. Waters and J. R. Barry, "The Chase family of detection algorithms for multiple-input multiple-output channels," *IEEE Trans. Signal Proc.*, vol. 56, No. 2, pp. 739-747, Feb. 2008. 23

[48] S. Liu, C. Ling, and D. Stehlé, "Randomized lattice decoding: Bridging the gap between lattice reduction and sphere decoding," *IEEE Int. Symp. Inform. Theory*, Austin, US, June 2010. 23, 24

[49] C. Ling, "On the proximity factors of lattice reduction-aided decoding," *IEEE Trans. Signal Process.*, submitted for publication. [Online]. Available: http://www.commsp.ee.ic.ac.uk/~cling/ 24

[50] C. Ling, "Towards characterizing the performance of approximate lattice decoding," in *Int. Symp. Turbo Codes/Int. ITG Conf. Source Channel Coding' 06*, Munich, Germany, Apr. 2006. 36

[51] H. Daudé and B. Vallée, "An upper bound on the average number of iterations of the LLL algorithm," *Theoret. Comp. Sci.*, vol. 123, pp. 95-115, 1994. 37, 100

[52] C. Ling and N. Howgrave-Graham, "Effective LLL reduction for lattice decoding," in *Proc. IEEE Int. Symp. Inf. Theory (ISIT),* Nice, France, Jun. 2007. 37, 100

[53] R. Nabar, D. Gore, and A. Paulraj, "Optimal selection and use of transmit antennas in wireless systems," presented at the *Int. Conf. Telecommun.(ICT'00),* Acapulco, Mexico, May 2000. 40, 93, 109

[54] I. Berenguer and X. Wang, "MIMO Antenna Selection with Lattice-Reduction-Aided Linear Receivers," *IEEE Trans. on Veh. Tech,* 53 (5), pp. 1289–1302, 2004. 41, 42, 93, 109

[55] G. J. Foschini and M. J. Gans "On limits of wireless communications in a fading environment when using multiple antennas," *Wireless Personal Communications*, vol. 6, pp. 311-335, Mar. 1998. 46

[56] I. E. Telatar "Capacity of multi-antenna Gaussian channels, " *European Transactions on Telecommunications*, vol. 10, no. 6, pp. 585-595, Nov.-Dec. 1999. 46

[57] R. A. Horn and C. R. Johnson. *Matrix Analysis.* Cambridge: Cambridge University Press, 1985. 47

[58] C. Berrou, A. Glavieux, and P. Thitimajshima, "Near Shannon limit error-correcting coding and decoding:Turbo-codes," in *Proc. IEEE ICC*, vol. 2, pp. 1064-1070, 23-26 May. 1993. 49

[59] P. Robertson, E. Villebrun, and P. Hoeher, "A comparison of optimal and sub-optimal MAP decoding algorithms operating in the log domain," in *Proc. IEEE ICC*, vol. 2, pp. 1009-1013, 18-22 Jun. 1995. 50

[60] J. S. Hammerschmidt, N. Graef, and S. A. Mujtaba, "A maximum a posteriori MIMO detector using recursive metric computations," *IEEE Trans. on Signal Processing*, vol. 54, pp. 3555- 3565, Sep. 2006. 51

[61] A. V. Zelst, R. V. Nee, and G. A. Awater, " Turbo-BLAST and its performance," in *Proc. IEEE VTC Spring*, vol. 2, pp. 1282-1286, 2001. 51

[62] B. M. Hochwald and S. T. Brink, "Achieving near-capacity on a multiple-antenna channel," *IEEE Trans. on Communications*, vol. 51, pp. 389- 399, Mar. 2003. 51

[63] D. Wubben, R. Bohnke, J. Rinas, V. Kuhn, and K. D. Kammeyer, "Efficient algorithm for decoding layered space-time codes," *Electronics Letters*, vol. 37, no. 22, pp. 1348-1350, 25 Oct., 2001. 54

[64] J. Choi, *Adaptive and Iterative Signal Processing in Communications*, Cambridge University Press, 2006. 56

[65] L. Bai, C. Chen, and J. Choi, " Lattice reduction aided detection for underdetermined MIMO systems: a pre-voting cancellation approach" *IEEE Vehicular Tech. Conf.*, Taipei, Taiwan, Spring 2010. 62, 63

[66] E. Biglieri, G. Taricco, and A. Tulino, "Performance of space-time codes for a large number of antennas," *IEEE Trans. Infor. Theory*, vol. 48, pp. 1794-1803, July 2002. 73

[67] M. Taherzadeh, A. Mobasher, and A. K. Khandani, "LLL reduction achieves the receive diversity in MIMO decoding," *IEEE Trans. Inform. Theory*, vol. 53, pp. 4801-4805, Dec. 2007. 76, 78

[68] Z. Wang and G. B. Giannakis, "A simple and general parameterization quantifying performance of fading channels," *IEEE Trans. on Communications*, no.51, pp. 1389-1398, Aug. 2003. 81, 118, 119, 120, 121

[69] A. Edelman, *Eigenvalues and condition numbers of random matrices*, Ph.D. Dissertation. MIT. May 1989 (http://www-math.mit.edu/edelman/homepage/papers/Eig.pdf, June 30, 2010). 80, 121

[70] A. J. Paulraj and C. B. Papadias, "Space-time processing for wireless communications," *IEEE Signal Processing Mag.*, vol. 14, pp. 49-83, Nov. 1997. 92

[71] L. C. Godara, "Applications of antenna arrays to mobile communications,Part I: Performance improvement, feasibility, and system considerations," *Proc. IEEE,* vol. 85, pp. 1031-1060, July 1997. 92

[72] L. C. Godara, "Applications of antenna arrays to mobile communications, Part II: Beam-forming and direction-of-arrival considerations," *Proc. IEEE,* vol. 85, pp. 1195-1245, July 1997. 92

[73] H. Y. Fan, R. D. Murch, and W. H. Mow, "Near maximum likelihood detection schemes for wireless MIMO systems," *IEEE Trans. on Wireless Comm.*, vol. 3, no. 5, pp. 1427-1430, Sep. 2004. 92

[74] Y. Li and Z. Q. Luo, "Parallel detection for V-BLAST system," in *Proc. IEEE ICC,* vol. 1, pp. 340-344, Apr. 2002. 92

[75] C. Windpassinger, L. H. J. Lampe, and R. F. H. Fischer, "From lattice-reduction-aided detection towards maximum-likelihood detection in MIMO systems," in *Proc. IEEE Information Theory Workshop*, pp. 144-148, Mar. 2003. 92

[76] R. W. Heath, Jr., S. Sandhu, and A. Paulraj, "Antenna selection for spatial multiplexing systems with linear receivers," *IEEE Commun. Lett.*,vol. 5, pp. 142-144, Apr. 2001. 93

[77] A. Gorokhov, D. A. Gore, and A. J. Paulraj, "Receive antenna selection for MIMO flat-fading channels: Theory and algorithms," *IEEE Trans. Inform. Theory,* vol. 49, pp. 2867-2696, Oct. 2003. 93

[78] A. Gorokhov, D. A. Gore, and A. J. Paulraj, "Receive antenna selection for MIMO spatial multiplexing: Theory and algorithms," *IEEE Trans. Signal Proc.,* vol. 51, pp. 2796-2807, Nov. 2003. 93, 109

[79] M. Gharavi-Alkhansari and A. B. Gershman, "Fast antenna subset selection in MIMO systems," *IEEE Trans. on Signal Proc.*, vol. 52, pp. 339-347, Feb. 2004. 93, 109

[80] M. Fuchs, G. DelGaldo, and M. Haardt, "Low complexity space-time-frequency scheduling for MIMO systems with SDMA," *IEEE Trans. on Vehicular Tech.,* vol. 56, no. 5, pp. 2775-2784, 2007. 93

[81] A. Bayesteh and A. K. Khandani, "On the user selection for MIMO broadcast channels," *IEEE Trans. on Information Theory,* vol. 54, pp. 1086-1107, March 2008. 93

[82] Z. Shen, R. Chen, J. G. Andrews, R. W. Heath, and B. L. Evans, "Low complexity user selection algorithms for multiuser MIMO systems with block diagonalization," *IEEE Trans. on Signal Proc.,* vol. 54, pp. 3658-3663, Sept. 2006. 93

[83] T. Ji, C. Zhou, S. Zhou, and Y. Yao, "Low complex user selection strategies for multi-User MIMO downlink scenario," *IEEE WCNC 2007,* pp. 1532-1537, 11-15 March 2007. 93

[84] S. Lee and J. S. Thompson, "QoS-guaranteed sequential user selection in multiuser MIMO downlink channels," *IEEE VTC 2007,* pp. 1926-1930, April 2007. 93

[85] R. Nabar, H. Bolcskei, and A. Paulraj, "Transmit optimization for spatial multiplexing in the presence of spatial fading correlation," in *Proc. IEEE Globecom,* San Antonio, TX, pp. 131-135, Nov. 2001. 95, 116

[86] S. Nam and K. Lee, "Transmit power allocation for an extended V-BLAST system," in *Proc. IEEE PIMRC,* pp. 843-848, Sept. 2002. 95, 116

[87] V. K. N. Lau, "Proportional fair space-time scheduling for wireless communications," *IEEE Trans. on Communications,* vol. 53, pp. 1353-1360, Aug. 2005. 95, 116

[88] L. Yang, M. Kang, and M.-S. Alouini, "On the capacity-fairness trade off in multiuser diversity systems," *IEEE Trans. on Vehicular Tech.,* vol. 56, pp. 1901-1907, July 2007. 95, 116

[89] J. Choi, *Optimal Combining and Detection: Statistical Signal Processing for Communications*, Cambridge University Press, 2010. 123